Heidi Gibson

TECHNICAL REPORT
NATICK/TR-90/028

AD A 241 335

PROCEEDINGS OF THE FIRST INTERNATIONAL SYMPOSIUM ON NONLINEAR OPTICAL POLYMERS FOR SOLDIER SURVIVABILITY

13 - 14 JUNE 1989

UNITED STATES ARMY NATICK
RESEARCH, DEVELOPMENT AND ENGINEERING CENTER
NATICK, MASSACHUSETTS 01760-5020

SOLDIER SCIENCE DIRECTORATE

DISCLAIMERS

The findings contained in this report are not to be construed as an official Department of the Army position unless so designated by other authorized documents.

Citation of trade names in this report does not constitute an official endorsement or approval of the use of such items.

DESTRUCTION NOTICE

For Classified Documents:

Follow the procedures in DoD 5200.22-M, Industrial Security Manual, Section II-19 or DoD 5200.1-R, Information Security Program Regulation, Chapter IX.

For Unclassified/Limited Distribution Documents:

Destroy by any method that prevents disclosure of contents or reconstruction of the document.

REPORT DOCUMENTATION PAGE

Form Approved
OMB No. 0704-0188

1. AGENCY USE ONLY (Leave blank)	2. REPORT DATE	3. REPORT TYPE AND DATES COVERED
	September 1990	Final 13 Jun 89--14 Jun 89

4. TITLE AND SUBTITLE

PROCEEDINGS OF THE FIRST INTERNATIONAL SYMPOSIUM ON NONLINEAR OPTICAL POLYMERS FOR SOLDIER SURVIVABILITY (U)

5. FUNDING NUMBERS

PE 1L162786
PR A1SL

6. AUTHOR(S)

7. PERFORMING ORGANIZATION NAME(S) AND ADDRESS(ES)

U.S. Army Natick Research, Development and Engineering Center
Kansas Street Attn: STRNC-Y
Natick MA 01760-5000

8. PERFORMING ORGANIZATION REPORT NUMBER

NATICK/TR-90/028

9. SPONSORING MONITORING AGENCY NAME(S) AND ADDRESS(ES)

10. SPONSORING MONITORING AGENCY REPORT NUMBER

11. SUPPLEMENTARY NOTES

The First International Symposium on Nonlinear Optical Polymers was held 13-14 June 1989 at Natick, MA. Symposium Director: Abner Salant, Director, Soldier Science Directorate; Symposium Coordinators: Jane A. Simpson and Thomas Sklarsky.

12a. DISTRIBUTION AVAILABILITY STATEMENT

Approved for public release; distribution unlimited.

12b. DISTRIBUTION CODE

13. ABSTRACT (Maximum 200 words)

This report incorporates 13 abstracts and 9 papers presented at the First International Symposium on Nonlinear Optical Polymers, held 13-14 June 1989 at the U.S. Army Natick RD&E Center, Natick MA.

14. SUBJECT TERMS

LASERS
LOW POWER
BATTLEFIELDS
EYE DAMAGE
RANGE FINDERS
TARGET DESIGNATORS
THREATS
NONLINEAR OPTICAL POLYMERS
LASER SAFETY

15. NUMBER OF PAGES

115

16. PRICE CODE

17. SECURITY CLASSIFICATION OF REPORT	18. SECURITY CLASSIFICATION OF THIS PAGE	19. SECURITY CLASSIFICATION OF ABSTRACT	20. LIMITATION OF ABSTRACT
Unclassified	Unclassified	Unclassified	

DEPARTMENT OF THE ARMY
U.S. ARMY TROOP SUPPORT COMMAND
NATICK RESEARCH, DEVELOPMENT AND ENGINEERING CENTER
NATICK, MA
01760-5002

REPLY TO
ATTENTION OF

STRNC-T

24 MAY 1989

MEMORANDUM FOR SEE DISTRIBUTION

SUBJECT: Proceedings of the First International Symposium on Nonlinear Optical Polymers for Soldier Survivability

1. The U.S. Army Natick Research, Development and Engineering Center held a symposium on 13-14 June 1989, the theme of which was, "Nonlinear Optical Polymers for Soldier Survivability." Our goal was to provide a forum that stimulates the exchange of ideas between academia, industry, and government agencies. In fact, the symposium was highly successful in accomplishing our goal, providing a lively scientific exchange among the attendees.

2. Twenty-two (22) papers were presented by the attendees, and two keynote addresses were given by very distinguished individuals in the field of Nonlinear Optical Polymers.

3. This volume includes all abstracts from the symposium and nine complete papers. It is of value to the symposium attendees and other professionals interested in the field of Nonlinear Optical Polymers. It is approved for public release. -- The Soldiers' Command

FOR THE COMMANDER:

ROBERT W. LEWIS
Technical Director

STRNC-T
SUBJECT: Proceedings of the First International Symposium on Nonlinear Optical Polymers for Soldier Survivability

DISTRIBUTION:
Dr. Byong H. Ahn, Center for Night Vision & Electro-Optics, Laser Division, CECOM, Ft. Belvoir, VA 22060-5677
Mr. James Bartley, MIT Lincoln Laboratory, Room L257, 244 Wood Street, Lexington, MA 02173
Dr. Joseph Bornstein, Dept. of Chemistry, Boston College, Chestnut Hill, MA 02167
Dr. Toch, Electro-Optical Products Division, ITT, 7635 Plantation Road, Roanoke, VA 24019
Professor Sergey Broude, Dept. of Physics, University of Lowell, Lowell, MA 01853
Dr. Charles T. Butler, Physical Sciences, Inc., 635 Slaters Lane, Suite G-101, Alexandria, VA 22314
Dr. Wempeng Chen, Non-Linear Optics Dept., Martin Marietta Labs, 1450 South Rolling Road, Baltimore, MD 21227
Dr. Nori Chu, American Optical Corporation, P.O. Box 1, Southbridge, MA 01550
Dr. Joseph Perry, Jet Propulsion Laboratory, California Institute of Technology, Materials Research & Spectroscopy Group, 4800 Oak Grove Drive, Pasadena, CA 91109
Professor Larry R. Dalton, Polymer Materials Research Center, D.P. & K.B. Loker Hydrocarbon Research Institute, University of Southern California, University Park, Los Angeles, CA 90089-0482
Dr. G. Thomas Davis, Dept. of Commerce, National Institute of Standards & Technology, Polymers Division, Building 224, Room B320, Gaithersburg, MD 20899
Professor Andrew Dienes, Dept. of Electrical Engineering & Computer Science, University of California at Davis, Davis, CA 95616
Dr Lawrence H. Domash, Foster-Miller, Inc., 350 Second Avenue, Waltham, MA 02254
Dr. Mark Druy, Foster-Miller, Inc., 350 Second Avenue, Waltham, MA 02254
LT Scott Dudevoir, Laser Microwave Division, U.S. Army Environmental Hygiene Agency, Aberdeen Proving Ground, MD 21010-5422
Mr. Mark Guaradlben, Laboratory for Laser Energetics, College of Engineering & Applied Science, University of Rochester, 250 East River Road, Rochester, NY 14623-1299
Dr. Shekhar Guha, Martin Marietta Labs, 1450 South Rolling Road, Baltimore, MD 21227
Dr. Robert Honeychuck, George Mason Institute, George Mason University Fairfax, VA 22030
Dr. G. Ronald Husk, U.S. Army Research Office, Chemical & Biological Sciences Division, P.O. Box 12211, Research Triangle Park, NC 27709-2211
Professor Samson A. Jenekhe, Dept. of Chemical Engineering, College of Engineering & Applied Science, University of Rochester, 206 Gavett Hall, Rochester, NY 14627
CPT Klenke, Combined Arms Combat Development Activity, ATTN: ATZO-CAG, Ft. Leavenworth, KS 66027
Professor Greg Kowalski, Dept. of Mechanical Engineering, Northeastern University, 360 Huntington Avenue, Boston, MA 02115

STRNC-T
SUBJECT: Proceedings of the First International Symposium on Nonlinear Optical Polymers for Soldier Survivability

DISTRIBUTION (Cont'd):
Dr. R. Sai Kumar, Dept. of Chemistry, College of Pure & Applied Science, University of Lowell, One University Avenue, Lowell, MA 01854
Ms. Sudha Kumar, Dept. of Physics, College of Pure & Applied Science, University of Lowell, One University Avenue, Lowell, MA 01854
Professor Robert Lenz, Polymer Science & Engineering Dept., University of Massachusetts at Amherst, Amherst, MA 01003
Dr. Michael Lesiecki, Candela Laser Corporation, 530 Boston Post Road, Wayland, MA 01778
Dr. Steve Letts, Lawrence Livermore National Laboratory, P.O. Box 808, L482, Livermore, CA 94550
Dr. Geoffrey A. Lindsay, Dept. of the Navy, Naval Weapons Center, Code 3858, China Lake, CA 93555-6001
Dr. David Lund, Letterman Army Institute of Research, Presidio of San Francisco, CA
Mr. Thomas A. Mooney, BARR Associates, 2 Liberty Way, Westford, MA 01886
Mr. Anthony P. Munie, McDonnell Douglas Electronic Systems Company, Mail Code 2871240, P.O. Box 516, St. Louis, MO 63166-0516
Mr. Arthur Nassucco, Arthur D. Little, 15 Acorn Park, Cambridge, MA 02140
Dr. Peter Nebolsine, Physical Sciences, Inc., P.O. Box 3100, Andover, MA 01810
Professor Peter Palffy-Muhoray, Liquid Crystal Institute, Kent State University, Kent, OH 44242
Dr. David G. Pelka, Physical Optics Corporation, 20600 Gramercy Place, Suite 101, Torrance, CA 90501
Professor Rolfe G. Petschek, Dept. of Physics, Case Western Reserve University, Cleveland, OH 44106-2624
Dr. Jack Preston, Research Triangle Institute, Research Triangle Park, NC 27709
Professor D. Rao, Dept. of Physics University of Massachusetts at Boston, Boston, MA 02125
Mr. Jerome Reid, Globalinx Corporation, 125 Second Avenue, Waltham, MA 02154
Professor John R. Reynolds, Dept. of Chemistry, University of Texas at Arlington, Box 19065, Arlington, TX 76019
Ms. Anita Robinson, Laser Microwave Division, U.S. Army Environmental Hygiene Agency, Aberdeen Proving Ground, MD 21010-5422
Dr. Daniel J. Sandman, GTE Laboratories, 40 Sylvan Road, Waltham, MA 02254
Dr. Gajendra D. Savant, Physical Optics Corporation, 20600 Gramercy Place, Suite 101, Torrance, CA 90501
Dr. Michael A. Schen, National Institute of Standards & Technology, Polymers Division, Building 224, Room B320, Gaithersburg, MD 20899
Mr. Ansgar Schmid, Laboratory for Laser Energetics, College of Engineering & Applied Science, University of Rochester, 250 East River Road, Rochester, NY 14623-1299
Dr. Robert E. Schwerzel, Battelle, Columbus Division, Dept. of Organic and Polymer Chemistry, 505 King Avenue, Columbus, OH 43201-2693
Dr. M.J. Soilleau, University of Central Florida, CREO-1, Orlando, FL
Dr. Donald Ulrich, Air Force Office of Scientific Research, Directorate of Chemical & Atmospheric Sciences, Bolling Air Force Base, Washington, D.C. 20332-6448

STRNC-T
SUBJECT: Proceedings of the First International Symposium on Nonlinear Optical Polymers for Soldier Survivability

DISTRIBUTION (Cont'd):
Dr. Wilfred Veldkamp, MIT Lincoln Laboratory, Room L270, 244 Wood Street, Lexington, MA 02173
Dr. Fred Yamagishi, Hughes Research Labs (MS RL70), 3011 Malibu Canyon Road, Malibu, VA 90265
Dr. Katherine Burns, U.S. Army Materials Technology Laboratory, Watertown, MA 02172-0001
Dr. Wenzel Davidsohn, U.S. Army Materials Technology Laboratory, Watertown, MA 02172-0001
Mr. Peter Dehmer, U.S. Army Materials Technology Laboratory, Watertown, MA 02172-0001
Mr. Mike Gilbert, U.S. Army Materials Technology Laboratory, Watertown, MA 02172-0001
Ms. Karen Kinsley, U.S. Army Materials Technology Laboratory, Watertown, MA 02172-0001
Ms. Emily McHugh, U.S. Army Materials Technology Laboratory, Watertown, MA 02172-0001
Mr. Charles Pergantis, U.S. Army Materials Technology Laboratory, Watertown, MA 02172-0001
Dr. Nate Schneider, U.S. Army Materials Technology Laboratory, Watertown, MA 02172-0001
Dr. M.S. Sennett, U.S. Army Materials Technology Laboratory, Watertown, MA 02172-0001
Dr. Robert E. Singler, U.S. Army Materials Technology Laboratory, Watertown, MA 02172-0001
Dr. R. A. Willingham, U.S. Army Materials Technology Laboratory, Watertown, MA 02172-0001
Ms. Pearl Yip, U.S. Army Materials Technology Laboratory, Watertown, MA 02172-0001
U.S. Army Armament RDE Center, ATTN: SMCAR-CO, SMCAR-TD, Dover, NJ 07801-5000
U.S. Army Chemical RDE Center, ATTN: SMCCR-CO, SMCCR-TD, APG, MD 21010-5423
U.S. Army Communications-Electronics RDE Center, ATTN: AMSEL-DCGD, AMSEL-TDD, Fort Monmouth, NJ 07703-5000
U.S. Army Belvoir RDE Center, ATTN: STRBE-Z, STRBE-ZT, Fort Belvoir, VA 21005-5066
U.S. Army Aviation RDE Center, ATTN: AMSAV-GRD, AMSAV-GTD, 4300 Goodfellow Boulevard, St. Louis, MO 63120-1798
U.S. Army Atmospheric Sciences Laboratory, ATTN: SLCAS-D, WSMR, NM 88002-5501
U.S. Army Vulnerability Assessment Laboratory, ATTN: SLCVA-D, WSMR, NM 88002-5513
U.S. Army Missile RDE Center, ATTN: AMSMI-R, Redstone Arsenal, AL 35898-5000
U.S. Army Tank Automotive RDE Center, ATTN: AMSTA-CF, AMSTA-CR, Warren, MI 48397-5000
U.S. Army Ballistic Research Laboratory, ATTN: SLCBR-D, APG, MD 21005-5066
U.S. Army Electronics Technology and Devices Laboratory, ATTN: SLCET-D, Fort Monmouth, NJ 07703-5302

STRNC-T
SUBJECT: Proceedings of the First International Symposium on Nonlinear Optical Polymers for Soldier Surviviability

DISTRIBUTION (Cont'd):
U.S. Army Harry Diamond Laboratories, ATTN: SLCHD-D, 2800 Powder Mill Road, Adelphi, MD 20783-1145
U.S. Army Human Engineering Laboratory, ATTN: SLCHE-D, APG, MD 21005-5001
U.S. Army Materials Technology Laboratory, ATTN: SLCMT-D, Watertown, MA 02172-0001
U.S. Army Materiel Command, ATTN: AMSTR-E, 5001 Eisenhower Avenue, Alexandria, VA 22333-0001
U.S. Army Materiel Systems Analysis Activity, ATTN: AMXSY-D, Aberdeen Proving Ground, MD 21005-5071
U.S. Army Armament, Munitions and Chemical Command, ATTN: AMSMC-CG, Rock Island, IL 61299-6000
U.S. Army Aviation Research and Technology Activity, ATTN: SAVDL-D, Ames Research Center, Moffett Field, VA 94035-1099
U.S. Army Laboratory Command, ATTN: AMSLC-TD, AMSLC-TP-PO, 2800 Powder Mill Road, Adelphi, MD 20783-1145
U.S. Army Research Office, ATTN: SLCRO-ZC, Research Triangle Park, NC 27709-2211
U.S. Army Electronic Warfare Vulnerability Assessment Laboratory, ATTN: SLCEV-M-D, White Sands Missile Range, NM 88002-5513
U.S. Army Test and Evaluation Command, ATTN: AMSTE-TD, Aberdeen Proving Ground, MD 21005-5055

First International Symposium on
Nonlinear Optical Polymers for Soldier Survivability
13-14 June 1989
U.S. Army Natick RD&E Center, Natick, Massachusetts

TABLE OF CONTENTS

* Complete paper

The format of the abstracts and papers in this volume is intended to reduce the costs of publication. The contributions are presented in substance as received from the authors.

NONLINEAR OPTICAL POLYMERS FOR LASER EYE PROTECTION

Dr. John Cornell
Polymer Section, MSB, PSD, SSD
U.S. Army Natick RD&E Center
Kansas Street (STRNC-YSM)
Natick, MA 01760-5020

The mission of the U.S. Army Natick Research Development and Engineering Center is to provide personal protection for the soldier against battlefield threats or those encountered in training. Recently a new threat has developed through the use of low power lasers in rangefinders and target designators and potential tunable weapons systems. Coherent radiation from these devices is capable of inflicting severe damage to the retina of the eye. One mode of protecting against such threats involves the development of nonlinear optical polymers which permit the transmission of visible light at ambient intensities but will reversibly block visible and near infrared radiation at intensities harmful to the eye.

At Natick RD&E Center a program of nonlinear optical polymers that can be incorporated in devices for laser eye protection is in progress. The program involves two phases (a) selection and synthesis of candidate polymers and (b) evaluation of the nonlinear optical properties.

A synthesis program has been initiated based on structural characteristics which we expect to demonstrate nonlinear optical properties. These include extended pi electron systems, permanent dipoles and anisotropic structures. Up until now the synthesis program has been carried out with three types of polymers having the required structures: Polyanilines and derivatives, polyazobenzenes and derivatives and polypyrroles. These polymers are generally intractable when prepared by bulk polymerization. Transparent tinted films of good optical properties comprising these polymers have been prepared by gas phase polymerization of the monomers on substrates of polyvinyl alcohol or polyvinylpyrrolidone.

These films will be evaluated in a facility that is now being completed at these laboratories. The test facility will employ a degenerate four wave mixing technique. A Rhodamine 6G dye laser pumped by a neodymium YAG unit will be used as a source for these experiments.

Plans for further work involve preparation and evaluation of polymers with conjugated segments in the main chain or in pendant groups. Investigation of nonlinear optical effects in liquid crystal and rigid rod polymers is also planned. Incorporation of the best optical materials into multiple layer films is also projected.

SYNTHESIS AND CHARACTERIZATION OF PROCESSABLE ORGANIC AND ORGANOMETALLIC MATERIALS WITH LARGE SECOND AND THIRD ORDER OPTICAL NONLINEARITIES AND FAST RESPONSE

Seth R. Marder, Joseph W. Perry and Daniel R. Coulter
Jet Propulsion Laboratory
California Institute of Technology
Pasadena, Ca. 91109

The Jet Propulsion Laboratory currently has a small program aimed at developing and characterizing processable organic and organometallic materials with large second and third order optical nonlinearities, fast response times and optical transmission in the visible and infrared regions of the spectrum for applications in optical computing, optical processing and eye and sensor protection. The main elements of the program include: 1) development of organic/organometallic donor-acceptor compounds with large $\chi^{(2)}$ values and transparency in the visible and near ir, 2) development of amorphous, processable, low scattering conjugated organic polymers with large $\chi^{(3)}$ values and near ir transparency, and 3) development of organic/organometallic dyes with nonlinear transmission properties in the visible. In the area of donor-acceptor compounds, a strategy which combines synthesis of molecules possessing large first hyperpolarizabilities (β's) with novel engineering of crystal structures has resulted in preparation of a number of materials with powder second harmonic generation efficiencies in the range of 100-2100 times urea and transparency ranging from the visible to the near ir. These efficiencies are up to an order of magnitude larger than previously reported for organic or inorganic materials. In the area of $\chi^{(3)}$ polymers, a number of conjugated materials have been made which have either soluble precursors or are themselves soluble. Characterization of thin films of these materials has shown nonlinearities approaching polyacetylene with in some cases reduction in scattering losses of up to three orders of magnitude relative to that material. Finally, studies have been under way on nonlinear transmission in dyes including metallophthalocyanines and their derivatives. Optical limiting studies with 30 psec pulses on solutions with 58% nominal transmission in the visible have shown a threshold for nonlinear absorption of <20 μjoules and a clamped output of ≈60 μjoules. Studies have also been conducted with longer pulses and pulse trains of up to 100 nsec duration and limiting has been observed (although with somewhat higher clamped output levels) thus indicating an impressive temporal dynamic range of at least four orders of magnitude. Any or all of the materials described above may have applicability in a variety of passive or active laser eye and/or sensor protection schemes.

Polydiacetylenes: The Best Defined Nonlinear Optical Polymers

Daniel J. Sandman
GTE Laboratories Incorporated
40 Sylvan Road
Waltham, MA 02254

Polydiacetylenes (PDA) are nonlinear optical polymers (NLOP) whose main chain involves completely conjugated segments manifested by intense visible absorption. The orientation of PDA is assured by their synthesis involving topochemical and topotactic solid state polymerizations of monomer crystals resulting in macroscopic fully crystalline experimental samples. As researchers deduced by degenerate four wave mixing studies on single crystal waveguide samples, PDA have the largest value of the degenerate third order susceptibility X(3) of any material in the transparent spectral region where the temporal response is in the femtosecond regime. The crystal structure-linear spectrum relationship for PDA is a sensitive function of the local crystal packing environment and is critical to enhancing the magnitude of X(3) in NLOP in general.

NEW THIRD-ORDER NONLINEAR OPTICAL POLYMERS: DESIGN, SYNTHESIS, AND CHARACTERIZATION BY DEGENERATE FOUR-WAVE MIXING*

Samson A. Jenekhe and W.C. Chen
Department of Chemical Engineering
University of Rochester
Rochester, NY 14627

S.K. Lo and D.J. Rogers
Honeywell System and Research Center
Minneapolis, MN 55418

S.R. Flom
Department of Chemistry
University of Minnesota
Minneapolis, MN 55455

ABSTRACT

Third-order ($\chi^{(3)}$) nonlinear optical processes in materials are of interest for optical switching and bistable optical devices. Conjugated polymers have been shown to exhibit the largest known nonresonant third-order nonlinear optical susceptibility ($\chi^{(3)}$) values. In an attempt to understand the structure-nonlinear optical property relationship in conjugated polymers and to maximize their nonlinear optical properties, we have designed and prepared a series of structurally diverse but related heteroaromatic polymers and measured their third-order nonlinear optical properties using picosecond and nanosecond degenerate four-wave mixing experiments. Our results show that the third-order nonlinear optical properties (γ and $\chi^{(3)}$) of the new polymers are larger than those of previously reported conjugated polymers by orders of magnitude.

*This research was partly funded by Naval Air Development Center (NADC) under contract no. N62269-87-C-0261.

Measurement of the Third-order Nonlinearity of an Organometallic Polymer in Thin Film and Solution Forms

S.Guha, C.C. Frazier, W.P. Chen, P. Porter and K. Kang
Martin Marietta Laboratories
1450 South Rolling Road
Baltimore, Maryland 21227

Transition metal-organic polymers are expected to possess large values of third-order hyperpolarizability because of the presence of extended π electron delocalization along long conjugated chains and also because of the interactions of the d orbitals of the transition metals with the organic π electrons, which provide an additional delocalized electronic system within the polymer chain. Measurements of these polymers in solution form have shown that the values of the third-order hyperpolarizability are indeed large.

For implementation of nonlinear materials in optical devices and full utilization of their large hyperpolarizabilities, the materials must generally be in the form of bulk crystals or thin films. We report here the measurement of the third-order nonlinear susceptibility (χ^3) of a transition metal-organic polymer in a dilute solution and as a thin film. Both the real and the imaginary parts of χ^3 were determined using the optical Kerr effect and intensity-dependent transmission using picosecond lasers. The nonlinear absorption coefficient of the polymer measured at visible wavelengths was large, making the material suitable for power limiting and sensor protection applications. We also will report on the measurement of the damage threshold of the polymer.

SELF-INDUCED BRAGG REFLECTION SHIELDS (SIBARS) FOR HARDENING AGAINST DIRECTED ENERGY THREATS

D.G. Pelka (1,2), G. D. Savant (1), C.P. Kuo(1), and J.B. Shellan (3)

(1) Physical Optics Corporation, Research Division, 20600 Grammercy Place, Suite 101, Torrance, California 90501

(2) Department of Electrical Engineering, Northrop University, Los Angeles, California 90045

(3) JBS Technologies, 631 Kendale Lane, Thousand Oaks, California 91360

ABSTRACT

Physical Optics Corporation is investigating the development of broadband agile laser reflection filters which should be effective from 350nm to 1400nm. The two approaches presented in this paper both use non-linear optical materials (NLOM) to induce appropriate Bragg structures which are then highly reflective to agile laser frequencies. The first device presented is completely passive and uses NLOM as the medium to induce back propagating Bragg planes which, in effect, cause the agile threat to induce its own countermeasure reflection filter. The second technology presented is a coherently coupled, holographic etalon, which can be made as either an active or passive device. Previous experimental data[1] suggest both technologies will have high laser damage thresholds of the order of 1-3 GW/cm^2.

1. INTRODUCTION

Protecting military personnel against retinal damage resulting from laser energy in the visible and near infrared (IR) spectrum represents a very difficult technology challenge. The major problem is discriminating between "good" visible light required for vision and "bad" visible and near IR light of sufficient intensity to cause eye damage. Full-time, or static, protection concepts such as dye absorbers or holograms block unacceptable amounts of "good" light, especially as the number of concurrent discrete wavelengths under consideration increases. Luminous transmissivity is reduced, causing degraded mission performance and increased field safety hazards. In addition, protection at discrete wavelengths is easily defeated by frequency agile lasers.

Emerging part-time or on-demand protection concepts against frequency agile lasers are expected to require advanced non-linear optical materials which change their index of refraction automatically when exposed to laser hazards. Since these unique materials may not be available in the near future, alternative concepts must be developed as interim solutions. There are several DOD programs underway to procure static, fixed, multiple-wavelength eyewear that will offer partial protection until better protection is available.

Physical Optics Corporation (POC) is exploring concepts that extend the fixed wavelength holographic Bragg structures to agile wavelength protection. We report on two such devices in this paper.

2. BRAGG STRUCTURE DEVICES

2.1 Fabrication of Holographic Filters

The basic technique for making holographic Bragg structures is illustrated in Figure 1. A laser beam of wavelength λ_o is incident on a layer (typically 10-20μm) of photo-sensitive holographic

emulsion. This laser beam passes through the holographic emulsion and is reflected by a mirror. This reflected beam now interferes with the incoming beam to set up a standing wave pattern[2] in the holographic emulsion. This standing wave pattern produces a set of interference fringes. Where constructive interference occurs within the material, a greater amount of energy is deposited, and

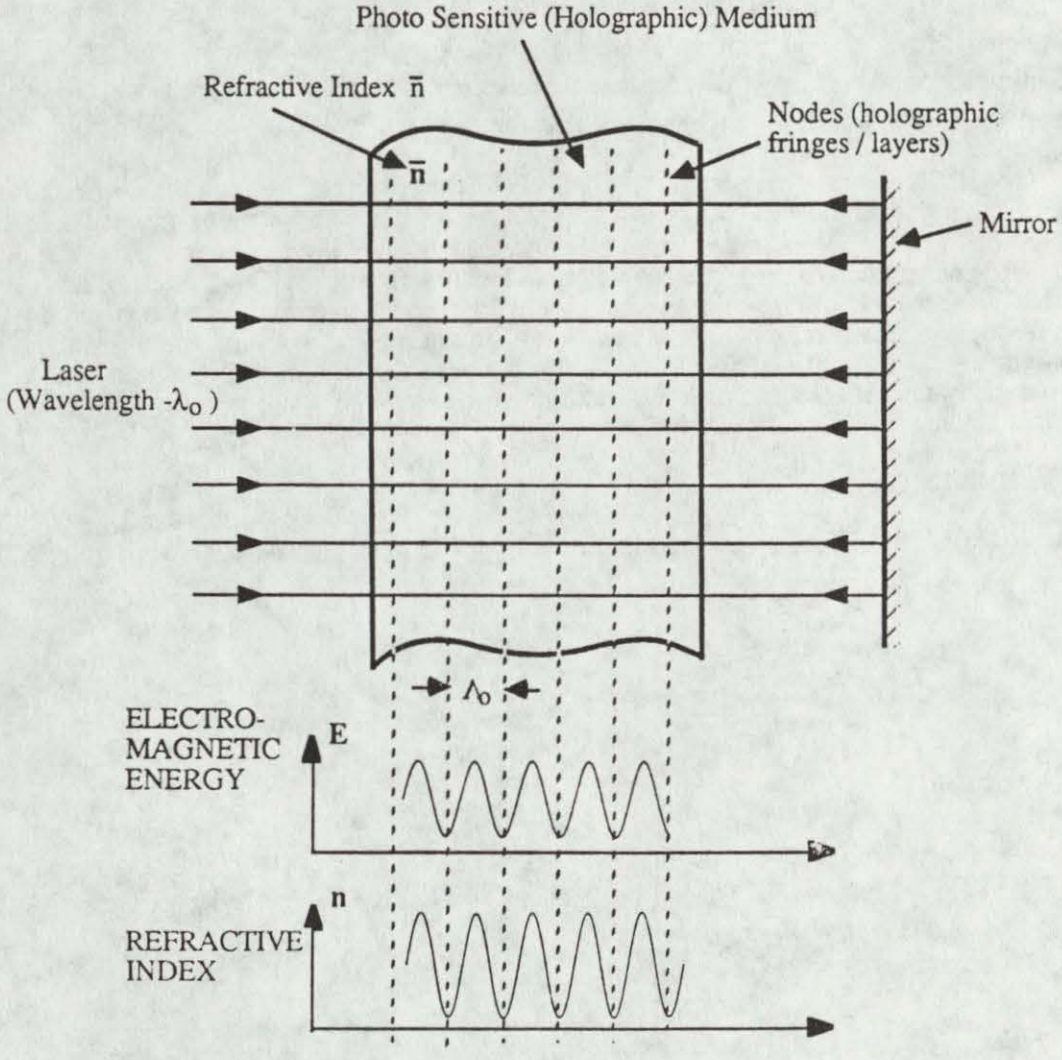

Figure 1. Standing Wave Holographic Recording (Normal Incidence)

where destructive interference occurs virtually no energy is deposited. Those planes with maximum deposition of energy (constructive interference) cause changes in the index of refraction of the material, thus creating scattering Bragg planes.

Recall that for interference structures the distance between successive Bragg planes is given by

$$\Lambda_o = \lambda/2 = \lambda_o/2n \qquad (1)$$

where λ is the wavelength of the laser radiation in the holographic emulsion, while λ_o is the free space wavelength and n is the retractive index of the holographic recording medium, typically $n \cong 1.50$. Simple calculation shows that the number of holographic reflection planes in an emulsion 20μm thick for λ_o=0.53μm is approximately 110.

Physical Optics Corporation has shown that these holographic filters are remarkable structures capable of having absolute reflectives in excess of 99.9%, optical densities in excess of 6, extremely small absorption, laser damage thresholds of a few GW/cm^2, and bandwidths typically from 10nm to greater than 500nm. The only shortcoming that fixed wavelength filters of this type have is that as the number of threat wavelengths in the visible portion of the spectrum increase and become frequency agile (i.e., tunable), the ability to superimpose many such fixed wavelength filters degrades the photoptic efficiency to such an extent that the laser protection becomes ineffective. However, it is clear that one would like to build in the major benefits of the Bragg structure for tunable protection devices if at all possible.

2.2 Self-Induced Bragg Reflection Structures

In analogy to Figure 1., the structure that suggests itself for an agile laser filter is shown in Figure 2.

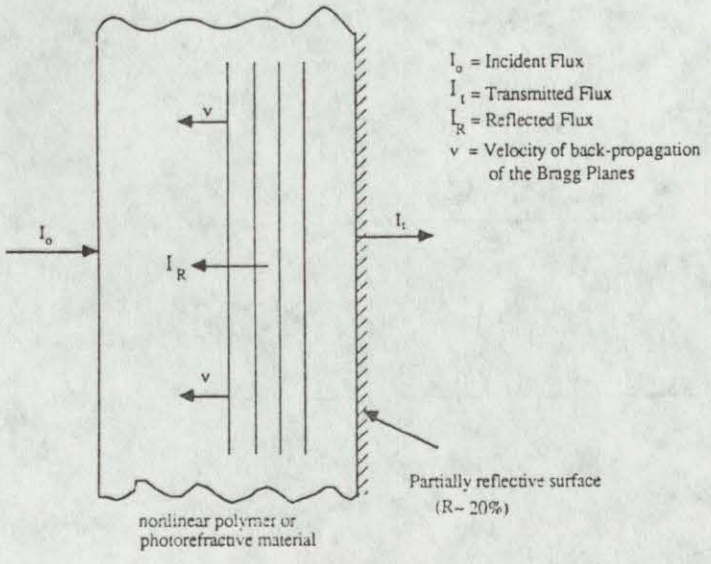

Figure 2. Self Induced Bragg Reflection Shield (SIBARS)

A nonlinear Kerr medium, whose back surface is coated with a partially reflective layer is the basis for this device. The index of refraction modulation in a Kerr medium is proportional to the local intensity (electric field squared).

This is in contrast to the Pockels effect in which case the index modulation is directly proportional to the electric field. For low incident power, nearly all of the reflected light can be attributed directly to the reflection from the back surface of the slab. At higher fluxes, however, the intensity of the radiation is high enough to generate significant index of refraction modulation of the Kerr medium. The standing wave in the slab, which initially was formed by the partially reflecting back surface, generates an index modulation which forms a Bragg reflector. The effectiveness of the self generated Bragg reflector increases with intensity and the incident field so that the SIBARS acts as a flux limiter to protect the eyes or sensors behind the slab. It can be shown that for a non-linear optical polymer with response times on the order of picoseconds that the amount of radiation transmitted to the eye or sensor before the back propagating Bragg structure is in place is much below injury or damage thresholds.

In analysis currently underway for the US Army Tank Command, POC has shown, using coupled mode theory, that in the limit of high reflectivity for SIBARS (high incident fluxes), the intensity transmitted to the sensor array is given by:

$$I(\ell) = \frac{I_\circ}{1 + \frac{4\pi}{\lambda} B \ell I_\circ} \qquad (2)$$

where $I_\circ$ = incident radiation; λ = wavelength of light; ℓ = thickness of the slab; β = nonlinear coefficient; $I(\ell)$ = intensity transmitted through the slab

The nonlinear coefficient relates the index of refraction modulation δn to the local intensity I by

$$\delta n = \beta I \qquad (3)$$

In the limit of high incident fluxes $I_\circ$, equation (2) indicates that the transmitted intensity is clamped at the maximum value I_ℓ^{max}, where

$$I_\ell^{max} = \frac{\lambda}{4\pi\beta\ell} \qquad (4)$$

2.3 Discussion of Results

In this section, we will evaluate equation (4) for typical Kerr materials to assess the usefulness of the SIBARS device. As will be seen in what follows the results are quite encouraging and indicate the concept is feasible.

The nonlinear coefficient β can be expressed in terms of the tabulated Kerr coefficient K by:

$$\beta = \frac{\lambda}{\varepsilon_o c} K \tag{5}$$

where c = speed of light $\varepsilon_o = 8.85 \times 10^{-12}$ f/m

Thus, we may rewrite equation (4) as:

$$I_\ell^{max} = \frac{\varepsilon_o c}{4\pi K I_d} \tag{6}$$

We wish to evaluate equation (6) for typical Kerr materials to determine the feasibility of the POC SIBARS concept. We begin by rewriting equation (6) as follows:

$$\ell_d = \frac{\varepsilon_o c}{4\pi K I_d} \tag{7}$$

In equation (7), ℓ_d represents the damage flux level and ℓ_d is the slab thickness required to reduce the incident flux to a level no higher than I_d. Consider the case for a pulsed laser with a 10ns pulse and a damage level to the slab of $10J/cm^2$ per pulse, and a material such as nitrobenzene ($K=2.44\times10^{-12}m/v^2$), $I_d = 10^{13}w/m^2$. For this case equation (7) predicts that the slab must be 8.7μm thick, a reasonable value. Note that we have not considered transient effects or the response time of the nitrobenzene in this analysis. Also, we have simply used damage levels which correspond roughly to the damage levels of coatings which may be used in the device.

The performance of the SIBARS can be improved substantially if the nitrobenzene is replaced with a high Kerr coefficient crystal. For crystals such as $BaTiO_3$, $KTaO_3$ or KH_2PO_4(KDP), the electro-optic tensor Sij is usually specified, rather than the Kerr coefficient. Roughly speaking, however, they are related by:

$$S = \frac{K\lambda}{n^3} \tag{8}$$

Then equation (7) may be cast into the form

$$\ell_d = \frac{\varepsilon_o c \lambda}{4\pi n^3 S I_d} \tag{9}$$

As Sij is a tensor, its value depends on the orientation of the crystal in the slab and the polarization of the incident radiation. For simplicity we have dropped the tensor subscripts ij in equations (8) and (9) since we are only interested in order of magnitude performance estimates at this time. If we use $\lambda = 0.5\mu m$, $S=10^{-14}m^2/v^2$ and n=2.4 (BaT_iO_3), equation (9) yields:

$$\ell_d = \frac{760}{I_d} \qquad \text{(MKS units)} \tag{10}$$

Consider the case of protecting a TH7863 CCD array manufactured by Thomson Electronics. This is a high performance array of 384x576 pixels which has a saturation exposure of 0.18 $\mu J/cm^2$.

For a clocking cycle of 10hz, this corresponds to a saturation intensity of $1.8 \times 10^{-2} w/m^2$. The SIBARS can be used to best advantage for this application in its focusing mode shown in Figure 3.

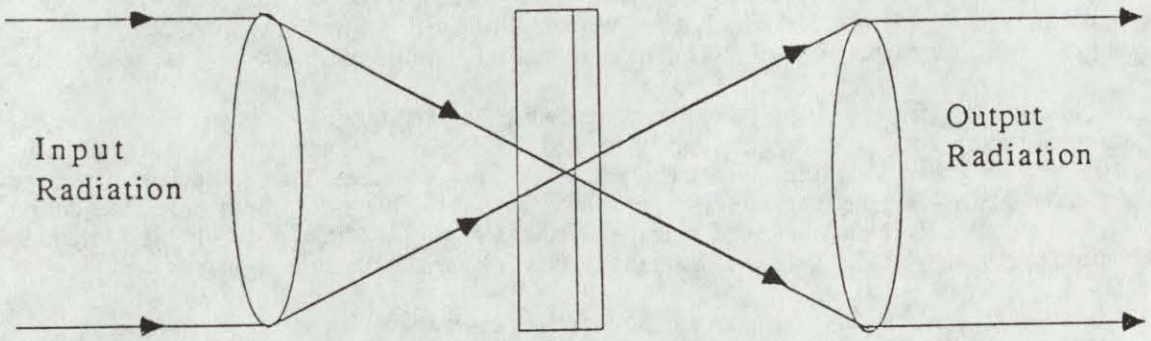

Figure 3 Focused Beam SIBARS Geometry

Assume a 10cm diameter input lens and a focused beam diameter in the SIBARS of 10μm. The intensity within SIBARS is then given by

$$I_o = (0.1m/10^{-5}m)^2 x 1.8x10^{-2} w/m^2 \qquad (11)$$
$$= 1.8x10^6 w/m^2$$

If we use this intensity in place of I_d in equation (10), we find that the $BaTiO_3$ slab must be 420μm thick. As a check on self consistency, we must verify that the assumed beam diameter of 10μm can be maintained within the entire length of the 420μm thick slab. The Rayleigh length l_R for a focused beam of diameter d is given by

$$\ell_R \approx \frac{\pi d^2}{\lambda} \qquad (12)$$

For the case d = 10μm and λ =0.5μm, equation (11) predicts l_R = 630μm. The beam can thus maintain its 10μm spot size throughout the thickness of the slab as required in this example.

Although it is probably only necessary to protect sensors from damage and not saturation, we have considered the above example to demonstrate the options possible with the SIBARS configuration.

3. COHERENTLY COUPLED HOLOGRAPHIC ETALONS

A relatively simple yet powerful technique for high resolution spectroscopy, narrow band filtering, or coherence filtering is based on the properties of the Fabry-Perot (FP) etalon. This device consists of a couple parallel highly reflective surfaces which can transmit a high fraction of incident radiation at certain periodic frequencies. At these frequencies a large fraction of the light that would ordinarily be reflected by each surface interact coherently and thus most of the radiation can be transmitted through the device.

Recently, Physical Optics Corporation has been able to fabricate coherently coupled holographic etalons which have shown characteristic Fabry-Perot circular fringes. These etalons have been constructed by taking liquid crystal material sandwiched between glass and coating holographic emulsion on both sides of the glass. Upon exposure of both sides of this glass as reflection holographic mirrors simultaneously, one observes that a coherently coupled FP etalon is obtained. By application of small amounts of voltage (approximately 2.5) volts, the effective optical path length between the two coherently coupled mirrors may be changed and the device will change from being highly reflective to highly transmissive over a characteristic bandwidth. Many remarkable features have been observed experimentally for this simple inexpensive device that makes it applicable to the fields of laser hardening, optical computing, spatial light modulators, etc.

The quality of the fringes observed experimentally was surprisingly good, given the poor optical quality of the microscope slide glass which formed the FP cavity. Furthermore, POC found that when the holographic coatings were recorded on the two surfaces during separate exposures (expose one side, develop, and then expose and develop the other side), the interference fringes were not visible. It is also believed that these fringes would not have been visible if standard evaporated coatings had been deposited on the surfaces of the glass cavity.

Modulation of the transmission characteristics of this cavity when the voltage across non-linear liquid crystal material is varied has been shown to be on the order of 10^{-3}s. By replacing this slow liquid crystal material by faster switching electro-optic polymer materials, switching times on the order of nanoseconds or faster can be predicted. Various configurations of both active and passive such devices show good promise for application to the field of agile laser countermeasures.

3.1 Physical Description of the Coherently Coupled Etalon (C^2E)

The basic physical embodiment of the coherently coupled etalon (C^2E) is shown in Figure 4. It consists of a non-linear material placed between a couple of coherently exposed holographic mirrors. The non-linear material can then be made to change its optical path length by the application of an electric field as shown in Figure 4 or by an intensity (passive) induced change. Both active and passive types of such etalons have been produced at POC, and the switching (or tuning) speeds of such optical devices has been shown to be directly dependent on the switching speed of the non-linear optical material.

Recall that the FP equations can be written as[3]

$$\Delta\upsilon = \frac{c}{2n\ell_\circ \cos\theta} \tag{13}$$

$$\Delta\lambda = \frac{\lambda_\circ^2}{2n\ell_\circ} \tag{14}$$

where c = speed of light, n = index of light

$\ell_\circ$ = length of the FP cavity, $\lambda_\circ$ = peak wave-length

θ = angle of incidence

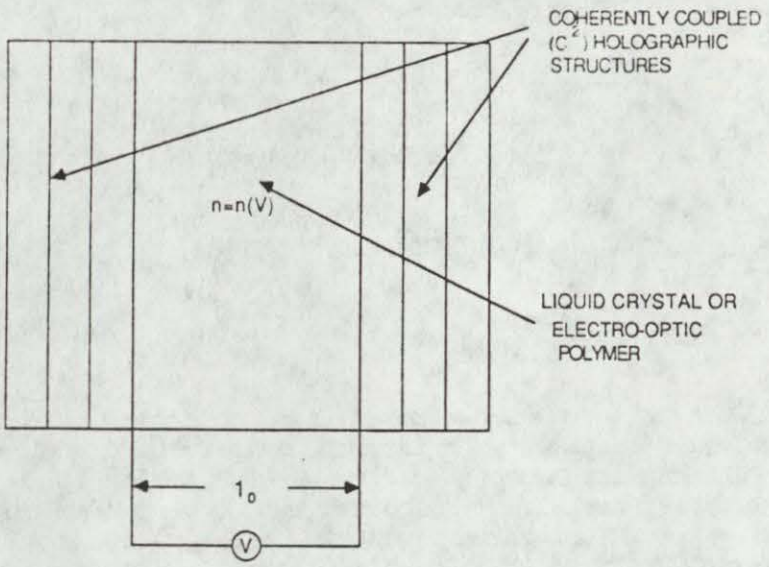

Figure 4. Coherently Coupled Tunable Holographic Etalon

The typical transmission versus frequency curve of a FP cavity is shown in Figure 5.

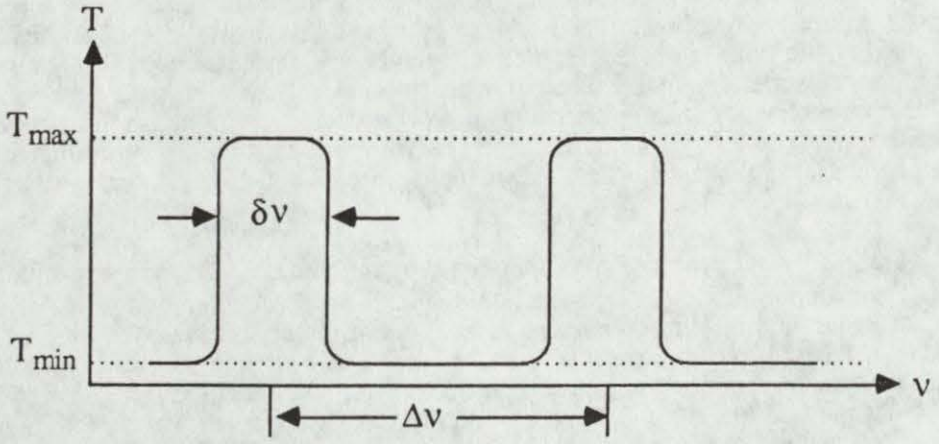

Figure. 5 Typical Fabry-Perot Characteristics

One can observe that for ℓ_o = 1 um, $\Delta\lambda \approx 80nm$. Only holographic etalons constructed in the manner outlined above can achieve such a broad free spectral range. This makes such devices interesting technology to use as countermeasures against frequency-agile tunable lasers.

The advantages of coherently coupled etalons when compared to classical FP etalons are:

1. The ability to use inexpensive optical substates.
2. Small cavity lengths result in large free spectral ranges and therefore high photoptic efficiencies.

1054-nm Damage Thresholds for Monomeric and Polymeric-Side-Chain Liquid Crystal Systems

Mr. Mark Guardalben
Dr. Ansgar Schmid
Dr. Steve Jacobs
Dr. Shaw-Horng Chen
LABORATORY FOR LASER ENERGETICS
University of Rochester
250 East River Road
Rochester, NY 14623-1299

ABSTRACT

Among the most important material parameters of non-linear organics are the magnitude and speed of the nonlinearity and the material damage threshold. A material with large nonlinearity paired with a low damage threshold is less useful than one with a higher threshold. Here, 1-nsec., 1054-nm. damage thresholds for monomeric and polymeric-side-chain liquid crystal systems are reported. A comparison between aliphatic and equivalent aromatic systems establishes a causal link between damage and the compound's electron delocalization. Rules of thumb for raising the damage threshold are derived and trade-offs for device designs are discussed.

BACKGROUND

Organic, conjugated π-electron molecular and polymeric materials offer great promise for high-power laser applications. Their advantage over conventional materials lies in the flexibility that organic synthesis offers for their design. By the same approach that leads to the design of other organic compounds, especially pharmaceutical ones, organic materials with specific linear or nonlinear optical properties can now be defined, designed, and calculated in terms of response. The most important properties in this regard are absorption at certain wavelengths, nonlinear susceptibilities, fast response times, and high-power laser-damage thresholds.

The OMEGA laser is among the first to employ organic optical devices in significant numbers.[1] The majority of these devices are liquid-crystal-based, circular polarizers developed and manufactured in-house. They comprise a eutectic mixture of nematic and twisted-nematic compounds whose relative mole fraction determines the coupling to the specific laser wavelength. All polarizers operating in the OMEGA Nd:glass chain are tuned to 1053 nm. However, other mole-ratio devices have been prepared, covering small wavelength intervals across the whole visible range. One particular device of this kind is the sequential combination of two circular polarizers of opposite handedness. In combination, they act as laser blocking filters. Still other devices use mixtures free of twisted-nematic compounds. There the intrinsic birefringence of the monomeric molecules leads to retardation effects in transmitted light similar to those observed in crystalline waveplates. In preparing any devices for 5 J cm^{-2}/1-ns applications, the question arises whether an improved laser-damage threshold can be engineered in an acceptable tradeoff with other parameters by changing the eutectic's composition. After elimination of compounds because of unsuitable linear absorption properties, the choice is between highly conjugated and more saturated compounds.

There are predictions that the nonlinear optical susceptibilities of organic systems are affected by the degree of π-electron conjugation. For $\chi^{(2)}$, ample experimental evidence[2] supports this contention. For $\chi^{(3)}$, fewer data exist. Because $\chi^{(3)}$ affects self-focusing, and because in the absence of extrinsic impurities self-focusing is a dominant mechanism for laser damage in many transparent materials, we tested the extent to which the damage threshold in some organic materials is affected by the degree of conjugation.

EXPERIMENTS

Three model compounds were chosen for this test: two monomers and one polymer. We report first on the nematic monomers and then on the cholesteric polymer. One monomeric, π-electron-rich compound was 4-octyl-cyanobiphenyl, which is a liquid crystal with a nematic mesophase at room temperature. Its saturated counterpart, 4-octyl-cyanobicyclohexyl, was also tested.

Fully Saturated Electron System Raises 1053-nm Damage Threshold in Liquid Crystals

Damage Threshold Comparison of Two Model Compounds (800-ps pulse length, 100-μm path length, 5-mm spot size, linear polarization)

Compound	K-15	ZLI-1185
Structure	CH_3-$(CH_2)_4$- 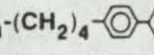 -CN	CH_3-$(CH_2)_4$- 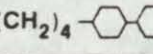 -CN
Mesophase	nematic (22°C)	nematic (62°C)
1-on-1 (J/cm^2)	9.6±2.4	>16.6*
N-on-1 (J/cm^2)	5.4±1.3	14.6±0.5

• Liquid crystals unaligned; alignment layers usually lower threshold

*for given spot size, transport optics damage at 20 J/cm^2

G2247

Fig. 1 A comparison between a highly conjugated and an equivalent highly saturated liquid-crystal system shows that the laser polarizability of the saturated system rises the near-IR laser damage threshold.

As shown in Fig. 1, the two compounds differ structurally only in their aromatic and saturated cores. The bicyclohexyl compound is commercially available under the trade name ZLI-S-1185 and has a nematic phase starting at 62°C.[3] Laser interaction tests were conducted at 1053 nm (fundamental of Nd:phosphate glass laser), where neither material exhibits any resonance. This is substantiated by the two absorption scans in Fig. 2, obtained from 1-cm-path-length cells at elevated temperatures keeping the compounds in their respective isotropic phases. The 1053-nm absorption coefficient for the biphenyl compound was 3.6×10^{-2} cm^{-1}. For the saturated compound, the residual absorption was three times larger. Absorption measurements were done in the isotropic phase to minimize the scattering contribution to the extinction.

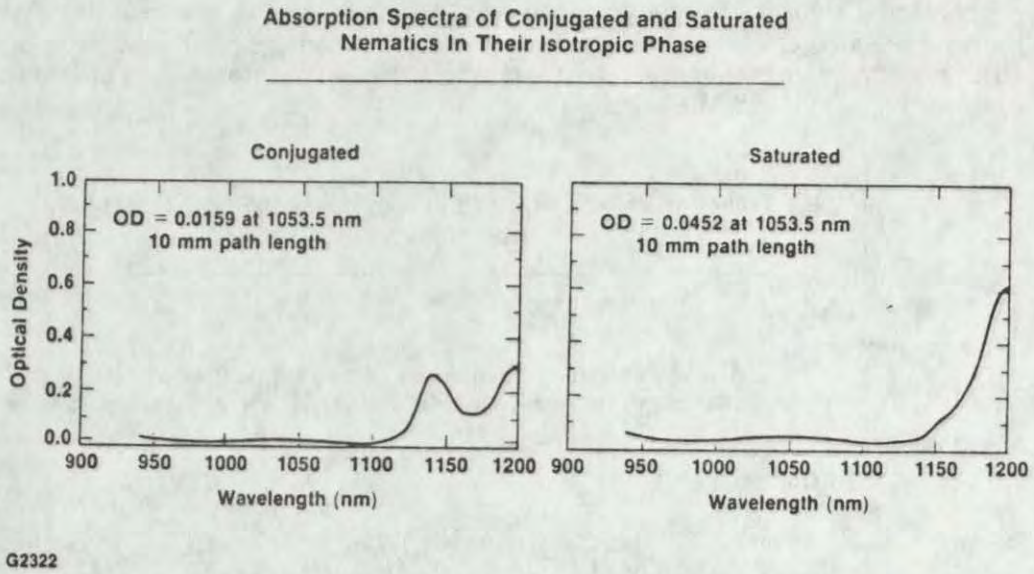

Fig. 2 The damage-test experiments were carried out at a wavelength where neither of the liquid-crystal samples exhibit any resonances. The residual linear absorption of 1053 nm of the saturated compound is higher than that of the conjugated, and yet its damage threshold is also higher.

Tests with linearly polarized incident pulses of 800-ps length were conducted identically for both monomeric materials. Unaligned cells of 100-μm path length were prepared from 30-60-90 borosilicate prisms and uncoated, fused-quartz cuvette covers and were sealed by high-temperature epoxy. (A clarification for this choice of sample geometry is published elsewhere.[4]) Cells were filled, by capillary action, with materials in their isotropic-fluid phase. Because this involves elevated temperatures, cells were not equipped with the organic alignment layers that are often used in aligning liquid crystals in either homeotropic or homogeneous configurations. It is also important to note that to date we have not found an alignment material that by itself shows a damage threshold in excess of the ones reported here

for liquid crystals. What is frequently measured in tests of liquid-crystal/alignment-layer systems is therefore not the damage threshold of the liquid crystal but that of the alignment layer. A project currently under way aims at sorting out the alignment materials with the highest damage threshold.

Irradiation by high-peak-power laser pulses occurred at normal incidence. The beam was weakly focused to a spot size of about 3 mm. Laser-induced sample changes that in liquid crystals usually appear as small bubbles can be observed with a long-working-distance microscope. The detectability of bubbles was limited by the lifetime of bubbles that redissolve into the liquid matrix. One-on-1 and N-on-1 irradiation modes were chosen. In N-on-1 testing, each separate sample site was irradiated by series of ten pulses each (8% pulse-to-pulse energy stability) of slowly increasing fluence levels. In that mode, occurrence of damage was checked after each shot. After the appearance of a bubble, irradiation was terminated even if that bubble happened to redissolve. In N-on-1 testing, the interval between pulses was 5 s. A record of peak fluence and its location within the beam was obtained for each shot.

RESULTS

Results for the monomeric materials are listed in Fig. 1. For both the aromatic and saturated compounds, the N-on-1 threshold is lower than the 1-on-1 threshold. This is in general agreement with many other monomeric liquid-crystal compounds tested earlier. However, in both 1-on-1 and N-on-1 results, a significant difference is apparent between the π–electron-rich and the fully saturated nematic. In fact, the beam transport optics for this experiment suffered damage of its own before any site of the saturated compound showed single-shot bubble formation. The corresponding fluence level is twice that of the single-shot threshold average for the aromatic compound. The N-on-1 threshold comparison shows an improvement over the aromatic compound by nearly a factor of 3.

To eliminate from consideration that impurities may cause these threshold differences, we analyzed sample stock by gas chromatography. At the 1-part-in-10^5 sensitivity level, no extraneous signals were observed from either compound. The only unusual feature was an isomer signature from the bicyclohexyl material. Within the stated sensitivity limit, impurities must be ruled out as a damage-dominating mechanism. Similarly, the opposing trends of damage thresholds and linear-absorption coefficients between the two nematics make linear absorption an unlikely damage mechanism.

The polymeric material was tested in a different approach. Here, the π-electron-rich phenyl functional group, one of several of the polymer's functional groups, was simply removed in the preparation of the control-sample polymer. The liquid-crystal polymer comprised a polysiloxane backbone with lateral, mesogenic side groups. The structure of the repeat unit is shown below:

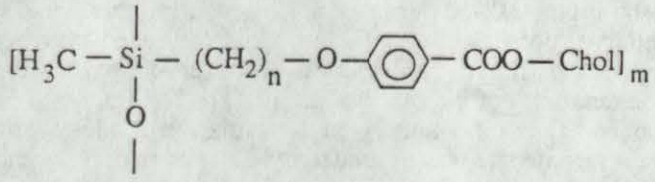

Chol stands here for cholesterol; *m* is usually 4 or 5. The cholesterol functional group with its alkyl tail introduces chirality into the polymer, offering interesting optical properties. Among them is the coupling between the molecular helix and the proper-handed, circularly polarized light of a wavelength λ that matches the pitch of the helix. By varying the pitch of the chiral structure, tuned optical devices can be prepared.[5] One method for varying the pitch of a chiral nematic polymer is to prepare a variable-weight copolymer of the design

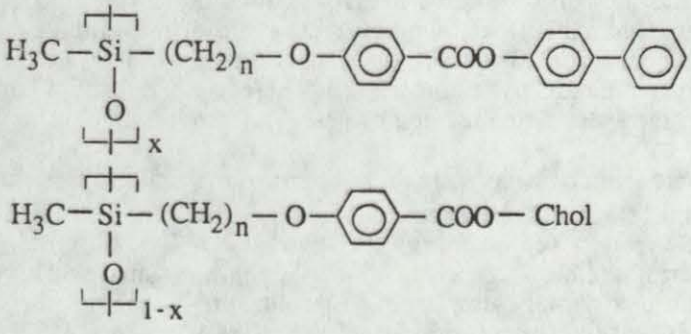

in which the density x of interleaved copolymer pendants determines the degree of pitch dilation along the backbone direction. By virtue of the π-electron distribution in the copolymer, changing this density means increasing or decreasing the nonlinear optical susceptibility of the total system in accordance with copolymer content. Testing the damage threshold of chiral copolymer samples tuned to different (nonresonant with regard to the 1053-nm incident wavelength) wavelengths provides further corroboration for the postulated link between $\chi^{(3)}$ and the degree of conjugation.

Damage-test samples of the copolymer were prepared by dissolving the material in toluene and spraying about 100-μm-thick films onto carefully cleaned, 30-60-90 borosilicate glass prism surfaces. Film thicknesses were uniform to better than 10% across individual samples but varied by up to 20% from sample to sample. The three copolymers reported here had cholesteric weight percents of 14%, 21%, and 35%, corresponding to tuned-response peak wavelengths of 1170 nm, 760 nm, and 450 nm, respectively. In 1-on-1 tests conducted in the same way as for monomeric materials, an important trend emerged: the copolymer with the highest cholesterol content--i.e., that with the lowest volume density of conjugation--showed the highest damage threshold; the one with the lowest cholesterol content and therefore the highest volume density of conjugation showed the lowest threshold. This trend is evident in Table 1.

TABLE 1

Damage Thresholds of Cholesteric Copolymers

Weight % Cholesteric	Peak Wavelength (nm)	Film Thickness (μm)	1-on-1 Threshold (J/cm^2)	N-on-1 Threshold (J/cm^2)
14	1170	108	0.8 ± 0.1	<0.8
21	760	104	2.4 ± 0.3	0.8
35	450	83	5.1 ± 1.2	<0.8
Smectic-C	not applicable	105	5.8 ± 0.3	13.8 ± 3.0

Catalysts used in the synthesis of these polymers were thought to affect these thresholds through platinum trace residues. Platinum inclusions in laser glass have been widely acknowledged as prime damage-inducing impurities.[6] However, tests with especially purified copolymer samples yielded only marginally higher damage thresholds than those listed in Table 1. We surmise that the role of impurities in the IR laser damage of these materials is as insignificant as in the monomeric compounds. The damage morphology in polymers differed from monomers in that no bubbles were observed. Damage was monitored at the same spatial resolution as in the case of bubbles, except that here permanent structural modifications in the form of microscopic pits were recorded.

Finally, a cholesteric polymer was prepared that totally lacked the copolymer pendants used in the previous examples for wavelength tuning. It also lacked the phenol group in the cholesteric pendant. Except for one conjugated bond on the cholesterol itself, this system was entirely π-electron free. These reductions affected not only the laser damage threshold but other physical properties as well. The polymer glass transition temperature, affecting the material's processability, was raised and its mesogenic phase behavior changed. The chiral

nematic room-temperature phase changed to smectic-C. Again, special efforts were made to keep this compound platinum-free. The platinum content was verified to be <1 ppm. When films of this material were prepared from a toluene solution in the same manner as for previous polymer samples, laser-damage thresholds could be measured. The 1054-nm, 1-on-1 threshold was 5.8±0.3 J/cm^2, a 10% improvement over the best copolymer mentioned earlier. A more dramatic improvement was observed for the N-on-1 threshold. Whereas the π-electron-rich copolymers exhibited a common, precipitous threshold drop with large scatter in data to about 0.8 J/cm^2 when tested in the N-on-1 mode, the smectic-C sample showed a significant rise in threshold to 13.8±3.0 J/cm^2. To date, we have no compelling explanation for these diverging trends. These measured thresholds compare well with the ones obtained for traditional, dielectric thin films.[7]

SUMMARY

To summarize, we conclude that, once impurities have been removed as a major cause of damage in organic optical materials, the volume density of conjugation in a compound becomes the dominant laser-damage factor. Because of this link, a reformulation of liquid-crystal polarizer compositions has dramatically enhanced the damage resistance of liquid-crystal optical elements used in the OMEGA laser. The guiding principle here is to substitute, wherever possible, highly saturated compounds for conjugated ones. One trade-off in this case is a drop in birefringence associated with the loss in π-conjugation, a trade-off easy to accommodate. The same principle will also help make other liquid-crystal devices high-power compatible, such as soft apertures,[8] cholesteric laser end mirrors,[9] or active devices, such as shutters and modulators.[10]

ACKNOWLEDGMENT

Dr. F. Kreuzer of Consortium fur Elektrochemische Industrie, Munich, West Germany, kindly provided the polymeric sample materials and their analytical characterization. He also offered valuable advice.

This work was supported by the U.S. Department of Energy Office of Inertial Fusion under agreement No. DE-FC08-85DP40200 and by the Laser Fusion Feasibility Project at the Laboratory for Laser Energetics, which has the following sponsors: Empire State Electric Energy Research Corporation, New York State Energy Research and Development Authority, Ontario Hydro, and the University of Rochester. Such support does not imply endorsement of the content by any of the above parties.

REFERENCES

1. S. D. Jacobs, K. A. Cerqua, K. L. Marshall, A. Schmid, M. J. Guardalben, and K. J. Skerrett, SPIE Proceedings Vol. 895, 120 (1988).
2. J. F. Nicoud, Mol. Cryst. & Liq. Cryst. 156, 257 (1988); H. E. Katz et al., J. Amer. Chem. Soc. 109, 6561 (1987).
3. Materials supplied by EM Chemicals, 5 Skyline Drive, Hawthorne, NY 10532.
4. S. D. Jacobs, K. A. Cerqua, K. L. Marshall, A. Schmid, M. J. Guardalben, and K. J. Skerrett, "Liquid-Crystal Laser Optics: Design, Fabrication, and Performance," J. Opt. Soc. Amer. B, 5, 1962 (1988).
5. I. P. Il'Chisin, E. A. Tikhonov, V. G. Tishechenko, and M. T. Shpak, Sov. Phys. - JETP 32, 24 (1980).
6. D. Milam, C. W. Hatcher, and J. H. Campbell, Seventh Annual Symposium on Optical Materials for High Power Lasers, Boulder, CO, 1985, National Bureau of Standards, Special Publication (to be published).
7. T. Walker, A. Guenther, and P. Nielsen, IEEE J. Quantum Electron. QE-17, 2041 (1981).
8. LLE Review 24, 188 (1985).
9. Yu. V. Denisov, V. A. Kinzel, V. A. Orlov, and N. F. Perevozchirov, Sov. J. Quantum Electron. 10, 1447 (1980).
10. R. A. Soref, Opt. Lett. 4, 155 (1979).

Self-focusing in Polymers

D.V.G.L.N. Rao James H. Bickford

Physics Department,
University of Massachusetts at Boston

A. Shere M. Muthukumar

Department of Polymer Science,
University of Massachusetts at Amherst

Abstract

Self-focusing of light is an interesting third order nonlinear effect which results from wavefront distortion of a single mode laser beam with a gaussian transverse profile, propagating in a nonlinear medium with index of refraction $n = n_0 + n_2E^2$. n_0 is the field independent index and E is the electric field of the optical wave. The nonlinear coefficient n_2 contains both electronic as well as nuclear orientation contributions. The intensity of the optical field is a maximum along the axis of propagation and hence the field-induced index is also a maximum at the center and falls off at the edges. As a result the central part of the beam slows down relative to the edges and the incident plane wave front becomes progressively concave in the direction of propagation creating a converging lens effect. Self-focusing is often responsible for optical damage in transparent materials and hence is an important consideration in the design of laser optical systems. In highly nonlinear materials it can occur at relatively low powers. Polymeric materials are currently receiving a lot of attention in nonlinear optical experiments for possible device applications. We describe experimental investigations on what we believe to be the first direct observation of self-focusing in polymers. Interesting results are obtained in n-Hexane solutions of the polymer Poly (di-n-Hexyl silane). Our results indicate that values of the nonlinear coefficient n_2 of the polymer solutions are about the same order or better than a strongly self-focusing liquid like CS_2. Detailed experimental results and the applications of the technique as a probe for the study of polymers will be presented and discussed.

Side-Chain Stilbazolium Polyether Synthesis and Langmuir-Blodgett Film Fabrication for Optical Second Harmonic Generation

J. M. Hoover, R. A. Henry, J. W. Fischer and G. A. Lindsay
Chemistry Division, Research Department
Naval Weapons Center, China Lake, CA 93555-6001

B. L. Anderson, B. G. Higgins, P. Stroeve and S. T. Kowel
Organized Research Program on Polymeric Ultrathin Film Systems
University of California, Davis, CA 95616

ABSTRACT

Side-chain polymers comprised of hydrophilic backbones and hydrophobic pendent groups were synthesized by substitution reactions on the chloromethyl groups of poly(epichlorohydrin). The side chains were stilbazolium chromophores attached to aliphatic tails. Multilayer, noncentrosymmetric films were deposited on glass slides by Langmuir-Blodgett processing (vertical dipping). Optical absorption shifts and second harmonic generation (SHG) as a function of film thickness and geometry were observed.

INTRODUCTION

New nonlinear optical polymers (NLOP) are under development in many laboratories because they offer properties superior to traditional single crystals in both performance and processability. Device scenarios are being proposed which make use of nonlinear optical materials for eye protection against lasers. However, materials development at this point is lagging behind requirements of the device engineers.

Langmuir-Blodgett (LB) processing technology has long been known as a laboratory technique for depositing ultrathin organic films in very precise arrangements.[1] Recent reports on depositing noncentrosymmetric multilayer LB films comprised of amphiphilic chromophores, we believe, will lead to the development of new, useful nonlinear optical materials.[2-4] However, these nonpolymeric films are rather fragile. Our effort and that of others have extended this work to polymeric nonlinear optical films prepared by LB deposition which are more robust.[5-9]

Stilbazolium chromophores are attractive due to their large second-order polarizabilities. This paper will describe our recent attempts to develop NLOPs based on the stilbazolium chromophores (SZC) attached as side groups pendent to a polyether backbone, and fabricated into noncentrosymmetric films by the LB technique. Our group has synthesized SZC-substituted polyethers (SZP) with different degrees of SZC on the polymer repeat units.[5,8] The noncentrosymmetric films are formed by one of two techniques: interleaving the SZP with an inert layer (having a low dipole moment, such as a fatty acid) or by forming ABAB . . . bilayers of two different SZPs with their donor-acceptor groups in the opposite sense to each other, in both cases using Y-type deposition.[9]

Our earlier studies involved alkoxy-substituted SZCs which absorb near 395 nm.[5,8] More recently, we have prepared amine-substituted SZCs, which absorb near 485 nm, and have a 100-fold stronger SHG per monolayer.[10] Figure 1 shows the SZP we report here and a hemicyanine dye, trans-4'-dimethylamino-n-docosyl stilbazolium bromide, which has been studied extensively.[2,3,10,11]

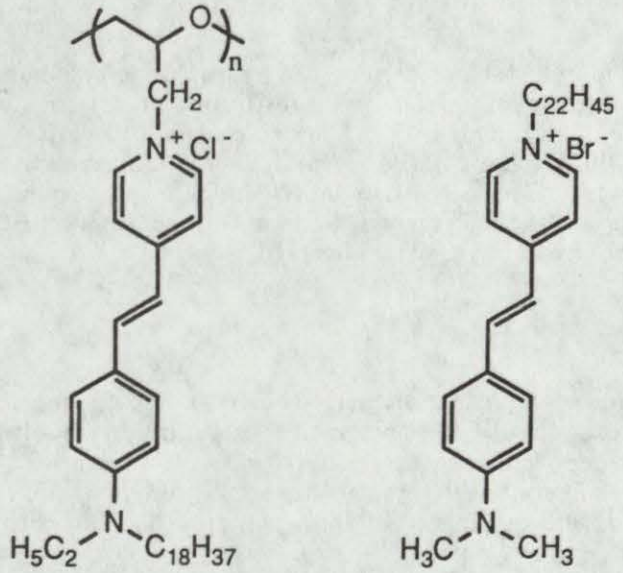

A B

Figure 1. (A) Chemical structure of stilbazolium-PECH (polyepichlorohydrin); (B) Chemical structure of the hemicyanine dye trans-4'-dimethylamino-n-docosyl stilbazolium bromide.

EXPERIMENTAL PROCEDURES

SYNTHESIS. Polyepichlorohydrin (PECH) from the 3M Company was dissolved in 4-picoline and refluxed overnight under nitrogen. Unreacted picoline was stripped under vacuum. A methanol solution of the resulting polymer was extracted with cylohexane and was shown to be about 90% substituted by proton NMR. Recrystallized 4-ethyloctadecylaminobenzaldehyde, prepared by the Vilsmeir reaction, was refluxed with a solution of the picolinium-substituted PECH in chloroform overnight. The mixture was cooled and volatiles removed under reduced pressure to yield a dark red glassy solid. This polymer was purified by preparative gel permeation chromatography. Differential scanning calorimetry and polarized optical microscopy show this polymer to be amorphous with a glass transition temperature over 150°C.

LANGMUIR-BLODGETT DEPOSITIONS. A computer-controlled, double-compartment trough made by NIMA Technology Ltd., Coventry, England, was used to deposit the LB multilayers on glass microscope slides. The SZP monolayers were deposited at 35 mN/m on the upstroke. Behenic acid layers were deposited at 27 mN/m on the down strokes. All depositions were performed at 10 mm/min.

OPTICAL MEASUREMENTS. SHG measurements were performed with a Q-switched Nd:YAG laser with a pulse duration of 10 ns and a repetition rate of 10 Hz. The laser beam was incident to the NLOP film at 60°. After filtering the p-polarized incident radiation, the intensity of the p-polarized SHG was detected in transmission with a photomultiplier detector averaged over 300 pulses. A quartz reference was used, and uncertainty in the measurement was about 15%. Reference 6 gives a schematic of the optical train. A Perkin-Elmer Lambda 4B UV-VIS spectrophotometer was used for linear absorption measurements over the range of 300 to 650 nm.

RESULTS AND DISCUSSION

OPTICAL ABSORPTION AND SHG MEASUREMENTS. As described in the Experimental Section, alternating layers of SZP and behenic acid were deposited. Surprising shifts in absorption maximum were observed as a function of the number of layers on the glass slide as shown in Figure 2. The first layer is blue-shifted by about 13 nm from the absorption of the same polymer in chloroform solution (479 vs. 492 nm). This shift may be a solvatochromic shift caused by the hydrophilic glass surface. However, the position of the absorption peak of the SZP monolayer also depends on the deposition surface pressure. As the pressure is increased from 20 to 45 mN/m, the peak blue-shifts from 485 to 474 nm. These shifts are considerably smaller than the 156-nm blue shift already reported for similar hemicyanine monolayers,[10] which was attributed to H-aggregation. Perhaps the shifts in our study are due to different interactions of the local fields imposed by the various chromophore configurations.

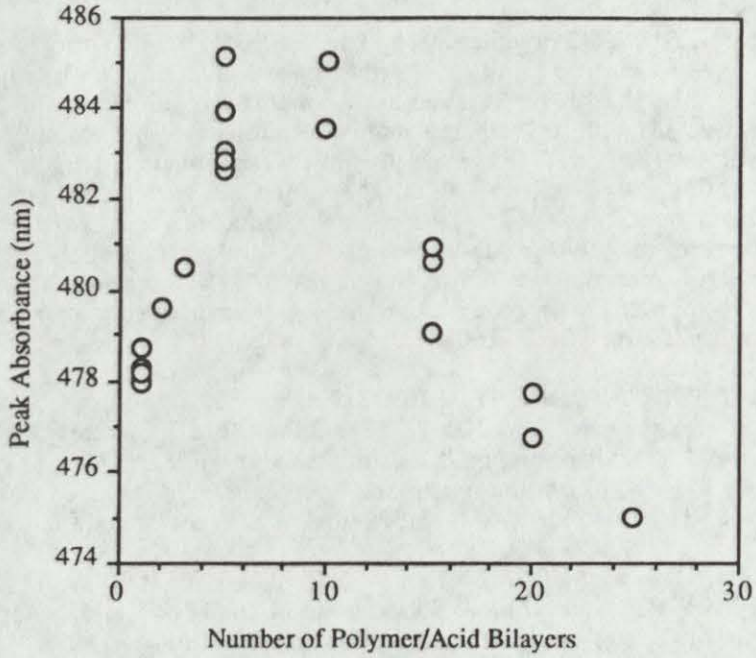

Figure 2. Variations of λ_{max} with the number of interleaved stilbazolium-PECH layers.

In multilayers, as shown in Figure 2, the absorption peak shifts to the red as the number of layers increases to about seven, then shifts to the blue again. This behavior has not yet been explained.

As one might suspect, the SHG signal for these films also depends on the deposition pressure. Since the second harmonic at 532 nm lies in the shoulder of the absorption peak, as the absorption envelope shifts one way or the other, the SHG will increase or decrease due to the variation in resonance enhancement.

The SHG for multilayers is shown in Figure 3. The increase in SHG with number of layers is roughly quadratic until the one reaches about ten layers, then it becomes more of a linear increase. In Figure 3, films with 10 dye layers or less and two of the films with 15 dye layers were interleaved with one layer of behenic acid. Films with 20 and 25 dye layers and one of the 15 dye layer films were also interleaved with one layer of behenic acid except that after each fifth dye layer, three layers of behenic acid were deposited.

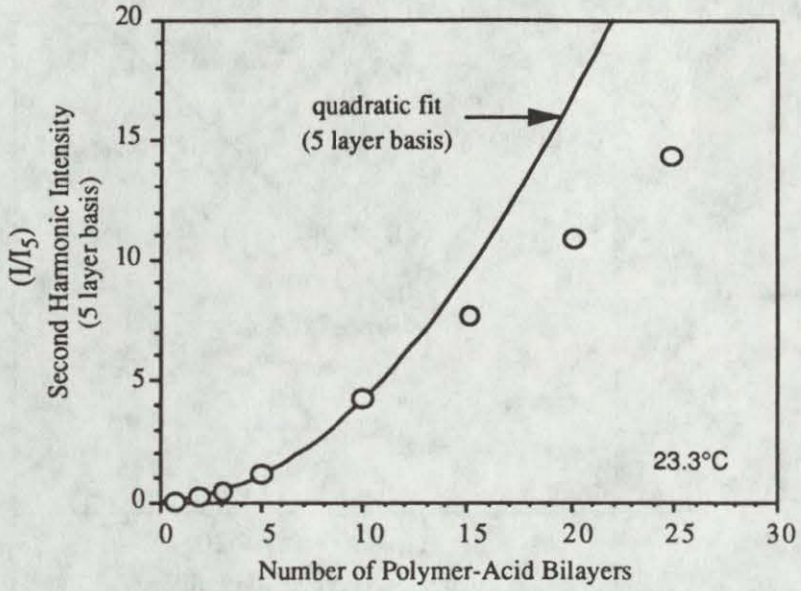

Figure 3. Data points are the normalized SHG enhancement for a multilayer LB film of stilbazolium-PECH interleaved with behenic acid. I is the measured film SHG intensity and I_5 is the intensity of the SHG from a 5-dye layer film. The dye was deposited on the upstroke at a surface pressure of 35 mN/m and the behenic acid was deposited on the downstroke at a surface pressure of 27 mN/m. -

The data points in Figure 3 were normalized with the fifth dye layer thickness as the basis. We did this because the first dye layer is thought to be unduly influenced by the substrate. The reason for the lack of quadratic behavior beyond ten dye layers is unclear, but one might speculate that they are less well ordered than the films in the first ten layers. Behenic acid is perhaps too mobile. A better choice for interleaving would be an inert polymer, such as poly(methyl methacrylate) (PMMA).

The peak absorption increased linearly, as shown in Figure 4, with the number of dye layers deposited, and the deposition ratio for SZP was 0.98 ± 0.03 and 0.92 ± 0.03 for behenic acid. This indicates that full and reproducible coverage was achieved. The deviation for the 20- and 25-layer films may indicate a less ordered stilbazolium alignment.

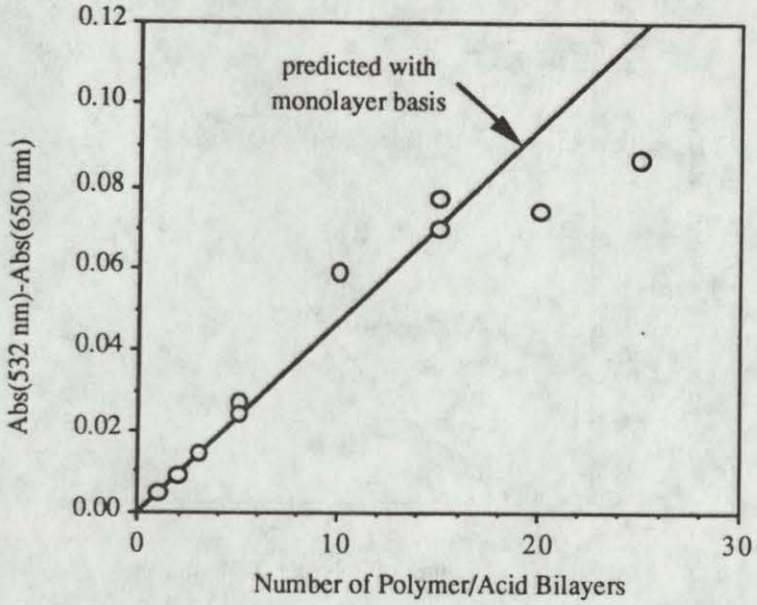

Figure 4. Absorbance at a wavelength of 532 nm, A_{532}, relative to that at 650 nm, A_{650}, as a function of the number of stilbazolium-PECH layers interleaved with behenic acid. The solid line indicates a linear increase in absorbance based on the absorbance of a dye monolayer. The error in measured absorbance is less than 5%.

By changing the number of interleaved behenic acid layers between the dye layers, one may be able to measure the effect of the local fields of one dye layer on the adjacent dye layers. Figure 5 shows the absorbance of five SZP layers interleaved with one, three, five and nine layers of behenic acid. Surprisingly, the absorbance decreased for the case of five and nine layers of interleaved behenic acid. Furthermore, the SHG also decreased as the number of interleaved behenic acid layers increased. These results are unexplained.

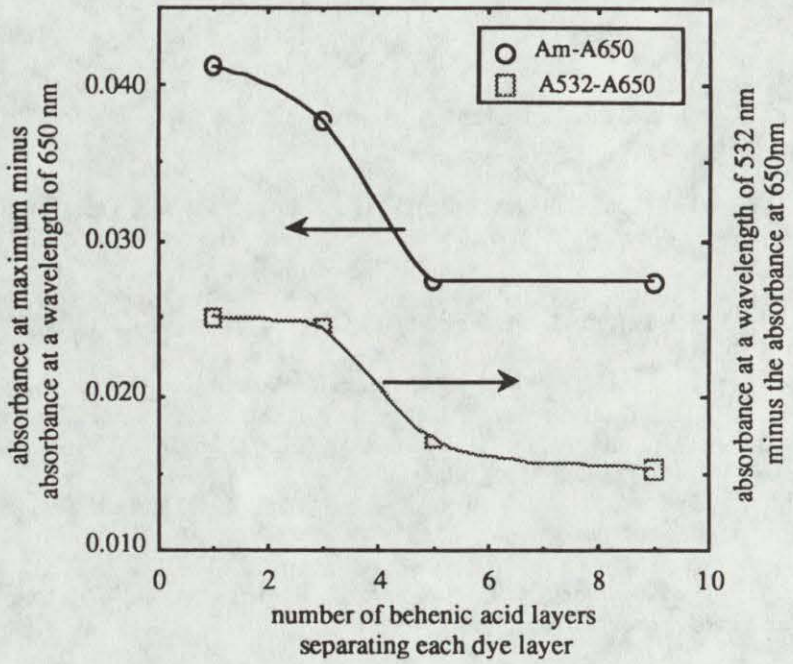

Figure 5. The effect of the number of behenic acid spacer layers on the absorbance of LB films with 5 stilbazolium-PECH layers. The top curve is the maximum absorption, A_{max}, minus the absorption at 650 nm, A_{650}. The bottom curve is the absorbance at 532 nm, A_{532}, minus that at 650 nm. The error in absorbance data is less than 5%.

ACKNOWLEDGMENTS

The synthetic work at the Naval Weapons Center was supported by the office of Naval Research, and the LB and optical work was supported in part by the National Science Foundation (CTB Division) and the Lawrence Livermore National Laboratory. We thank A. Knoesen for technical assistance with the SHG measurements.

REFERENCES

1. Gaines, G. L., Jr., "Insoluble Monolayers at Air-Water Interfaces," Interscience (New York, 1966).

2. Neal, D. B., Petty, M. C., Roberts, G. G., Admad, M. M., Feast, W. J.,Girling, I. R., Cade, N. A., Kolinsky, P. V., and Peterson, I. R., *Electron. Lett.*, **22** (1986) 460.

3. Girling, I. R., Cade, N. A., Kolinsky, P. V., Jones, R. J., Peterson, I. R., Ahmad, M. M., Neal, D. B., Petty, M. C., Roberts, G. G. and Feast, W. J., *J. Opt. Soc. Am. B*, 4:6 (1987) 950.

4. Ledoux, I., Josse, D., Fremaux, P., Piel, J.-P, Post, G., Zyss, J., McLean, T., Hann, R. A., Gordon, P. F., and Allen, S., *Thin Solid Films*, **160** (1988), 217.

5. Hall, R. C., Lindsay, G. A., Kowel, S. T., Hayden, L. M., Anderson, B. L., Higgins, B. G., Stroeve, P., and Srinivasan, M. P., *Proceedings of SPIE*, **824** (1987), 121.

6. Hayden, L. M., Anderson, B. L., Lam, J. Y. S., Higgins, B. G., Stroeve, P., Kowel, S. T., *Thin Solid Films*, **160** (1988) 379.

7. Tredgold, R. H., Young, M. C. J., Jones, R., Hodge, P., Kolinsky, P., Jones, R. J., *Electron. Lett.*, **24** (1988) 308.

8. Hall, R. C., Lindsay, G. A., Anderson, B. L., Kowel, S. T., Higgins, B. G., and Stroeve, P., *Proceedings of Materials Research Society*, **109** (1988) 351.

9. Anderson, B. L., Hall, R. C., Higgins, B. G., Lindsay, G. A., Stroeve, P., and Kowel, S. T., *Synthetic Metals*, **28** (1989) D683.

10. Schildkraut, J. S., Penner, T. L., Willand, C. S., Ulman, A., *Optics Letters*, **13**:2 (1988) 134.

11. Neal, D. B., Kalita, N., Pearson, C., Petty, M. C., Lloyd, J. P., and Roberts, G. G., *Synthetic Metals*, **29** (1988) D711.

Corona-Onset Poling of New Side-Chain Polymers for Optical Second Harmonic Generation

J. M. Hoover, R. A. Henry, and G. A. Lindsay
Chemistry Division, Research Department
Naval Weapons Center, China Lake, CA 93555-6001

M. A. Mortazavi, A. Knoesen and S. T. Kowel
Organized Research Program on Polymeric Ultrathin Film Systems
University of California, Davis, CA 95616

L. M. Hayden
Unisys Corp. MS U1L14
St. Paul, MN 55164-0525

ABSTRACT

Polymer-bound dyes have proven to be superior to guest-host polymer-dye mixtures as materials for optical second harmonic generation (SHG) in terms of long-term retention of nonlinearity. New comb-shaped polymers were prepared, comprised of a variety of side chains, such as azo, azomethine, and coumarin; and a variety of main chains, such as, poly(methyl methacrylate), poly(styrene), and poly(t-butyl styrene). The glass transition temperatures (T_g) of the purified copolymers ranged from 80 to 130°C. Above the T_g, thin films were exposed to a strong electric field at the onset of corona discharge in air, and then cooled to room temperature under the electric field. In the absence of an applied electric field, at room temperature, the second order nonlinear optical properties (NLOP) of these films are quite stable with time.

INTRODUCTION

The fast optical response time (femtoseconds), the ease of processability, the ruggedness, and the high nonlinearity of polymeric chromophores make them attractive candidates for eye protection devices. Our ultimate goal is to fabricate a shield which would generate and filter out the second harmonic of a visible laser pulse, thereby limiting the power of transmitted light. This paper reviews our first attempts to synthesize NLOPs by electric-field poling, and to

measure their ability to double the frequency of a Nd:YAG laser.[1,2] We are also preparing NLOP by Langmuir-Blodgett (LB) processing techniques.[3]

EXPERIMENTAL PROCEDURES

Polymer-dye compositions were synthesized by copolymerizing monomeric new chromophores with conventional vinyl monomers, and by attaching chromophores to preformed polymer backbones. The former case is limited to monomers that will not interfere with the polymer propagation mechanism.

We found that coumaromethacrylate (CMA) monomers, shown in Figure 1, copolymerize by free radical initiation with methyl methacrylate (MMA) and t-butyl styrene (TBS) monomers to yield high molecular weight copolymers. Other chromophores, shown in Figure 2, were chemically attached to a preformed copolymer of styrene and acrylic acid (PSAA), Joncryl 67, obtained from Johnson Wax Specialty Chemicals, Racine, WI. The dye-substituted polymers were purified by preparative gel chromatography to remove unreacted monomers and chromophores. Synthesis of the chromophores will be published elsewhere.

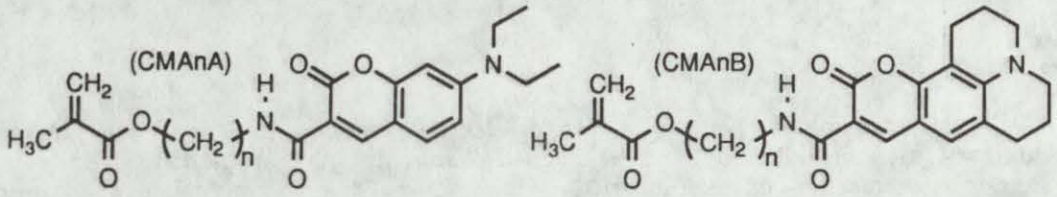

Figure 1. Coumaromethacrylate (CMA) monomers (where n = 2, 3, or 5).

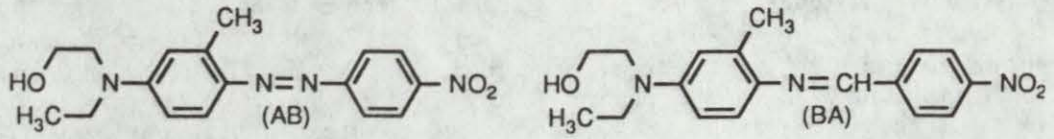

Figure 2. Azobenzene (AB) and benzylidene aniline (BA) chromophores.

Polymers were characterized by differential scanning calorimetry (DCS), proton nuclear magnetic resonance (NMR) spectroscopy, and ultraviolet-visible (UV-VIS) spectroscopy. Films of these polymers were deposited on glass slides by spin-coating or dip-coating techniques.

The pendent chromophores were oriented by corona-onset poling of the films at temperatures above the glass-rubber transition. The glass slide, polymer side up, was placed on an horizontal cathode (an aluminum plate), which in turn rested on a hot plate. The anode, a thin tungsten wire, was placed about one

centimeter above the film. About 5000 volts potential was required to establish onset of corona discharge (3 mAmps). Higher currents damage the films. Other details of the poling apparatus are described elsewhere.[1,2] Films were cooled after about 5 minutes of poling. For best results, the electric field was maintained across the films, even after cooling to room temperature for an hour or more, while the films continued to consolidate (short-term enthalpy relaxation).

Second harmonic measurements (SHG) were made in transmission with a pulsed ND:YAG laser incident to the films at about 60°. Signals generated by the NLOP were compared to a quartz reference. More details are given elsewhere.[1,2]

RESULTS AND DISCUSSION

Table 1 compares all of the NLOP of this study. The number of chromophores per cubic centimeter, N, was calculated from the mole fraction of chromophores (measured by NMR) and the specific gravity of the polymer. The second harmonic coefficient, d33 in picometers/volt, is the figure of merit used to compare the nonlinearity of these polymers.[1] These new chromophores are all promising candidates for optical devices. The poling temperatures and times have not yet been optimized.

Table 1. Characteristics of Dye Substituted Copolymers.

Sample	Backbone	Dye Type	$N/10^{20}$	T_g (°C)	d_{33} (pm/V)	λ_{max}
1220-22	PSAA	(none)	0	91	---	---
1220-25a	PSAA	BA	6.2	78	17	466
1220-25b	PSAA	AB	8.2	80	30	466
1220-26	PSAA	AB	9.2	84	41	486
1220-30	PMMA	CMA2A	9.8	116	~19	419
1220-37	PMMA	CMA2B	6.5	112	~19	435
1220-32	PMMA	CMA5A	7.7	92	~19	419
1220-29	PTBS	CMA2A	7.6	132	~19	419
1220-31	PTBS	CMA5A	6.1	100	~19	419

The dipole moment of the pendent dyes is roughly parallel with the geometric long axis of the chromophores. The chromophores take on an average alignment normal to the surface of the film, characterized by the angle, θ. An order parameter, ϕ, defined as [1 - (Ap/Ao)], where Ap is the absorption perpendicular to a poled film and Ao is absorption of an unpoled film, has been shown to be directly proportional to the birefringence induced by poling the dipoles.[1]

Figure 3 shows typical absorption spectra for a coumaromethacrylate-MMA copolymer.

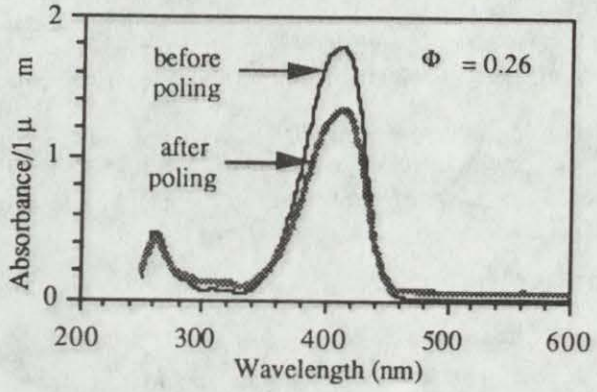

Figure 3. UV/Vis spectra of PMMA-PCMA.

Figure 4 shows the normalized SHG signal of a NLOP as the film is heated again from room temperature. The second harmonic signal is a sensitive measure of the average orientation of the chromophores. At a temperature about 40°C below the T_g, the chromophores relax noticeably in 30 minutes. Complete relaxation occurs in 30 minutes when the temperature is 40°C above the T_g. The relaxation of polymer-bound chromophores is much slower than that observed for guest-host systems in which the chromophore is dissolved in (but not chemically attached to) the polymer as other researchers have already reported.[4,5]

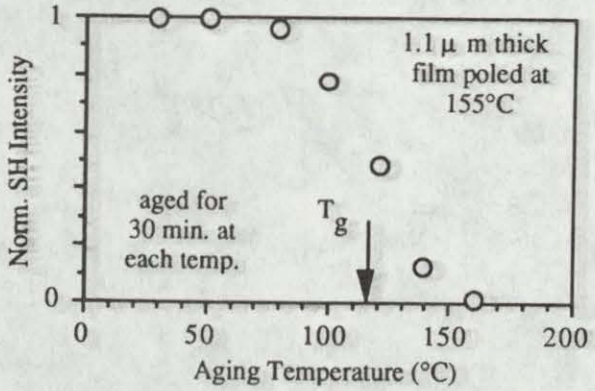

Figure 4. Aging of poled PMMA-PCMA film.

REFERENCES

1. Mortazavi, M. A., Knoesen, A., Kowel, S. T., Higgins, B. G., and Dienes, A. J. *Opt. Soc. of America*, **B 6**(4) (1989), 733.

2. Ore, F. R., Jr., Hayden, L. M., Sauter, G. F., Pasillas, P. L., Hoover, J. M., Henry, R. A., and Lindsay, G. A., *SPIE Symposium Proceedings: Nonlinear Optical Properties of Organic Materials II* (to be published, 1989).

3. Anderson, B. L., Hall, R. C., Higgins, B. G., Lindsay, G. A., Stroeve, P., and Kowel, S. T., *Synthetic Metals*, **28** (1989), D683.

4. Singer, K. D., Kuzyk, M. G., Holland, W. R., Sohn, J. E., and Lalama, S. J., *Applied Physics Letters*, **53** (1988), 1800.

5. Hubbard, M. A., Marks, T. J., Yang, J., and Wong, G. K., *Chemistry of Materials*, **1**(2) (1989), 167.

MOLECULAR DESIGN OF POLYMERIC LIQUID CRYSTALS WITH LARGE OPTICAL X^2S

Rolfe G. Petschek
Department of Physics
Case Western Reserve University
Cleveland, OH 44106-2624

ABSTRACT

Most monomeric and polymeric liquid crystals contain conjugated rings which are expected to have large non-linear optical polarizabilities. However all known non-chiral liquid crystalline phases have symmetries which are inconsistent with non-zero X^2's. All known chiral liquid crystalline phases have symmetries consistent with non-zero X^2's. These, however, are generally very small, presumably because there is relatively little coupling between the chiral group and the optically important group. The design of materials with large X^2's can therefore follow three distinct paths: design of non-chiral materials which will have phases consistent with X^2, design of chiral materials which have significant coupling of the chiral nature of the material to the optical properties, and design of materials which are easily polarizable into and frozen into phases with non-zero X^2. Each of these possibilities will be discussed.

A variety of main chain or side chain polymeric liquid crystal structures which are expected to form phases consisting of three different layers[1] which then lack inversion symmetry around the layer normal or long axis of the rod are discussed. The synthetic and physical issues in forming these phases are discussed. The nature of possible non-linear optical susceptibilities in known chiral liquid crystalline phases is discussed and structures which might result in large X^2's for nematic and tilted chiral smectics are discussed. Finally a polymeric structure which is expected to have a large dielectric susceptibility along the layer normal in smectic phases is discussed.

1) Petscheck, R. G. and R. M. Wiefling, Novel Ferroelectric Fluids, Phys. Rev. Lett. 59, 343 (1987).

POLY(ORGANOPHOSPHAZENES) FOR NLO APPLICATIONS

R.A. Willingham, M.S. Sennett, and R.E. Singler
Polymer Research Branch, SLCMT-EMP
U.S. Army Materials Technology Laboratory
Watertown, MA 02172-0001

ABSTRACT

The use of polymers as materials for nonlinear optical (NLO) applications is gaining increasing attention, because of the ability to tailor molecular structures which have inherently fast response times and large second and third order molecular susceptibilities. Polymers provide synthetic and processing options that are not available with other classes of NLO materials, as well as excellent mechanical properties, environmental resistance, and high laser damage thresholds.

In the design and synthesis of NLO materials, liquid crystalline polymers offer some advantages over other polymer types. Side chain liquid crystalline polymers are of particular interest due to the ease of synthesis and processing of these materials relative to main-chain liquid crystalline polymers.

Polyphosphazene chemistry represents an excellent opportunity to vary molecular weight, molecular weight distribution and side chain substituents in a single polymer system. Synthetic procedures will be presented which illustrate the wide variety of organic substituents which can be attached to a common phosphorus-nitrogen backbone, resulting in polymers with a range of properties. We have demonstrated that thermotropic liquid crystalline side chain polyphosphazenes can be prepared. Synthetic methods will be discussed which may lead to new polyphosphazenes with potential for NLO applications, such as high speed switching, sensors, and eye protection against low-power lasers.

BIOGRAPHY: Reginald A. Willingham, PhD.
PRESENT ASSIGNMENT: Research Chemist, U.S. Army Materials Technology Laboratory.
PAST EXPERIENCE: Senior Research Chemist, Dow Chemical Company, Freeport, Texas, 1982-84.

DEGREES HELD: Bachelor of Arts, Morehouse College, Atlanta, GA, 1975. Master of Arts, Harvard University, Cambridge, MA, 1977. PhD., Texas A&M University, College Station, TX, 1983.

POLY(ORGANOPHOSPHAZENES) FOR NLO APPLICATIONS

R. A. Willingham, Dr., M. S. Sennett, Dr., and R. E. Singler, Dr.
Polymer Research Branch, SLCMT-EMP
U.S. Army Materials Technology Laboratory
Watertown, MA 02172-0001

INTRODUCTION

The use of polymers as materials for Nonlinear Optical (NLO) applications is gaining increasing attention because of the ability to tailor molecular structures which have inherently fast response times and provide second- and third-order molecular susceptibilities. Polymers provide synthetic and processing options that are not available with other classes of NLO materials, as well as excellent mechanical properties, environmental resistance, and high laser damage thresholds (1).

In the design and synthesis of NLO materials, liquid crystalline polymers offer some advantages over other polymer types. Side-chain liquid crystalline polymers are of particular interest due to the ease of synthesis and processing of these materials relative to main-chain liquid crystalline polymers.

Phosphazene chemistry offers a new approach to the development of NLO materials and represents an excellent opportunity to vary molecular weight, molecular weight distribution, and side-chain substituents in a single polymer system. Phosphazene polymers are inorganic polymers with a phosphorus-nitrogen backbone and, thus, are unique when compared to other common polymer systems which have carbon, oxygen, nitrogen, or sometimes silicon in the backbone. However, phosphazene elastomers have been available in commercial form for several years. In addition, other phosphazene polymers are being developed for various uses, including fibers, membranes, conducting polymers, and drug-release agents. More recently, thermotropic, liquid crystalline polyphosphazenes have been reported (2,3).

SYNTHESIS

Figure 1 shows the general reaction scheme for the preparation of polyphosphazenes. We have a two-step process; first, a ring-opening polymerization to give poly(dichlorophosphazene) which is an inorganic macromolecule. The next step involves substitution reactions to prepare a series of hydrolytically stable poly(organophosphazenes). This is an excellent example of the inorganic macromolecule concept; prepare a reactive polymer and modify it to produce polymers of interest (4,5). Thus, from one polymer, a potentially endless variety of different polymers can be prepared.

Both the phosphazene polymerization process and the substitution reaction chemistry are important steps in the final determination of polymer properties. Most work to date has been centered on the uncatalyzed ring-opening polymerization which produces a high molecular weight poly(dichlorophosphazene). Various catalyst systems have been developed which increase the rate and yield in the polymerization process, but generally this is at the expense of lowering the molecular weight. We have recently demonstrated (6), however, that under certain conditions, one can control the molecular weight and molecular weight distribution of poly(dichlorophosphazenes) in a catalyzed process to give a range of molecular weights. Thus, it is possible to even further define the ultimate properties of polymers of interest.

LIQUID CRYSTALLINE POLYMERS

More recent work at MTL has focused on the synthesis and characterization of side-chain liquid crystalline polyphosphazenes (2). Liquid crystalline polymers can be prepared in a variety of ways. The concept of coupling a mesogenic group with a flexible spacer to a polymeric substrate to prepare side-chain liquid crystalline polymers has been demonstrated by Finkelmann and other workers (7). Our approach has been to attach low molecular weight mesogenic molecules to the phosphazene (PN) backbone via a flexible spacer group (Figure 2). The mesogenic molecules that are not liquid crystalline are able to induce mesomorphic behavior when attached to a suitable substrate. As noted above, phosphazenes offer a potential advantage in that a variety of different substituents can be attached to a common substrate to yield a wide range of materials with different properties.

Shown in Figure 2 is an example of a phosphazene copolymer. Small molecule nucleophiles (R) are substituted on the main chain to ensure complete chlorine displacement. The preparation of phosphazene homopolymers with only the flexible spacer/rigid rod groups has also been accomplished (3,8).

Some examples of phosphazene copolymers and homopolymers are shown in Figure 3. Polymers prepared show thermotropic liquid crystalline behavior. Mesogens include para-substituted phenylazophenols and para-cyanobiphenol. Both two-carbon and six-carbon spacer compounds have been prepared. Polymers have been studied by differential scanning calorimetry (DSC), optical microscopy, and, in two cases, X-ray diffraction. The nature of the mesophase(s), mesophase temperature range, and isotropization point are dependent on the spacer length and type of mesogen. Polymers are both film- and fiber-forming materials and are soluble in common solvents.

MOLECULAR MODELING

In addition to polymer synthesis and characterization, we have recently begun to evaluate the potential of computer-aided molecular modeling as a tool for designing new liquid crystalline polymers and NLO materials based on phosphazene chemistry. The molecular modeling system predicts the optimal conformation of molecules and can calculate intrinsic electronic properties, such as polarizability and dipole moment. Preliminary results show a correlation between experimental structure data from one of our polymers and the conformation predicted by the modeling program. An example is provided in Figure 4. We anticipate that modeling of the polymers and chromophores will provide insight as to how the NLO response of these materials can be optimized.

CONCLUSION

Although we have only begun to explore the potential of polyphosphazenes as NLO materials, we believe the versatility in the chemistry and the unique phosphorus-nitrogen polymer backbone make this an attractive system for consideration. We plan to prepare sufficient quantities of selected side-chain LC polyphosphazenes and other polyphosphazenes with NLO active chromophores for evaluation in device applications.

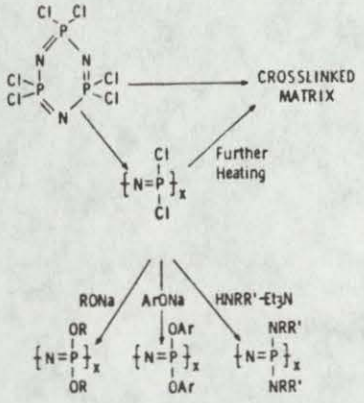

Figure 1. Polyphosphazene Synthesis

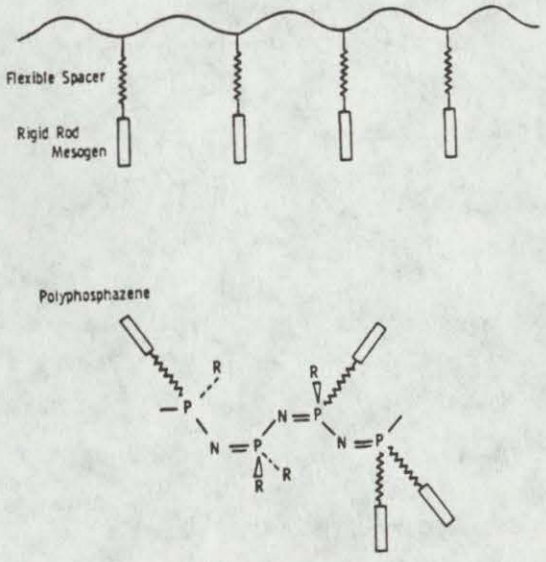

Figure 2. Liquid Crystalline Side-Chain Polymers

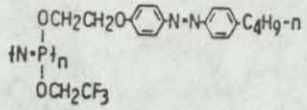

$\frac{\text{Mesogen}}{\text{Alkoxide}} \sim \frac{1.3}{0.7}$

ISOTROPIC STATE ABOVE 175°C

MESOPHASE BETWEEN 123°C AND 175°C

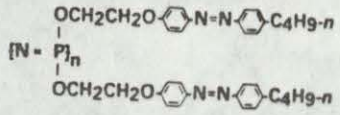

ISOTROPIC STATE ABOVE 171°C

MESOPHASE BETWEEN 144°C AND 171°C

FOCAL CONIC FAN TEXTURE - SMECTIC PHASE

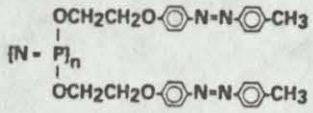

ISOTROPIC STATE ABOVE 135°C

MESOPHASE BETWEEN 114°C AND 135°C

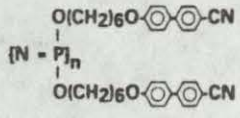

ISOTROPIC STATE ABOVE 110°C

MESOPHASE BETWEEN 58°C AND 110°C

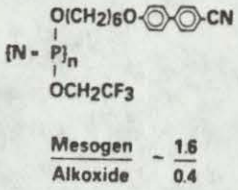

$\frac{\text{Mesogen}}{\text{Alkoxide}} \sim \frac{1.6}{0.4}$

ISOTROPIC STATE ABOVE 92°C

MESOPHASE BETWEEN 57°C AND 92°C

Figure 3. Liquid Crystalline Polyphosphazenes

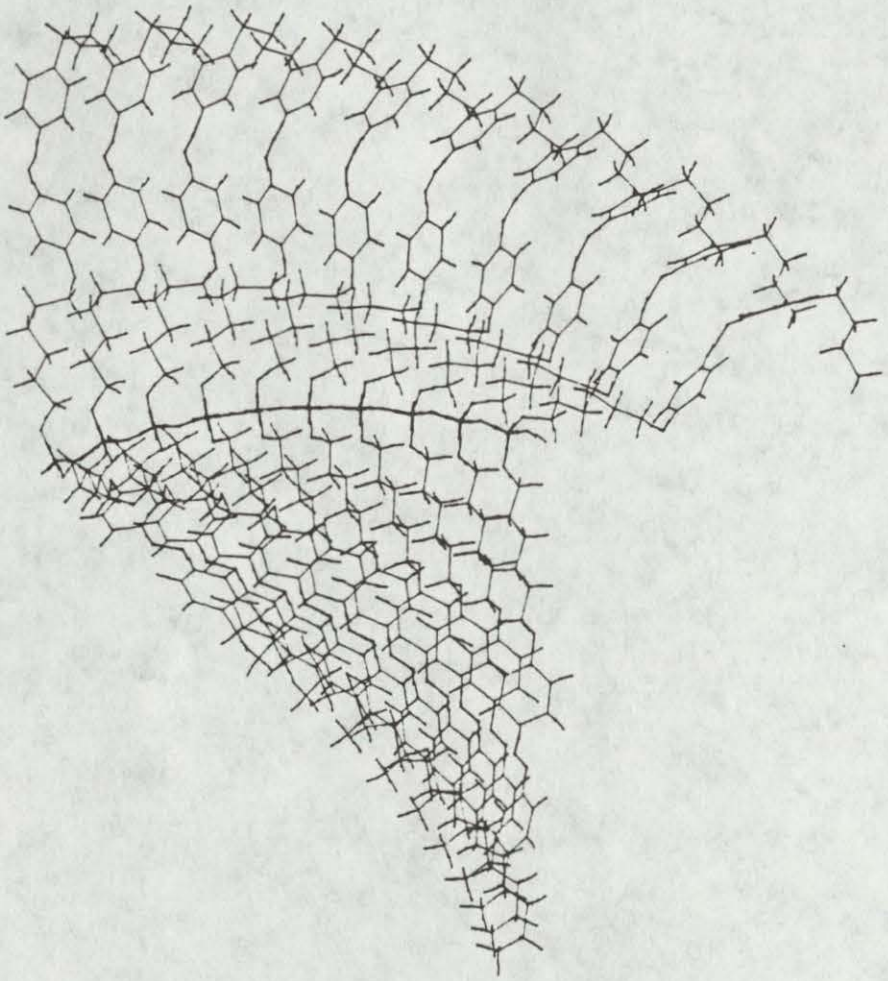

Figure 4. Computer-Generated Representation of a Liquid Crystalline Polyphosphazene with a n-Butylphenylazophenoxy mesogen.

REFERENCES

1. Ulrich, D. R.; Mol. Cryst. Liq. Cryst. 1988, 160, 1.

2. Singler, R. E.; Willingham, R. A.; Lenz, R. W.; Furukawa, A.; Finkelmann, H. Macromolecules 1987, 20, 1727.

3. Allcock, H.R. and Kim, C. Macromolecules 1987, 20, 1726.

4. Singler, R.E.; Hagnauer, G.L.; Schneider, N.S. Polym. Eng. Sci. 1975, 15, 321.

5. Allcock, H.R., "Inorganic Macromolecules" Chem. & Eng. News. March 18, 1985, p 22-36 .

6. Singler, R.E.; Sennett, M.S.; Willingham, R.A. In Inorganic and Organometallic Polymers; Zeldin, M. Ed.; Wynne, K.J.; Allcock, H.R. ACS Symposium Series, No. 360. American Chemical Society, Washington, D.C. 1988, p 268.

7. Finkelmann, H. In Polymer Liquid Crystals; Ciferri, A.; Krigbaum, W.R.; Meyer, R.B., Eds.; Academic Press, New York, 1982, Chapter 2.

8. Singler, R.E.; Willingham, R.A.; Noel, C.; Friedrich, C.; Bosio, L.; Atkins, E.D.T.; Lenz, R.W. Polym. Prepr. (Amer. Chem. Soc. Div. Polym. Chem.) 1989, 30(2), in press.

TITLE: **Polydiacetylene "Alloys": Experiments Directed Toward Nonlinear Waveguiding in Langmuir-Blodgett Multilayer Films**

*Robert E. Schwerzel, Dr., Kevin B. Spahr, John P. Kurmer, Dr., and Keith A. Ramsey
Battelle, 505 King Avenue, Columbus, OH 43201-2693

ABSTRACT: The polydiacetylenes have received much attention in recent years because of their large non-resonant third-order nonlinear optical response and because of the flexibility they offer in designing tailored molecular structures for specific applications. However, the fabrication of these materials into device-quality thin films has proven to be difficult, largely because of their propensity for forming highly scattering polycrystalline solids (with the exception of the few soluble polydiacetylenes, such as BCMU, which can be spin-coated by conventional techniques, albeit in the less-active yellow form of the polymer).

We have addressed this problem by developing a family of polydiacetylene "alloys": polymers derived from mixtures of similar diacetylene monomers having identical positioning of the diacetylene unit within the hydrocarbon chain, but with different "head" groups that provide varying degrees of affinity to water. The rationale here has been to design mixtures that would form a uniform, quasi-amorphous monolayer on the water surface in Langmuir-Blodgett multilayer fabrication, and thus avoid the scattering losses associated with grain boundaries that form within the monolayer on the water surface. To date, multilayer films up to 0.4 um thick have been fabricated by this approach, and photolithographic techniques have been developed for patterning strips down to 4 um wide in the films, without converting the blue form of the polydiacetylene to the red form in the process. Moreover, high quality films of polydiacetylene have been deposited successfully onto curved surfaces, such as polycarbonate lens blanks, using these compositions.

BIOGRAPHY OF PRESENTER: Dr. Robert E. Schwerzel
PRESENT ASSIGNMENT: Senior Research Scientist, Battelle, 505 King Avenue, Columbus, OH 43201-2693
PAST EXPERIENCE: Dr. Schwerzel has over 15 years of experience at Battelle, and has directed Battelle's research efforts in organic photochemistry and in nonlinear optical materials during that time. He is also a co-inventor of Laser-EXAFS spectroscopy, which received an IR-100 Award. Prior to joining Battelle, Dr. Schwerzel was with Syva Research Institute in Palo Alto, CA (1972-73). He conducted postdoctoral research in magnetic resonance spectroscopy at Brown University (1971-72) and in photochemistry at Cornell University (1970-71).
DEGREES HELD: B.S. (Chemistry), Virginia Polytechnic Inst., 1965
Ph.D. (Phys. Org. Chem.), Florida State Univ., 1970

Polydiacetylene "Alloys": Experiments Directed Toward Nonlinear Waveguiding in Langmuir-Blodgett Multilayer Films

*Robert E. Schwerzel, Dr.
Kevin B. Spahr
John P. Kurmer, Dr.
Keith A. Ramsey
Battelle, 505 King Avenue, Columbus, OH 43201-2693

Introduction

The polydiacetylenes have been studied extensively in recent years because of their intriguing photochromic properties[1-3] and because of their large third-order nonlinear optical response [4-6]. While diacetylene monomers are colorless, or nearly so, exposure of the solid monomers to ultraviolet light or ionizing radiation (or, in some cases, to heat) causes the initial formation of a deep blue polymer having an absorption maximum at around 630 nm[1-6]. Heating the blue form, or exposing it to any of a number of common solvents, leads to an irreversible reorientation of the polydiacetylene lattice which shifts the absorption maximum to around 540 nm, resulting in the red form of the polydiacetylene[1-3]. Continued heating or exposure to radiation ultimately causes still another absorption shift, to around 460 nm or so; this yellow form of the polymer is reversible with the red form for some polydiacetylene structures.

It is now well established that the blue forms of several carboxylic acid polydiacetylene derivatives have among the largest nonresonant third-order nonlinear optical coefficients measured [4-6] and that the response is truly electronic in nature, with a sub-picosecond time constant[5]. Unfortunately, it has proven difficult to fabricate these materials into device-quality thin films, because of their tendency to form highly scattering polycrystalline solids. While it has been possible in the case of a p-toluenesulfonate-terminated diacetylene to grow high quality single crystals up to a few mm in size[7], the "solution-shear" or "melt-shear" procedures employed are slow, requiring several weeks for the growth of each sample, and do not appear well suited to the deposition of active waveguide films on larger substrates. As a result, waveguide formation in polydiacetylene films applied to substrates has been demonstrated to date only for the red and yellow films which can be obtained by spin-coating solutions of the soluble, urethane-terminated polydiacetylene derivatives such as 3-BCMU[8] or 9-SMBU[9]. These films are less ordered, and less active, than the blue forms of the polymers. Thus, the promised desirable nonlinear optical properties of the polydiacetylenes have yet to be realized in a useful waveguide device.

We have addressed this problem by developing a family of polydiacetylene "alloys": blue-form polydiacetylene polymers derived from mixtures of two similar diacetylene monomers having identical positioning of the diacetylene unit within the hydrocarbon chain, but with different "head" groups that provide varying degrees of affinity to water. The structures of these monomers are shown below. Multilayer films of the pure monomers, and of mixtures of them having specified mole ratios, have been deposited on glass, quartz, and plastic (CR-39^{R}) substrates using the Langmuir-Blodgett technique[10-11].

$$CH_3-(CH_2)_5-C\equiv C-C\equiv C-(CH_2)_8-CO_2H$$

I ("CO2H")

$$CH_3-(CH_2)_{11}-C\equiv C-C\equiv C-(CH_2)_8-CONH(C_6H_5)$$

II ("C=ONH")

In this technique, a small amount of the material to be deposited as a film is first spread as a monolayer, usually from a highly pure chloroform solution, onto the surface of a hydrophobic trough filled with high-purity water containing a small concentration of cadmium or other metal ions. Typically, a surfactant derivative of the desired material is used, with a hydrophilic group (such as a carboxylic acid) on one end and a hydrophobic group (such as a hydrocarbon chain) on the other. The monolayer is then compressed with a moveable barrier which sweeps across the surface of the water, forming a tightly packed monolayer that ultimately resembles a two-dimensional polycrystalline array[12,13]. By then slowly dipping the substrate into the trough, individual monolayers may be transferred from the water surface to the desired substrate[11]. With care, and with stringent attention to cleanliness and purity, it is possible to transfer an arbitrary number of monolayers to the substrate, allowing films of useful thicknesses to be built up over a period of several days.

The difficulty for waveguide applications, of course, is that any trace of dust, bacteria, or crystalline grain boundaries in the monolayer on the water surface will quickly lead to unacceptable scattering losses in a multilayer film composed of several hundred monolayers. The rationale of the present work has been to design mixtures that would form uniform, quasi-amorphous monolayers on the water surface for use in Langmuir-Blodgett multilayer fabrication, and thus avoid the scattering losses associated with grain boundaries that form within the monolayer on the water surface[12,13] while using careful clean-room procedures to minimize or eliminate any contamination of the films by dust or bacteria. Here, compound I tends to form highly crystalline monolayers, while compound II, which is less strongly

bound to the water surface, tends to form much less ordered monolayers. In mixtures of the two monomers, therefore, the presence of compound II serves to moderate the crystallinity of compound I, leading to relatively uniform, glassy monolayers. By using different lengths for the hydrocarbon "tails" of the two compounds, any tendency of the films to form crystalline domains at the boundaries between layers is also discouraged, while still ensuring that adjacent layers will remain mutually compatible.

Experimental Procedures

The diacetylene monomers were synthesized according to standard literature procedures[14-16] using acetylenic precursors that were purchased from Farchan Chemical Co. (Gainesville, FL). Following synthesis and recrystallization of the monomers, all subsequent procedures (with the exception of routine uv-visible and infrared spectroscopy) were conducted under Class 100 clean room conditions. Langmuir-Blodgett multilayer depositions were carried out using a KSV (Helsinki, Finland) Model 2200 L-B trough; the temperature of the water surface in the trough was measured at the surface with a calibrated thermistor, and was maintained to approximately +/- 0.1 C by means of a Lauda-Brinkmann refrigerated circulator, which pumped a temperature-controlled glycol solution through a quartz tube in the trough. All solutions were filtered through Millipore 0.2 micron filters immediately before transfer to the trough. Polymerization of the multilayer monomer films was accomplished after all layers had been transferred by irradiating the coated substrate with far-uv light (primarily 253.7 nm) from a small low-pressure mercury arc lamp. Photolithographic patterning of the L-B films was carried out under Class 100 clean conditions, using standard procedures with reactive oxygen ion etching. Absorption spectra were recorded on a Cary Model 17DX spectrophotometer.

Results and Discussion

Representative pressure-area isotherms for the pure compounds I and II, measured on the L-B trough as a function of surface temperature, are shown in Figure 1. The strong ordering of compound I ("CO2H") is evident from the sharp rise in surface pressure at a mean molecular area of around 6-8 A^2/molecule. In contrast, it is clear that the monolayers of compound II are somewhat "mushy", and that they probably collapse to a multilayered, jumbled film on the water surface (as evidenced by the very small molecular areas where the rise in pressure occurs) without ever forming a tightly packed, quasi-crystalline monolayer as compound I does. The effect of increasing the temperature in both cases is to make the films pack somewhat more tightly (that is, smaller mean molecular area at a given surface pressure), perhaps by providing additional thermal agitation to "jiggle" the molecules into a close-packing arrangement.

Figure 2 shows representative isotherms for a series of the mixed polydiacetylene "alloys" at 22 C, ranging in composition from 75 mole percent

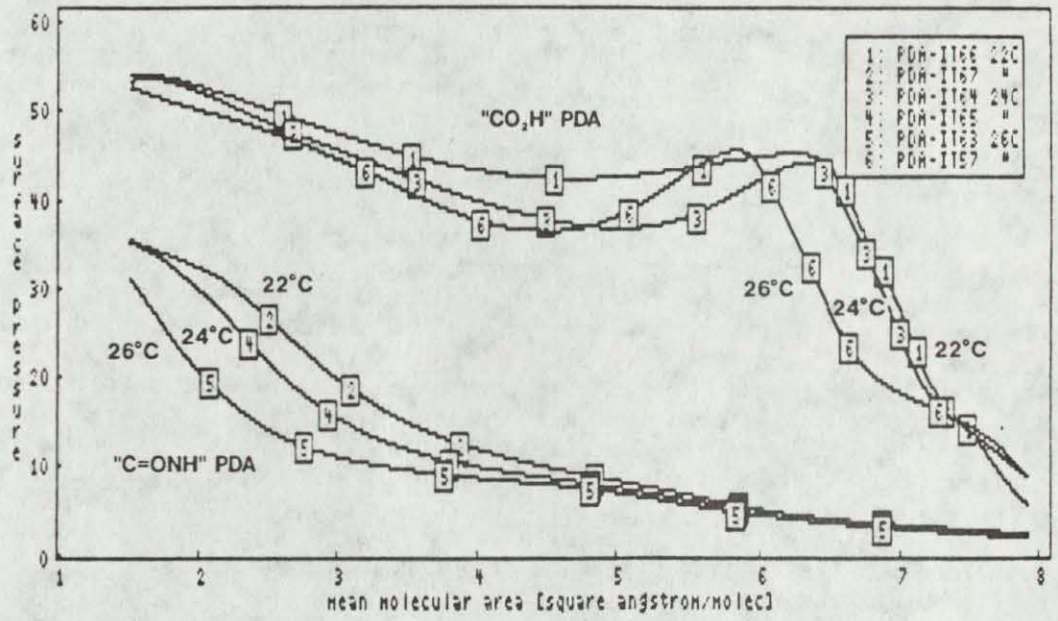

FIGURE 1. REPRESENTATIVE LANGMUIR-BLODGETT ISOTHERMS FOR PURE DIACETYLENES

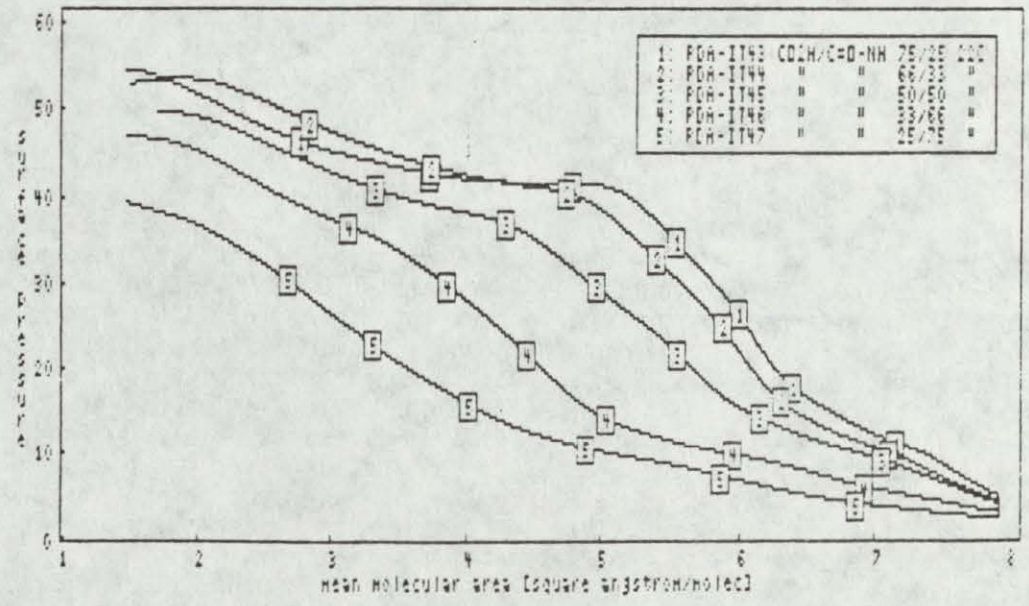

FIGURE 2. REPRESENTATIVE LANGMUIR-BLODGETT ISOTHERMS FOR POLYDIACETYLENE "ALLOYS"

compound I / 25 mole percent compound II (curve 1) to 25 mole percent compound 1 / 75 mole percent compound II. The isotherms show a smooth progression from the behavior shown by pure compound I to that shown by pure compound II as the mole fractions vary from one toward the other, as expected. These films, and those of the pure components shown in Figure 1, were deposited on scrupulously cleaned microscope slides.

In parallel with these studies, the optical quality of the films deposited with each composition was monitored by recording the visible absorption spectrum of the films at several points along the film, as illustrated by the insert in Figure 3. This was accomplished using a custom-made sample holder for the Cary 17 spectrophotometer, which allowed the sample to be mounted horizontally in the sample chamber of the instrument and then moved through the beam in controlled increments for successive scans of the spectrum. The technique relies on the fact that light scattering is wavelength-dependent, and is more pronounced at short wavelengths than at longer wavelengths. In the case of a uniformly coated sample, as shown in Figure 3, some differences in film thickness and/or polymerization efficiency are evident as the sample is scanned from top to bottom (position 1 corresponds to the top of the sample and position 4 to the bottom of the sample as it was dipped into the L-B trough), but there is essentially no divergence between the spectra at either the long-wavelength side or the short-wavelength side. With a poorly deposited sample, however, as illustrated by Figure 4, in addition to appearing visible cloudy in appearance there was a strong divergence in the spectra in the short-wavelength region. Thus, this technique provided an objective basis for evaluating the quality of the films as a function of composition and deposition conditions. While there was some variability from sample to sample even in replicate experiments, in general the 50:50 (CO2H:C=ONH) and 75:25 (CO2H:C=ONH) mixtures gave consistently better samples than did other mixtures or either of the pure components alone.

While waveguiding has not yet been demonstrated in our samples, photolithographic techniques for patterning the L-B films into waveguide configurations have been developed in anticipation of further improvements in optical quality. In this portion of our work to date, existing masks for simple line patterns and for Mach-Zehnder interferometers have been used to develop appropriate photolithographic conditions for patterning the films. A key consideration here has been to avoid converting the blue form of the polydiacetylenes into the red form during the patterning process. We have found that this can be accomplished by first vacuum-evaporating a thin layer of aluminum onto the PDA film, and then spin-coating American Hoechst AZ 4901 positive photoresist onto the aluminum layer. After the resist has been patterned and developed, reactive ion etching with oxygen then removes the PDA film in the desired areas. An example of this technique is given in Figure 5, which shows an optical micrograph (422x, so 1 mm = approx. 2.4 microns) of a Mach-Zehnder interferometer pattern that has been etched into a film of compound I using the above technique. Alternatively, Figure 6 shows a scanning electron micrograph (1000x, so 1 mm = 1 micron) of a line pattern which has first been etched into a quartz substrate by the above procedure and

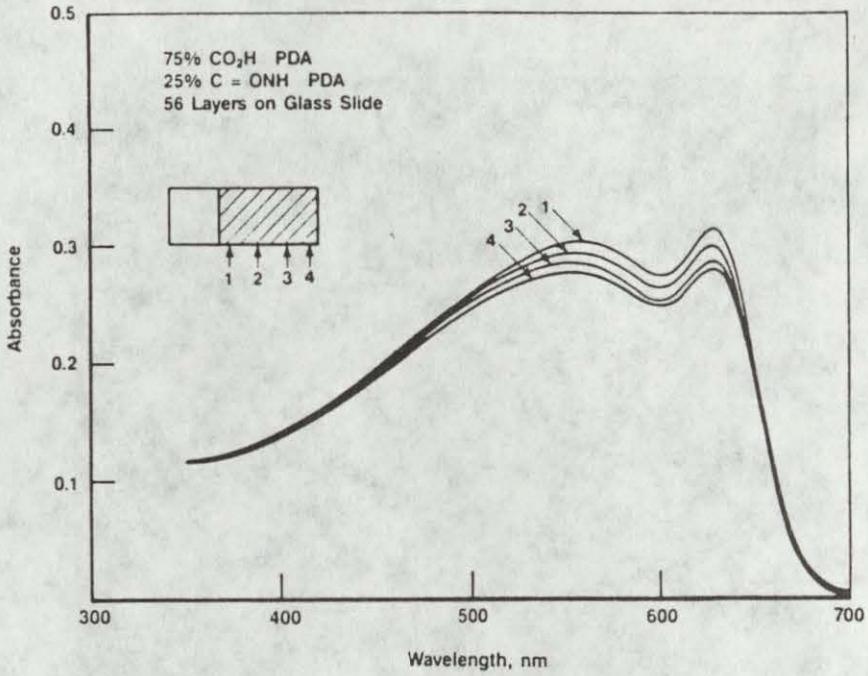

FIGURE 3. ABSORPTION SPECTRUM OF UNIFORMLY COATED POLYDIACETYLENE L-B FILM

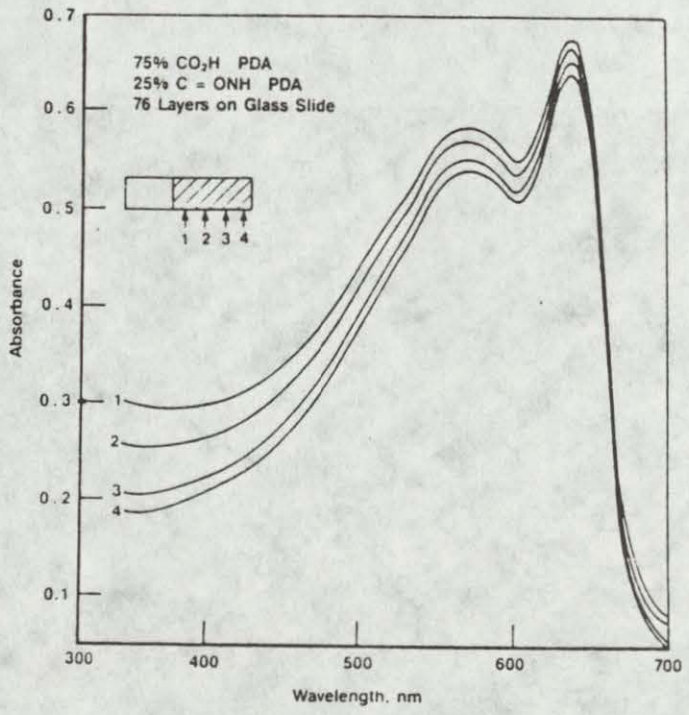

FIGURE 4. EFFECT OF SCATTER ON ABSORPTION SPECTRUM OF POLYDIACETYLENE L-B FILM

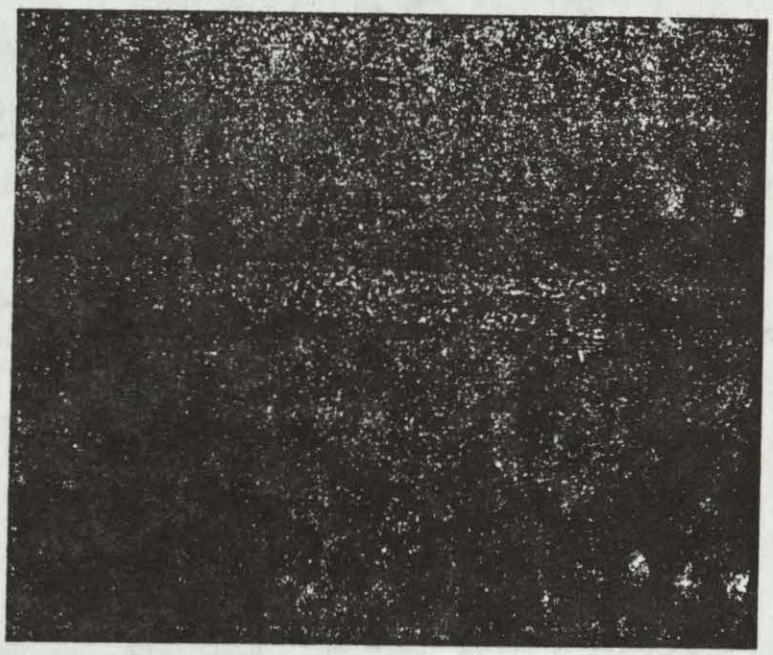

FIGURE 5. PHOTOMICROGRAPH OF PATTERNED POLYDIACETYLENE L-B FILM (422X)

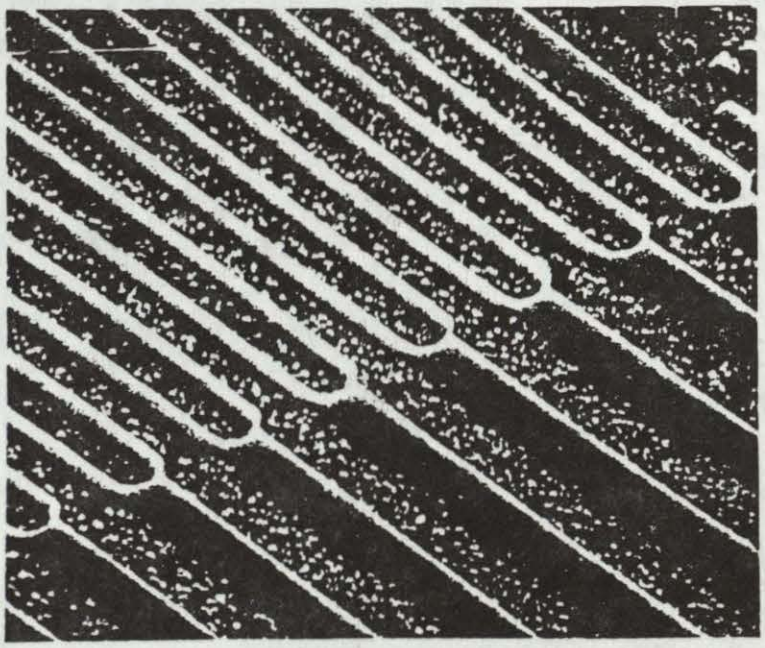

FIGURE 6. SEM PHOTOMICROGRAPH OF POLYDIACETYLENE FILM (70 LAYERS OF 75:25) DEPOSITED ONTO ETCHED QUARTZ LINE PATTERN (1000X)

then overcoated with 70 layers of 75:25 I:II to test the conformability of the L-B films. As can be seen, the film conforms well to the curvature of the lines (the small "flakes" between the lines are quartz fragments remaining from the initial etching prior to L-B deposition); this suggests that in the future it may be possible to deposit polydiacetylene films onto active substrates having complex curvatures or shapes.

Summary and Conclusion

In this paper, we have described our preliminary results toward the development of device-quality polydiacetylene nonlinear optical waveguides. We have shown that films of good optical quality can be deposited by means of Langmuir-Blodgett techniques by using "alloy" mixtures of similar diacetylene monomers, and we have shown that these films can be patterned using standard photolithographic techniques without converting the blue form of the polydiacetylene to the less active red form. We are optimistic that further improvements in film quality will permit low-loss waveguiding to be achieved in the relatively near future.

References

1. A. H. Adelman, A. F. Fentiman, R. L. Foltz, and R. E. Wyant (Battelle, Columbus, Ohio), unpublished results (1963-69); R.L. Foltz, "Photosensitive Element and Process", U. S. Patent No. 3501302 (issued March 17, 1970); R.L. Foltz and D.E. Trent, "Photoinduced Images and Process", U.S. Patent No. 3501303 (issued March 17, 1970); G.E. Cremeans, "Alkali Metal Salts of Polyacetylenic Polyoic Acids", U.S. Patent No. 3501297 (issued March 17, 1970), U.S. Patent No. 3679738 (issued July, 25, 1972); A. H. Adelman, "Composition and Process", U.S. Patent No. 3501308 (issued March 17, 1970).

2. G. Wegner, Z. Naturforsch., 24b, 824 (1969).

3. D. Bloor, in Crystallographically Ordered Polymers, D. J. Sandman, Ed., ACS Symposium Series 337, American Chemical Society, Washington, DC (1987), Chapter 10.

4. M. L. Shand and R. R. Chance, in Nonlinear Optical Properties of Organic and Polymeric Materials, D. J. Williams, Ed., ACS Symposium Series 233, American Chemical Society, Washington, DC (1983), Chapter 9.

5. T. Hattori and T. Kobayashi, Chem. Phys. Lett., 133, 230 (1987).

6. M. Schott and G. Wegner, in Nonlinear Optical Properties of Organic Molecules and Crystals, Vol.2, D. S. Chemla and J. Zyss, Eds., Academic Press, Orlando, FL (1987), Chapter x.

7. M. Thakur and S. Meyler, Macromolecules, 18, 2341 (1985).

8. J. L. Jackel, et al., in Nonlinear Optical Properties of Organic Materials, G. Khanarian, Ed., Proc. SPIE 971, The Society of Photo-Optical Instrumentation Engineers, Bellingham, WA (1988), pp. 239-244.

9. S. Mann, et al., in Nonlinear Optical Properties of Organic Materials, G. Khanarian, Ed., Proc. SPIE 971, The Society of Photo-Optical Instrumentation Engineers, Bellingham, WA (1988), pp. 245-251.

10. I. Langmuir, Trans. Faraday Soc., 15, 62 (1920).

11. K. B. Blodgett, J. Amer. Chem. Soc., 57, 1007 (1935).

12. G. M. Carter, Y. J. Chen, and S. K. Tripathy, in Nonlinear Optical Properties of Organic and Polymeric Materials, D. J. Williams, Ed., ACS Symposium Series 233, American Chemical Society, Washington, DC (1983), Chapter 10.

13. R. A. Hann and B. L. Eyres, Nature, 313, 382 (1985).

14. G. N. Patel, in Polymer Preprints, ACS Division of Polymer Chemistry, 19(2), 154 (1978); G. N. Patel and E. K. Walsh, J. Polymer Sci. Lett. Ed., 17, 203 (1979).

15. W. Chodkiewicz, Ann. Chim., 2, 819 (1957).

16. A. S. Hay, J. Org. Chem., 27, 3320 (1962).

AROMATIC SCHIFF BASES AND THEIR MESOMORPHIC DERIVATIVES FOR EFFICIENT NONLINEAR OPTICS

R. SAI KUMAR, SUDHA KUMAR, A. BLUMSTEIN,
SUKANT TRIPATHY AND JAYANT KUMAR

DEPARTMENTS OF CHEMISTRY AND PHYSICS
UNIVERSITY OF LOWELL
LOWELL, MA 01854

ABSTRACT

We have synthesized a set of aromatic Schiff base compounds posessing molecular structures capable of exhibiting large second- and third-order nonlinear optical effects. By incorporating these moieties as side groups on the diacetylene functionality, we have obtained unique materials in which enhanced second and third order nonlinear optical response is derivable on polymerization by topochemical means. Using a dc Kerr experiment in solutions containing these molecules, we have recently observed (electrooptic) modulation in the transmitted He-Ne laser light. This experiment gives a direct measurement of the Kerr constant and hence the third order nonlinear optical susceptibility, $\chi^{(3)}$. We are also carrying out an all-optical Kerr experiment with these materials in solution. Results of these experiments will be presented at the meeting.

Liquid crystalline derivatives containing these electroactive moieties have been synthesized in our laboratory. We are carrying out laser-field induced Kerr experiments on a representative mesomorphic compound in its isotropic state. Apart from the Kerr constant (and hence $\chi^{(3)}$) typically derivable from these experiments, one can also obtain information on the molecular dynamics and the pretransitional organization (in the isotropic phase) for these compounds. Results of these experiments and their application in optical limiting and other related phenomena will be presented at the meeting.

CRYSTALLINE AND AMORPHOUS POLYDIACETYLENES DERIVED FROM LIQUID CRYSTALLINE MONOMERS

Michael A. Schen, National Institute of Standards and Technology, Polymers Division, Blg.224/Rm.B320, Gaithersburg, MD 20899

For the successful implementation of a second order, χ^2, or third order, χ^3, polymeric nonlinear optical materials into an electro-optical or integrated optical device, developing appropriate material processing technologies for device fabrication that successfully combines the nonlinear optical performance of the material with the secondary device performance specifications becomes a key challenge to the material scientist. To this end, our work in the area of χ^3-active materials has focused on extending the realm of microphases under which polydiacetylenes, PDAs, will undergo polymerization to high polymer and investigating novel micromorphologies resulting from these new polymerizations. It has been found that continuous PDA films may be easily prepared from previously described liquid crystalline diacetylene monomers[1]. Depending on the microphase under which polymerization takes place and the degree of polymerization, resulting films exhibit microstructures ranging from pseudo-crystalline to fully amorphous. These films are currently under investigation for their linear and nonlinear optical responses.

1. (a)Schen M.A., Proc. SPIE, 824, 93(1987); (b)Schen, M.A., Proc. SPIE, 971, 178(1988).

Processing of Third-Order Polymeric Films for Optical Bistability

M. Druy, L. Domash, Foster-Miller, Inc.

and

P. Prasad, SUNY Buffalo

Abstract

Certain polymeric materials are promising for third-order nonlinear optical applications such as laser hardening because they possess substantial third-order nonlinear coefficients at subpicosecond speeds combined with excellent strength and environmental stability. We present a summary of our research in novel methods of processing films of three classes of delocalized conjugated polymer materials: polyphenylene benzobisthiazole (PBT), polyphenylene vinylene (PPV) and LARC-TPI, a polyimide. Data on chi-3, response speed, and optical quality improvements gained through processing innovations are presented. Recent progress includes one of the first demonstrations of purely dispersive optical bistability in a polymer film.

TITLE: Laser Protection Based on Optical Fibers and Nonlinear Organic Liquids

Lawrence Domash, Dr., Phil Levin, Mr.,Jay Ahn, Dr., Jayant Kumar, Dr., Sukant Tripathy, Dr.

ABSTRACT: Nonlinear optical organic liquids based on 2-methyl-4-nitroaniline (MNA)-type molecules in solution are potentially practical as third-order materials, featuring a large and fast intensity dependent index of refraction (n_2), low optical loss, insusceptibility to laser damage and a freely adjustable refractive index. The latter property makes them compatible with glass substrate devices and permits ease of fabrication for demonstration devices. Concepts and preliminary data are presented for a high speed, all-optical switch based on glass waveguides suspended in a nonlinear liquid cladding of index matched organic solutions.

BIOGRAPHY OF PRESENTER: Lawrence H. Domash

PRESENT ASSIGNMENT: Senior Scientist and Technology Area Manager for Nonlinear Optics at Foster-Miller, Inc.

PAST EXPERIENCE: Formerly he was a Research Fellow at Harvard University and a National Academy of Sciences Postdoctoral Fellow with NASA. Before joining Foster-Miller, he was Chief Scientist of Super/Radiant Systems, Inc., an optics research firm. Dr. Domash has also served as a consultant to Corning Glass, BDM, and other companies.

DEGREES HELD: Ph.D. in Physics from Princeton University, B.S. from the University of Chicago.

Laser Protection Based on Optical Fibers and Nonlinear Organic Liquids

Lawrence Domash, Dr.*, Phil Levin, Mr.*, Jay Ahn, Dr.^, Jayant Kumar, Dr.**, Sukant Tripathy, Dr.^

*Foster-Miller, Inc. Waltham, MA 02154-1196
^Dept. of Chemistry, University of Lowell, Lowell, MA 01854-2881
**Dept. of Physics, University of Lowell, MA 01854-2881

1. Introduction

All-optical waveguide devices based on ultrafast third-order nonlinear optical properties are desired for a variety of functions including fiber optic switching and optical limiting for laser protection. Materials potentially useful in these applications must possess (a) high third-order nonlinearity, (b) ultrafast response time, and (c) excellent additional requisite physical properties. These properties include superior transparency, freedom from scattering centers, uniformity, optically flat surfaces, chemical and environmental stability and processibility. Organic materials are often cited as having the best long range promise for such devices[1]. In spite of intensive research using organic materials, relatively few working devices have been demonstrated to date due to a variety of problems in selecting, processing and fabricating such materials into appropriate device configurations.

We discuss concepts for a class of switching devices intended to be easy to fabricate and test, based on combining nonlinear organic solutions with glass fiber waveguides. In constructing practical nonlinear waveguide devices for the application discussed above, many characteristics other than large, high speed n_2 effects become important. In particular, low loss (the sum of absorption and scattering) is significant. The effective nonlinear response for many device configurations is not the intensity-induced index modulation $n_2 I$, but the figure of merit, $n_2 I/\alpha\lambda$, where I is the intensity of the incident beam, α is the loss per cm and λ is the wavelength of the incident beam.

An often overlooked factor is that for maximum flexibility in device design it is desirable

that a third-order material should have a linear refractive index compatible with the other materials typically used in fiber optics and waveguide structures. For example, some high performance organic films or crystals have indices in the 1.6 to 1.9 range, making it difficult to integrate them with glass structures of index ≈ 1.45. In addition, laser damage threshold of the nonlinear material under consideration must be high enough to withstand the fields required to generate significant nonlinear effects. Finally, the usefulness of a material is severely limited unless a fabrication technology exists to produce high precision, low loss waveguide forms. Organic materials exist which satisfy each of these requirements, but no one material so far satisfies them all at once. In an attempt to develop approaches to maximize utilization of organic NLO materials and minimize processing and fabrication complexities, we employed NLO materials in solution form.

Solution form of NLO materials provides at least two advantages for research and feasibility demonstrations. First, adjusting the linear refractive index to match a given fiber cladding will be significantly easier than in the solid state. Second, the transparency problem will be drastically reduced since the scattering and inhomogeneity prevailing in most solid films will be avoided. As a tradeoff for these advantages, solutions raise problems such as concentration limits and temperature dependence of the refractive index. Therefore, several solvents must be evaluated to identify the range of refractive index available, and temperature must be controlled as accurately as possible to minimize the temperature-dependent changes of refractive index.

With these factors in mind, it is instructive to note that Friberg et al.[4] were able to demonstrate all-optical switching in a simple dual core optical fiber, operating as a Jensen coupler[5]. In their early experiments, the "nonlinear" material was ordinary silica, whose n_2 is only 1/10,000 that of a prototypical high performance polymer such as PDA, in the material's transparent regime[6]. Because of the extremely high transparency of silica, however, combined with the existing technology to form long low loss fibers, this small nonlinearity was available over a long optical path length (many cm) in a "pipelined" switching configuration capable of subpicosecond speeds. Switching power threshold was on the order of 1 kW. Using the organic NLO solutions of the present research, larger n_2 effects may yield switching times an order of magnitude faster with optical switching power on the order of 100mW.

2. Dual-Waveguide Switching Device Using Liquid Cladding

In view of the difficulty of fabricating high precision nonlinear thin film waveguides, it is clearly a practical advantage to work with devices based on glass fibers as an existing high quality waveguiding structure, provided more strongly nonlinear materials can also be intro-

duced. Clark, Andonovic and Culshaw[7] modeled dual waveguide devices in which the nonlinear material in a dual-core optical switch was located contiguous with the cladding, as shown schematically in Figure 1. A directional coupler is first fabricated which, under low power conditions, transfers 100 percent of the optical power from fiber 1 to fiber 2. Under the control of a separate optical pump beam, or else a simple increase in power of the signal itself, the nonlinear core or cladding index $n = n_o + n_2 \cdot I$ (where n_o is the linear refractive index) is modulated sufficiently to alter the coupling ratio between the two fibers. If the coupler length and power threshold are set correctly, this can cause the signal to exit 100 percent from fiber 1 instead of transferring to fiber 2, effecting an optically controlled switch. This class of devices is called nonlinear coherent couplers (NLCC). Figure 2 suggests that a simple NLCC can in principle be made by immersing a rather ordinary bidirectional coupler with etched cladding in an index-controlled bath of a nonlinear liquid. Although it is inherently less efficient to locate the active nonlinear material in the cladding than in the core, this can be compensated by large n_2 values, long path lengths, and very accurate index control of the nonlinear cladding element. The goal, in developing such a switch, is subpicosecond speed combined with a power threshold for switching on the order available from diode lasers, 10 to 100mW.

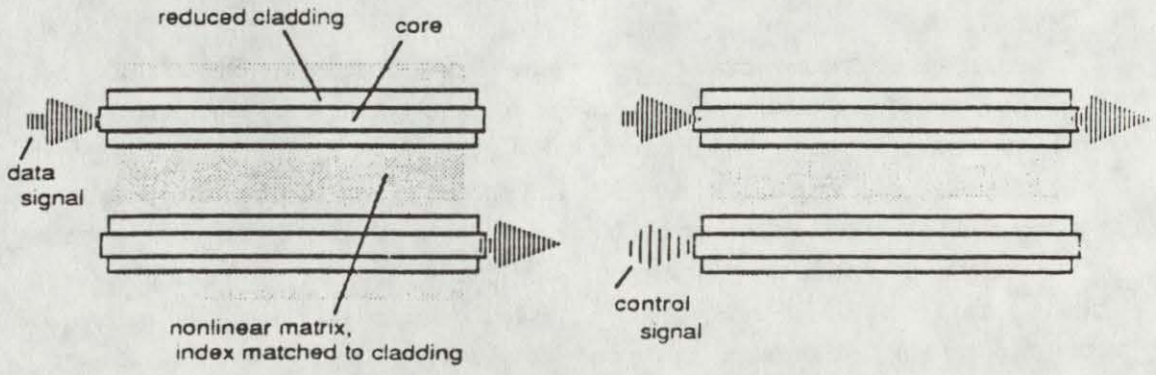

Figure 1. The Nonlinear Coherent Coupler, NLCC

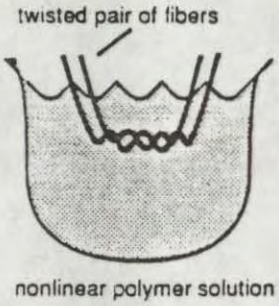

Figure 2. A Simple NLCC with Glass Fibers in a Nonlinear Liquid Bath

Highly transparent third-order materials whose linear index can be precisely adjusted to match glass cladding values are essentially limited to glasses, doped glasses or liquids. The latter have the advantage of potentially much larger nonresonant nonlinearities. Although liquid CS_2 is a standard for third-order nonlinear optics, relatively little effort has been devoted to developing new, higher performance liquids as practical device materials. Using high concentrations of NLO solutions, it is possible to precisely match the index to a range of desired values. In high concentrations, n_2 values comparable to the best solid organic materials may be possible, along with the low loss and self-healing characteristic of high purity liquids.

3. Device Model

The equations describing power transfer within an NLCC were derived by Jensen[5]. The NLCC is defined as two parallel waveguides spaced closely enough for evanescent wave overlap and separated by a nonlinear medium. For a coupler with active region equal to the characteristic coupling length, L_c, the coupler will operate in the "crossed state" at low powers (i.e., all of the power launched into one waveguide will exit the second waveguide).

Switching of the NLCC from the crossed to the parallel state is shown as a function of input power in Figure 3. The effect of a factor of two increase in the nonlinear index of the medium constituting and surrounding the coupler guides is shown by the two curves; the coupler with the higher nonlinearity shows 100 percent switching at a lower power. Since some nonlinearity is always present in the core, and the higher field there emphasizes this

contribution over that of the cladding, the effect of a nonlinear liquid bath is essentially to enhance the performance (i.e., reduce the power threshold for switching), which is already present due to the small nonlinearity of the glass core.

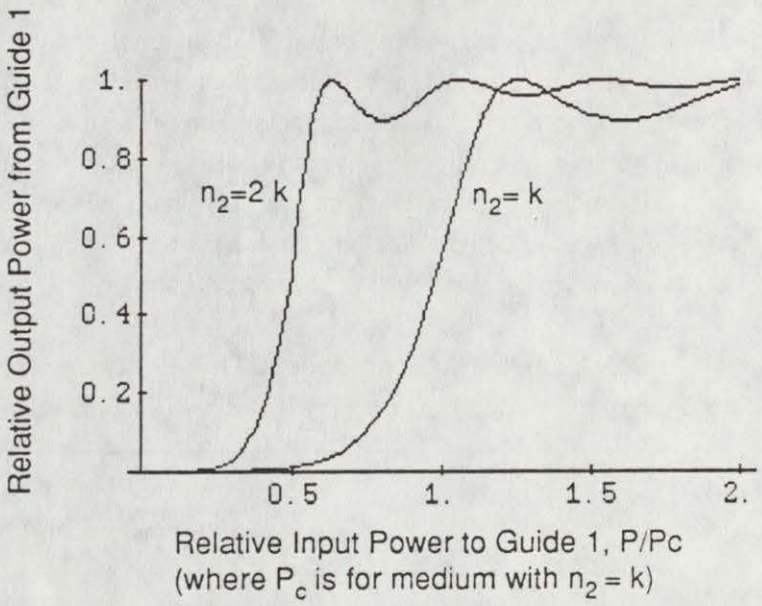

Figure 3. Signal Fraction Exiting Fiber 1 as a Function of Input Power

4. Characterization of Organic NLO Materials

Commercially available 2-methyl-4-nitroaniline (MNA), primarily known as a second order material[2], was selected for the preliminary demonstration of all-optical switching using NLO solutions. MNA also exhibits considerable third-order nonlinearity, whose high speed nonresonant nonlinear index of refraction ($n_2 = 25.0 \times 10^{-11}$esu) is 2 to 3 times greater than that of silicon or p-nitroaniline[3]. Exceptionally high solubility of MNA in polar solvents allows a wide range of refractive indices to be available. MNA also provides a wide range of transparent window (from mid visible to near infrared) where optical losses are minimal (Figure 4).

Solubilities of MNA in various solvents (HPLC grade) at room temperature were measured for the range of refractive index available (Table 1). Variation of refractive index of the MNA solution in various solvents at 20°C as a function of concentration was obtained using

an Abbe refractometer as shown in Figure 5. The thermal fluctuation of the refractive index in MNA-saturated solutions measured at 15°C and 25°C is tabulated in Table 2. Change of refractive index resulting from temperature variation turned out to be approximately 0.0004/°C, so that it is essential to control the solution temperature to better than ±0.1°C in this experiment in order for only electronic nonlinear refractive index change to be effective.

As a result, the refractive index can be tailor-made to the desired value by varying one or more of the following factors; (a) concentration of the NLO material, (b) solution temperature and (c) solvent type. It is true that the higher the number density of the NLO molecules in solution, the larger the nonlinear effects are. In practice, however, not only nonlinearity but optical loss, solvent volatility, stability of polymeric components in the device assembly, such as epoxy encapsulant and so on, must be taken into account. Consequently, nonvolatile propylene carbonate (PCB) was selected as the best choice for the test solvent in which epoxy encapsulant was found very stable for long periods of time.

Table 1. Solubilities of MNA in Dimethylformamide (DMF), P-dioxane, Propylene Carbonate (PCB) and Tetrahydrofuran (THF) at Room Temperature

SOLVENT	SOLUBILITY (grams/liter) DMF
DMF	527
p-DIOXANE	261
PCB	15
THF	349

Table 2. Thermal Fluctuation in Refractive Indices of MNA Saturated Solutions

	REFRACTIVE INDEX	
SOLVENT	15°C	25°C
DMF	1.5660	1.5613
p-DIOXANE	1.4766	1.4725
PCB	1.4580	1.4546
THF	1.4954	1.4817

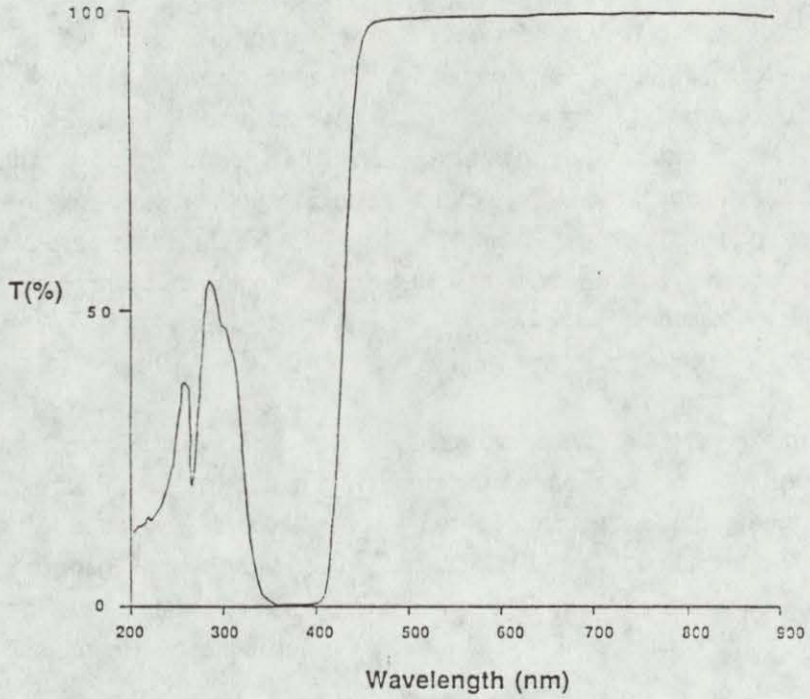

Figure 4. Ultraviolet-Visible Transmission Spectrum of MNA

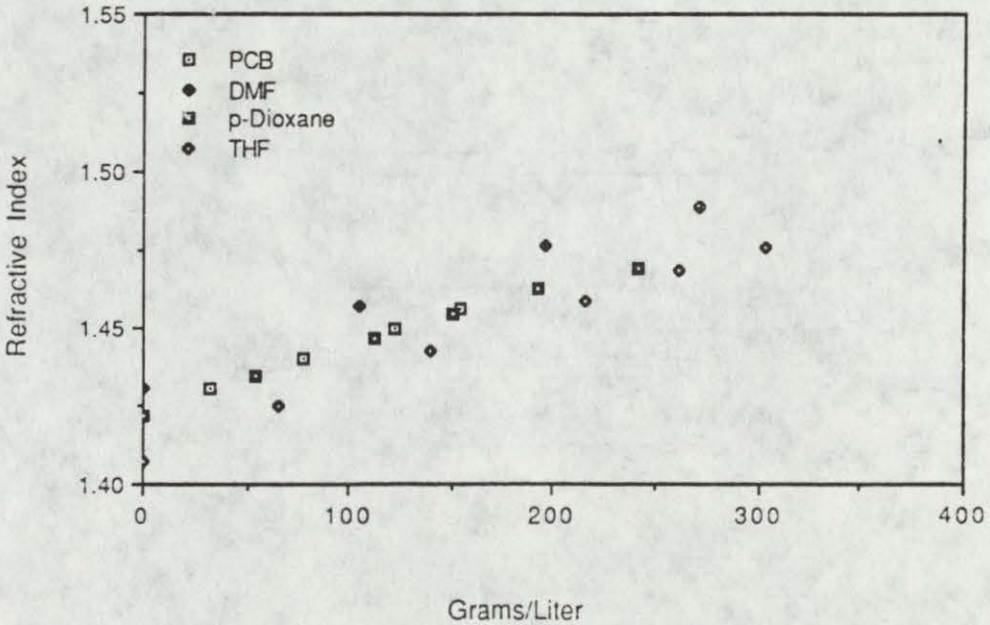

Figure 5. Refractive Indices of MNA Solutions as a Function of Concentration at 20 C

In MNA solution, excellent transparency is observed for the wavelength of 450 nm through near infrared with an absorption peak at 380 nm as shown in Figure 4.

A number of organic NLO molecular systems have been designed and synthesized in our laboratory[8], which are expected to possess significantly larger third-order nonlinearity than MNA. Polymerization of these molecules may result in soluble materials with significantly large nonlinear optical properties. Eventually, these new NLO materials are expected to improve the device performance by at least an order of magnitude leading to a switching power threshold of less than 100 mW.

5. Preliminary Experiments

As a preliminary test, we have constructed a device as shown in Figure 2, have developed a high precision laboratory method of matching liquid indices to glass cladding, and have demonstrated modulation of the probe beam by a pump beam at low speed using thermal effects. This demonstration, which has been carried out with thermal changes in the index of refraction of the surrounding liquids, gives some indication of the dynamics to be expected from electronic nonlinearities of the NLO solutions in subsequent experiments.

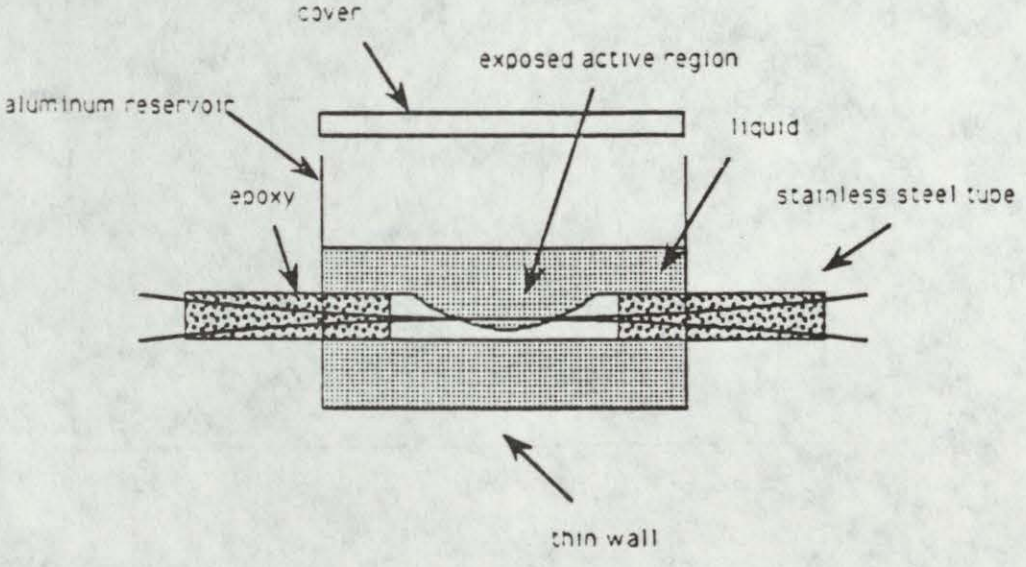

Figure 6. Cross Section of Liquid Test Apparatus for Nonlinear Coherent Couplers

A cross section of the experimental apparatus is shown in Figure 6. The basic coupler is of the fused type and is fabricated from two optical fibers with single mode cutoff at about 590 nm. The fused or "active" region of the coupler is about 1-cm long and has an estimated minimum diameter of about 40μ. At both ends of the active region, at the points of bifurcation, an epoxy encapsulant is used to anchor and seal the coupler. As shown, after encapsulation, only the active region remains available for exposure to the test liquids. The coupler sits within a stainless steel tube, with central section cut out. The tube passes diametrically through a liquid reservoir and serves as a liquid-tight bulkhead through which the input and output fiber ends of the coupler pass. As some of the test solvents are highly volatile, the reservoir is fitted with a removable cap to prevent evaporation. The liquids are tested by filling the reservoir until the active region is submersed.

The apparatus may be used with a single laser input beam of adjustable intensity which serves as both the pump beam and the probe beam, or else two lasers operating at different wavelengths may be used to separate the probe/signal and pump/control functions. In our initial tests it was convenient to use separate lasers for the probe and pump beams; the arrangement for launch and detection of transmitted optical signals is shown in Figure 6.

As a preliminary test of the device apparatus, an argon ion laser (Coherent Innova 90-6) producing 0.5 to 4 W at 515 nm was used as the pump beam in Figure 7. Optical modulation of the HeNe probe beam was demonstrated under control of the argon pump beam, by means of thermal modulation of the active region of the coupler, as shown in Figure 7. This effect was quite slow as expected, on the order of 10 ms, but served to demonstrate principles similar to those which will operate in subpicosecond experiments using purely electronic index modulations. Addition of an index matching fluid to the active region reduced the amplitude of the probe beam modulation, possibly because the liquid stabilized the active region temperature through convective cooling. Note that it is difficult to distinguish experimentally between the contributions of the core and cladding nonlinearities, whether thermally or electronically induced.

The experimental apparatus is now being readied for high speed all-optical switching experiments using a subnanosecond pulsed laser pump in conjunction with the organic NLO liquids as described above.

6. Concluding Remarks

To demonstrate all-optical switching using organic NLO solutions, MNA was selected as a test NLO material and its suitable solvent systems were identified. A test apparatus has been designed and assembled which enables optical interaction between a fiber optic single

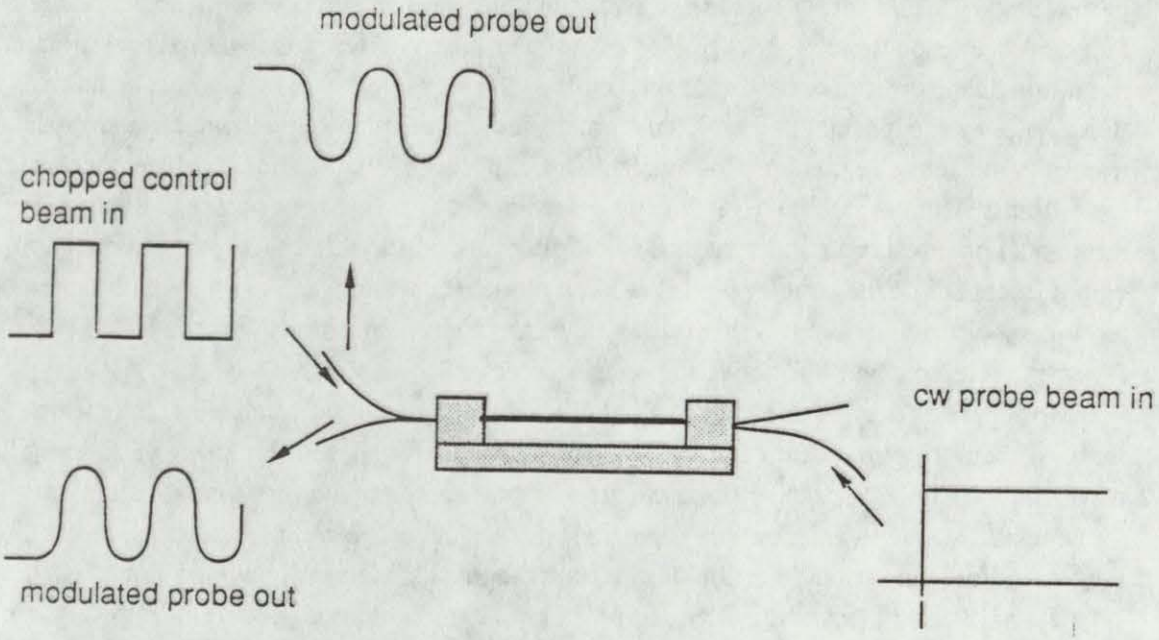

Figure 7. Optical Coupling due to Thermal Index Modulation

mode coupler and NLO liquids. Thermal modulation of an input signal has been demonstrated with this apparatus. Subpicosecond all-optical switching using organic NLO solution (e.g. MNA/PC), including new NLO materials synthesized in our laboratory, is now under investigation for enhanced switching efficiency.

ACKNOWLEDGEMENTS

This University of Lowell/Foster-Miller collaboration is supported by the Massachusetts Center of Excellence Corporation in Polymer Science, a state agency.

REFERENCES

1. G. Stegeman, C. Seaton, J. Appl. Phys., 58, R57(1985).
2. A. Yariv, "Quantum Electronics", 2nd Ed., John Wiley & Sons, Inc., New York, 1975.
3. T. Chang, Opt. Eng., 20, 220(1981).

4. S. Friberg, Y. Silverberg, P. Smith, Appl. Phys. Lett., 51, 1135(1987).
5. S. Jensen, IEEE JQE-18, 1580(1982).
6. D. Williams, "Nonlinear Optical Properties of Organic and Polymeric Materials", ACS, Washington DC, 1983.
7. D. Clark, I. Andonovic, B. Culshaw, Opt. Lett., 11, 540(1986).
8. R.S. Kumar, J. Kumar, S. Kumar, A. Blumstein, S. Tripathy, Proc. IUPAC MACRO 88, 32nd Int'l Sympo. Macromol., Kyoto, Japan, Blackwell Sci. Publ., 1988.

Polymer dispersed liquid crystal films and their nonlinear optical response

P. Palffy-Muhoray, J. Kelly, Michael A. Lee, J.L. West[†],
B.J. Frisken[†], J.Y. Kim, and H.J. Yuan

Liquid Crystal Institute[†] and Department of Physics
Kent State University, Kent, OH 44242

ABSTRACT

Polymer dispersed liquid crystals are composite materials consisting of inclusions of liquid crystals dispersed in a polymer binder. In this paper we report studies of optical field induced effects in these materials. We report observations of scattering by these films induced by the field of a CW Ar^+ laser through both reorientation and thermal effects. A simple theory is given to assess the relative contribution of these two mechanisms, and experimental results are compared with the theoretical predictions.

1. INTRODUCTION

Polymer dispersed liquid crystal (PDLC) films consist of liquid crystal droplets dispersed in a polymer binder. The liquid crystal is usually dispersed in the form of nearly spherical inclusions with diameters ranging from 0.1 to 10 μm. The mechanism for forming these droplets is phase separation of an initially homogeneous polymer-liquid crystal mixture. The phase separation mechanism, induced by polymerization, thermal quenching or solvent evaporation, has been described in detail elsewhere[1].

The optical properties of the PDLC films are sensitively dependent on the differences between the refractive index of the polymer binder and the refractive indices of the liquid crystal. In its normal state, the typical PDLC should be viewed as a collection of nonabsorbing birefringent liquid crystal droplets, nearly equal in size ($\pm 10\%$) and approximately spherical in shape, randomly distributed in a transparent isotropic polymer host. Typically ten to thirty

percent of the volume fraction of the sample is liquid crystal microdroplets. The local symmetry axis of the liquid crystal in the droplets is specified by the nematic director. Although a variety of director configurations are known to be possible[2], we consider here a typical bipolar configuration shown in Fig. 1.

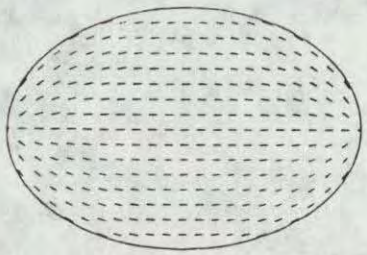

Fig. 1 Liquid crystal droplet with bipolar configuration. The director is parallel to the line segments.

Since in the nematic phase the liquid crystal is birefringent, the refractive index mismatch depends on both the orientation of the optic axis and the degree of orientational order of the liquid crystal. If the ordinary refractive index n_0 of the liquid crystal and refractive index n_p of the polymer are matched, the films are transparent when the liquid crystal in all the droplets is completely aligned with the director along the direction of light propagation. The films may easily be switched from an opaque scattering state to a transparent clear state by electric[3-6] or magnetic[7] fields which reorient the liquid crystal droplet.

Optical fields have also been shown to switch PDLC films both in a transparent state and in a scattering state[8-9]; in both cases we have observed optical field induced reorientation of the liquid crystal in the PDLC inclusions. The optical fields reorient the liquid crystal as a result of the anisotropic polarizability, and sample heating occurs due to absorption. We ascribe the laser induced changes in transmittance of the PDLC films to both reorientation and thermal effects and compare the experimental results to the predictions of theory.

2. PDLC FILMS

In general the heterogeneous structure of the PDLC films is a result of phase separation of the initial polymer-liquid crystal mixtures. The phase separation is induced by polymerization, thermal quenching or solvent evaporation. Both spinodal decomposition and droplet nucleation and growth have been observed in the process of phase separation. The size and morphology of the droplets can be controlled by the dynamics of phase separation process.

The PDLC films used were formed by mixing equal parts (by weight) of Epon 828, Capcure 3-800 and the liquid crystal E7. Epon 828 is the reaction product of epichlorohydrin and bisphenol A. Capcure 3-800 is a trifunctional mercaptan terminated liquid polymer and E7 is a eutectic liquid crystal mixture of cyanobiphenyls and triphenyls. The components are well mixed, forming a clear homogeneous solution. Glass spacers of given thickness are added to the solution which is poured on to a 3.0cm×2.5cm×1.14mm glass slide with a transparent layer of conducting indium tin oxide (ITO). An identical second glass slide is placed on the top of the

solution, and pressed to contact the glass spacers forming a film with given thickness. The glass sandwich is placed in an oven at a fixed temperature until phase separation and polymerization are complete. Typical samplet thicknesses are in the range of 10-40μm, and the curing temperatures are 60-75°C. A scanning electron micrograph of such a PDLC film is shown in Fig. 2.

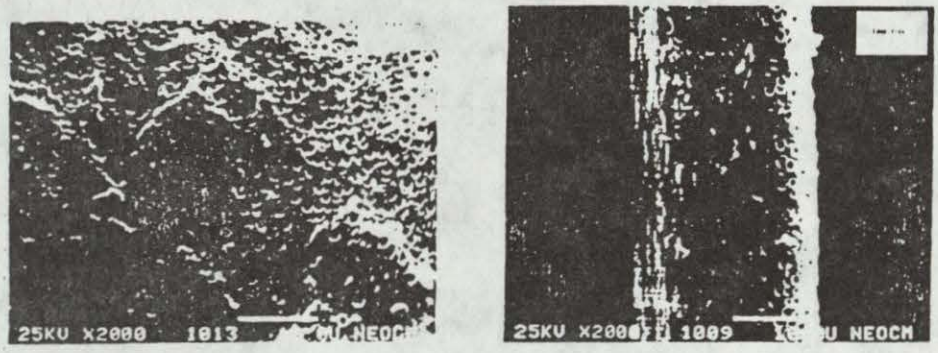

Fig. 2 Scanning electron micrograph of a PDLC film. The left and right panels are in plane view and edge view, respectively. The scale bar is 10 μm long.

3. NONLINEAR RESPONSE IN LIQUID CRYSTALS

The dielectric tensor ϵ_{ij} of liquid crystals depends on both on the degree of orientational order and the local direction of molecular orientation. It is customary to characterize nematic order by the order parameter tensor Q_{ij} defined by

$$Q_{ij} = S \cdot \frac{1}{2} (3n_i n_j - \delta_{ij}) \tag{1}$$

Here S is the scalar order parameter, and n_i are the components of the director $\hat{n}$. The dielectric tensor is then related to the order parameter tensor by

$$\epsilon_{ij} = \left(\frac{\epsilon_{||} + 2\epsilon_{\perp}}{3} \right) \delta_{ij} + \frac{2}{3} (\epsilon_{||} - \epsilon_{\perp}) Q_{ij} \tag{2}$$

where $\epsilon_{||}$ and $\epsilon_{\perp}$ are the principal values of ϵ_{ij} parallel and perpendicular to the local symmetry axis, respectively. Because the scalar order parameter S and molecular director $\hat{n}$ depend on the applied field $\vec{E}$, so does the tensor order parameter Q_{ij} and dielectric constant ϵ_{ij}. We expand Q_{ij} in powers of E,

$$Q_{ij} = a_{ij} + b_{ijkl} E_k E_l + \cdots \cdots \tag{3}$$

and it follows that the lowest order orientational contribution to the third order susceptibility is given by

$$\chi^{(3)}_{ijkl} = \frac{2}{3}\,\Delta\epsilon\, b_{ijkl} \tag{4}$$

where $\Delta\epsilon \equiv \epsilon_{||} - \epsilon_{\perp}$ is the dielectric anisotropy.

In the presence of both an AC electric field at frequency Ω, and an optical field at frequency ω, dominant contributions to the third order optical susceptibility are the AC Kerr effect $\chi^{(3)}(-\omega;\ \omega,\ \Omega,\ -\Omega)$ and the optical Kerr effect $\chi^{(3)}(-\omega;\ \omega,\ \omega,\ -\omega)$. In bulk PDLC films, these $\chi^{(3)}$ processes give rise to the field induced changes in the transmittance due to scattering.

4. DROPLET REORIENTATION MODEL

We wish to describe the reorientation process of a confined liquid crystal droplet due to an applied electric and/or an optical field. In such a system there are a number of competing effects that determine the overall orientation of a droplet. First, interactions at the liquid crystal - polymer interface usually favour alignment such that the director field is in the bipolar configuration. The droplets are not perfectly spherical, and to first order may be assumed to be ellipsoidal. Elastic torques arising from the eccentricity of the droplet shape tend to keep the direction of average orientation parallel to the long axis of the ellipse to minimize curvature strain. Second, applied fields exert a torquewhich tends to reorient the director. In the case of low frequency AC (or DC) fields, the alignment can be parallel or perpendicular to the field, depending on the sign of the dielectric anisotropy. Third, optical fields tend to orient the director along the direction of polarization, due to the positive refractive index anisotropy. We consider a simple model[10] where the configuration of liquid crystal in an inclusion is described by the droplet director $\hat{N}$, the direction of average orientation of molecules in the droplet. We assume that each cavity is ellipsoidal with eccentricity δ and symmetry axis $\hat{I}$. If the applied AC field $\vec{E}_{ac}$ and the optical field $\vec{E}_{opt}$ are perpendicular, then the average free energy density due to the contributions of elastic torques and external fields can be written[10] as

$$\frac{\mathfrak{F}}{\mathfrak{F}_0} \simeq -(\hat{N}\cdot\hat{I})^2 - \left(\frac{E_{ac}}{E_0}\right)^2 (\hat{N}\cdot\hat{E}_{ac})^2 - \frac{I}{I_0}(\hat{N}\cdot\hat{E}_{opt})^2 \tag{5}$$

where $I = \frac{1}{2}\epsilon_o c E_{opt}^{\ 2}$ is the intensity of the optical field, c is the speed of light,

$$E_0 = \frac{\delta}{R_{eff}}\left(\frac{K}{\epsilon_0\,\Delta\epsilon}\right)^{1/2} \tag{6}$$

$$I_0 = \frac{\delta^2\, K\, c}{2\, R_{eff}^{\ 2}\, \Delta n} \tag{7}$$

K is the average elastic constant, $1/R_{eff}$ is the effective curvature of the director field, $\Delta n \equiv n_{||} - n_{\perp}$ is the refractive index anisotropy. The characteristic intensity I_0 and the

field E_0 are obviously material properties. We assume that the orientation of $\hat{l}$ is randomly distributed in the PDLC films.

To characterize the change in scattering of a PDLC film induced by the optical field of a laser, both heating and reorientational effects must be considered. We have separately characterized these phenomena in the absence of other applied fields.

For refractive index matched PDLC films, the scattering cross section is negligible when droplets are oriented with $\hat{N}$ along the direction of propagation of light, but is large otherwise. To a good approximation, the total scattering cross section is given by

$$\sigma = 3\,\sigma_0\,(\,\hat{N}\cdot\hat{E}_{opt}\,)^2 \tag{8}$$

where σ_0 is a material constant which depends on the refractive index anisotropy, Δn, and the refractive index of the host polymer. Since there is some contribution from multiple scattering, σ_0 may be thought of as an effective scattering cross-section which is not stricly independent of the density of droplets. The transmittance of a PDLC film with droplet number density ρ and thickness d is then

$$t = e^{-\rho\,3\,\sigma_0\,<\,(\,\hat{N}\cdot\hat{E}_{opt}\,)^2\,>\,d} \tag{9}$$

where the average $<\ >$ denotes the volume average over all droplets in the sample. When the liquid crystal in a PDLC film is heated into isotropic phase, the corresponding transmittance is that of a collection of isotropic spheres with cross-section σ_i, that is,

$$t_i = e^{-\rho\,\sigma_i\,d} \tag{10}$$

The usual eletro-optic effect in PDLCs as reported by Doane et al.[3] is shown in Fig. 3.

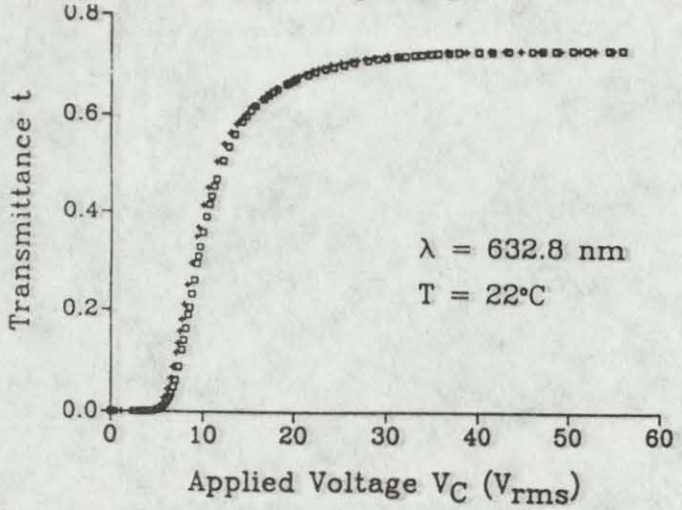

Fig. 3 Sample transmittance as a function of applied voltage. The symbol □ corresponds to increasing and + to decreasing applied voltage.

This figure gives the sample transmittance as function of applied voltage at the fixed temperature T=22 ^{o}C . As can be seen from Fig. 3, the sample is opaque before the application of a voltage or when the applied control voltage V_c is well below the threshold voltage V_{th}. After increasing the applied field so that $V_c \gg V_{th}$, the nematic director, and hence $\hat{N}$, the average direction of orientation in each droplet, aligns essentially parallel to the field. The sample (an index matched PDLC film) is transparent in this configuration as shown in Fig. 3.

Because the refractive indices of the liquid crystal, and, to a lesser extent, that of the polymer vary with temperature, the amount of light scattered by the sample shows a dependence on temperature. This effect is particularly pronounced in the vicinity of the nematic-isotropic transition of the liquid crystal. The transmittance of the sample without any applied field is shown in Fig. 4 as a function of temperature.

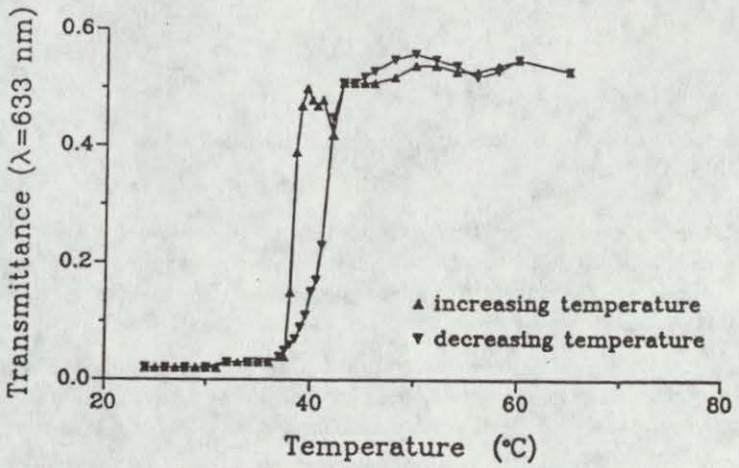

Fig. 4 Transmittance of a PDLC sample as a function of temperature.

The sample transmittance is low at low temperatures where the liquid crystal is in the nematic phase, due to the large average scattering cross section of the randomly aligned droplets. Above the nematic-isotropic temperature the transmittance increases, due to the small refractive index difference between the polymer and the liquid crystal, the scattering cross section of the droplets is reduced.

5. OPTICAL POWER LIMITING

There are two forms of optical power limiting behaviour which have been studied in PDLCs. The first employs the well known electro-optic effect, while the second involves switching phenomena using only optical fields.

a. Active Feedback Type

We have previously described [11] an OPL configuration of a PDLC which relies on an

optical sensor to control an AC driving voltage. The schematic diagram of the active feedback experiment system is shown in Fig. 5.

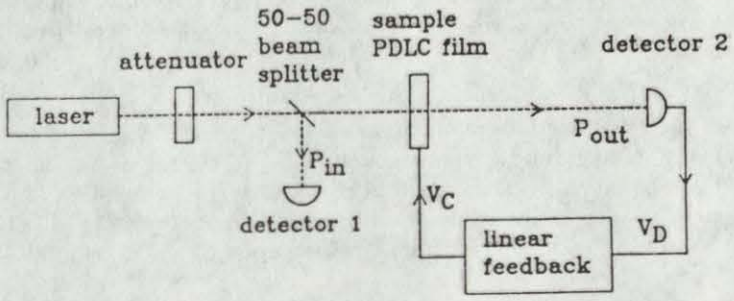

Fig. 5 Schematic of the experimental arrangement for active feedback type optical power limiting.

The intensity of the transmitted light is measured by a photodiode. The feedback circuit generates a voltage which is a linear function of the photodiode amplifier output, and this voltage is used to modulate the output of a signal generator. The 1 kHz sinusoidal output of the signal generator is applied to the sample cell via a step-up transformer.

The nonlinear dependence of the transmittance on the applied voltage V_c is responsible for the characteristic nonlinear response of the system in the presence of linear feedback. The power transmitted by the sample is $P_{out}=t\,P_{in}$, where t is the transmittance and P_{in} is the incident power.

The output voltage of detector 2 is proportional to P_{out}, and the voltage across the cell is a linear function of the detector output so that

$$V_c = V_0 + G\,t\,P_{in} \tag{11}$$

where V_0 is the offset and G is the gain of the feedback circuit. A very nearly ideal OPL action is obtained with **negative** feedback ($G<0$) as shown in Fig. 6. For low incident intensities, V_c and hence t are essentially constant, and P_{out} is proportional to P_{in}. As the incident power is increased, V_c decreases, reducing the transmittance and giving rise to optical power limiting behavior. By varying the feedback parameters, the characteristics of this behavior may be modified. For example, increasing V_0 increases the range where P_{out} is proportional to P_{in}, while changing G simply scales P_{in} and P_{out}, leaving the response otherwise unchanged. We have found this process to be easily achieved with response times on the order of one millisecond. Similar feedback effects have also been observed by others[12].

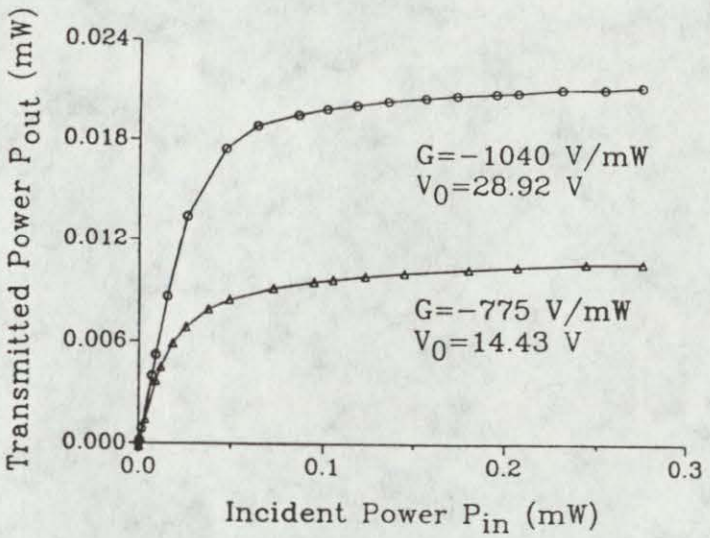

Fig. 6 Measured responses of the active power limiting system with different feedback parameters.

b. Passive Type

An all-optical OPL offers not only simplicity of design, but potential for faster response times as well. We have previously described[8] one arrangement where a PDLC with a stabilizing AC field was switched from a transparent to a scattering state. The experimental arrangement of the passive optical power limiter[8] is shown in Fig. 7. A CW Ar^+ laser was used as the pump beam and the sample transmittance was monitored using a 10 mW He-Ne laser. The beam of the Ar^+ laser is controlled by a pulse generator driven shutter, and is focused to a beam radius of 95 μm at the sample.

The sample transmittance for vertical and horizontal probe beam polarizations is shown as a function of the pump beam intensity in Fig. 8. The optical limiting behavior of these systems comes from both field induced reorientation of the liquid crystal in the sample and laser heating. Optical field induced reorientation produces an index mismatch and thus reduces the transmittance. Laser heating will change the inherent birefringence and eventually cause a phase transition of the liquid crystal from the nematic into the isotropic phase with a resulting increase in the scattering cross section. Power limiting behaviour by PDLC films have also been observed by others[13]; there the mechanism was attribued primarily to thermal effects.

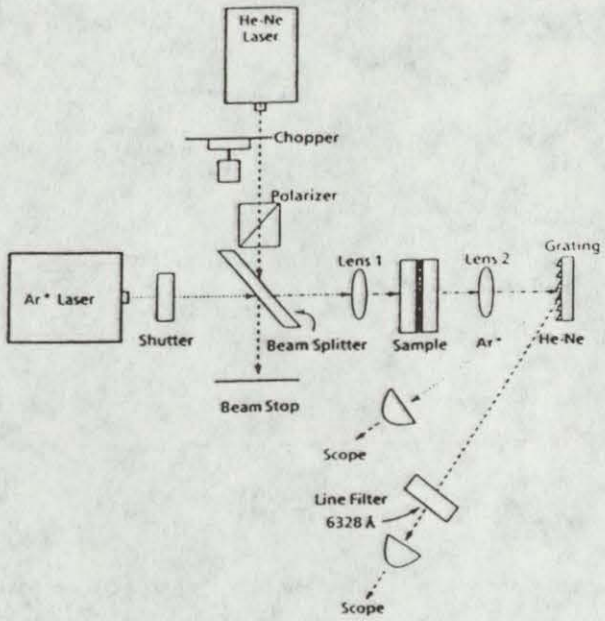

Fig. 7 Schematic of the experimental arrangement for passive type optical power limiting.

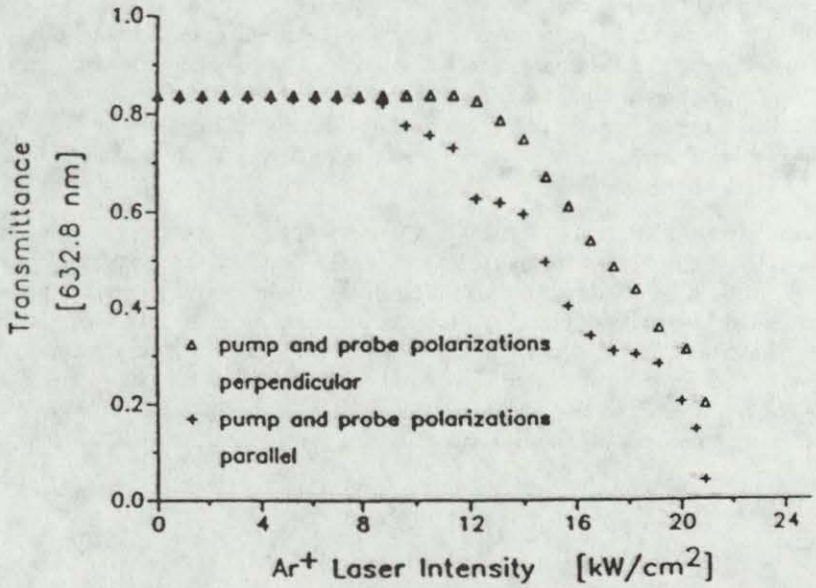

Fig. 8 Minimum transmittance as a function of pump beam intensity.

6. OPTICAL REORIENTATION vs. THERMAL EFFECTS

In order to characterize the relative contributions of optical reorientation and thermal effects, we have carried out detailed measurements of transmittance for two different geometries without any applied electric field. When the applied voltage $V_c=0$, the transmittance of a PDLC sample for parallel and perpendicular polarizations (the polarization of probe beam relative to that of pump beam) are

$$t_{||} = e^{-\rho\, 3\, \sigma_0 < (\hat{N} \cdot \hat{E}_{opt})^2 > d} \tag{12}$$

and

$$t_{\perp} = e^{-\rho\, \sigma_0\, \frac{3}{2} < 1 - (\hat{N} \cdot \hat{E}_{opt})^2 > d} \tag{13}$$

At low pump beam intensities the droplet directors are random, and $t_{||} = t_{\perp}$. It is expected that, with increasing intensity I, $t_{||}$ will decrease while $t_{\perp}$ will increase if the only effect of the pump beam is the reorientation of the droplet directors.

Fig. 9 shows the measured transmittance $t_{||}$ and $t_{\perp}$ of the sample as a function of the Ar^+ laser intensity.

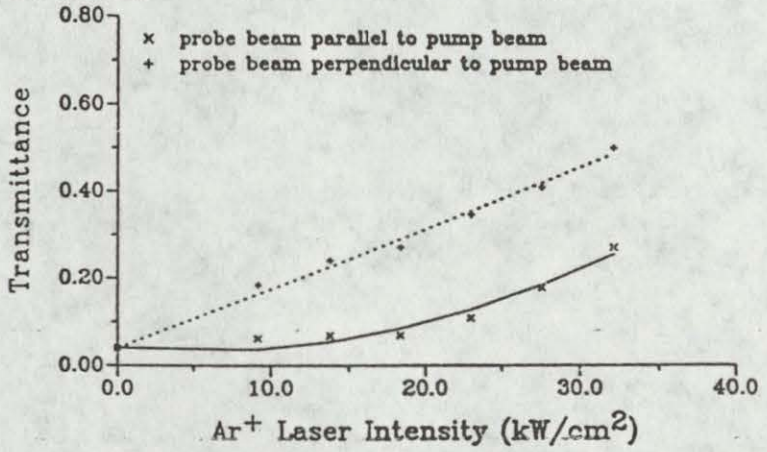

Fig. 9 Laser induced transmittance as a function of pump beam intensity for two different geometries.

The difference between $t_{||}$ and $t_{\perp}$ shows the existence of optical field induced reorientation; while the observed increase (instead of decrease) of $t_{||}$ with increasing pump beam intensity shows the existence of considerable laser heating. Increasing the temperature of the liquid crystal decreases the degree of orientational order. This reduces the birefringence, as well as the values of the elastic constants. The scattering cross-section of the droplets is therefore reduced due to changes in the refractive indices of the liquid crystal, as well as due to changes in the director field configuration. The detailed temperature dependence of the scattering cross section is difficult to calculate; however, we infer from Fig. 4, that the dominant effect is the change associated with the nematic-isotropic transition.

In order to separately assess the effects of laser induced reorientation and laser heating, we make the simplifying assumption that the sole effect of laser heating is to transform the nematic liquid crystal in some fraction y of the droplets into the isotropic phase. In this case, the transmittance for light polarized parallel and perpendicular to the pump beam polarization are[9]

$$t_{||} = t_i^{\,y} \cdot e^{-(1-y)\,\rho\,\sigma_0\,(1+2S_S)\,d} \tag{14}$$

and

$$t_{\perp} = t_i^{\,y} \cdot e^{-(1-y)\,\rho\,\sigma_0\,(1-S_S)\,d} \tag{15}$$

where the sample order parameter $S_S \equiv < P_2 (\hat{N} \cdot \hat{E}_{opt}) >$ and P_2 is the second Legendre polynomial. Eqs. 14 and 15 can be solved at once for y and S_S to give

$$y = \frac{\ln \left((t_{||}\, t_{\perp}^{\,2})^{1/3} / t_N \right)}{\ln (t_i / t_N)} \tag{16}$$

and

$$S_S = \frac{\ln (t_{||} / t_{\perp})\ \ln (t_N / t_i)}{3\ \ln \left((t_{||}\, t_{\perp}^{\,2})^{1/3} / t_i \right)\ \ln (t_N)} \tag{17}$$

where t_N is the transmittance of the unaligned nematic sample; that is, $t_N = t_{||} = t_{\perp}$ when $S_S=0$. The isotropic fraction y and the sample order parameter S_S as function of pump beam intensity are shown in Figs. 10 and 11, respectively.

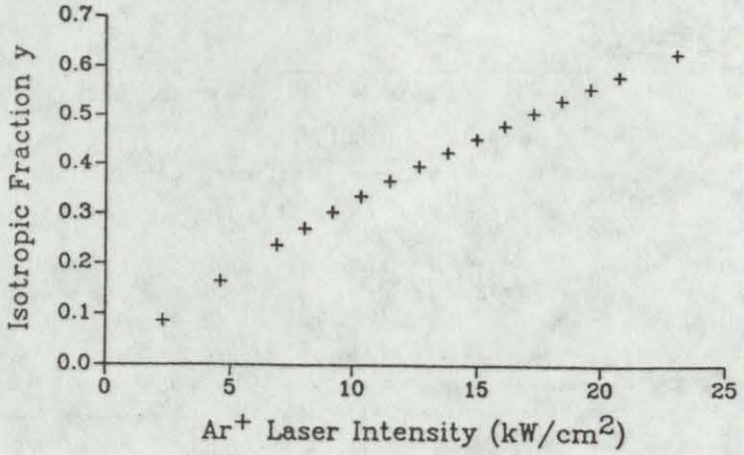

Fig. 10 Fraction y of isotropic droplets as a function of pump beam intensity.

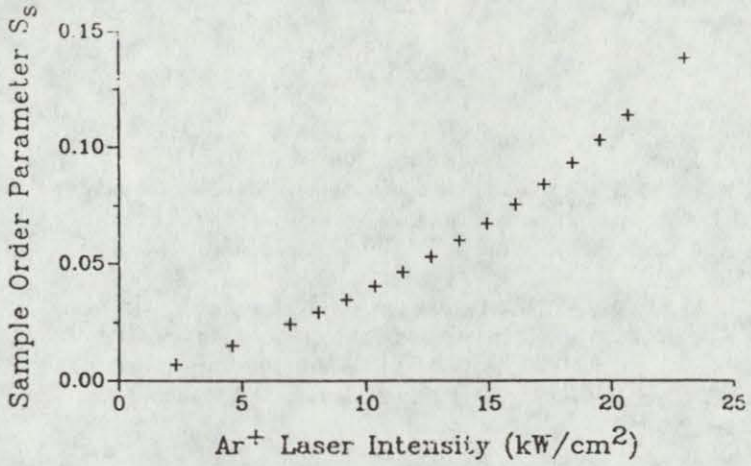

Fig. 11 Sample order parameter S_s as a function of pump beam intensity.

7. CONCLUSIONS

We have prepared the polymer dispersed liquid crystal samples and carried out measurements of the effects of optical fields on the transmittance of PDLC films. The nonlinear optical responses of PDLC films with or without applied voltage have been studied. Both optical field induced reorientation of the liquid crystal in the droplets and thermal effects are found in our measurements. We have proposed a simple formalism to separate these two effects and found the observed behaviour to be in reasonable agreement with the predictions of theory.

ACKNOWLEDGEMENTS

This work was supported by DARPA through US Army CECOM Center for Night Vision and Electro-Optics, contract DAAB07-88-C-F421. We gratefully acknowlege useful discussions with E. Von Stryland and M.J. Soileau of the Center for Research in Electro-Optics and Lasers as well as J. Pohlmann and E. Sharp at the U.S. Army Center for Night Vision and Electro-Optics.

REFERENCES

1. J.L. West, Mol. Cryst. Liq. Cryst.15, 427 (1988).
2. A. Golemme, S. Zumer and J.W. Doane, Phys. Rev. A 37, 559 (1988).
3. J.W. Doane, N.A. Vaz, B.-G. Wu and S. Zumer, Appl. Phys. 48, 269 (1986).
4. S. Zumer and J.W. Doane, Phys. Rev. A34, 3373 (1986).
5. J.W. Doane, A. Golemme, J.L. West, J.B. Whitehead, Jr. and B.-G. Wu, Mol. Cryst. Liq. Cryst. (in press).
6. B.-G. Wu, J.H. Erdmann and J.W. Doane, Liq. Cryst. (in press).
7. D. Allender, J. Kelly, P. Palffy-Muhoray and C. Rosenblatt (to appear).
8. P. Palffy-Muhoray and J.L. West, in Wave Propagation in Varied Media, SPIE Proc. 0927 (Orlando, 1988). P. Palffy-Muhoray, M.A. Lee and J.L. West, Mol. Cryst. Liq. Cryst. (in press).
9. P. Palffy-Muhoray, B.J. Frisken, J. Kelly and H.J. Yuan, SPIE Proc. 1105 (Orlando, 1989).
10. P. Palffy-Muhoray, in Liquid Crystal Chemistry, Physics and Applications, SPIE Proc. (in press) (Los Angles, 1989).
11. J.Y. Kim and P. Palffy-Muhoray, J. Appl. Phys. 66, 362 (1989).
12. R.L. Sutherland, SPIE Proc. 1080, (Los Angeles,1989)
13. F. Simoni, C. Cipparrone, C. Umeton, G. Arabia and G. Chidichimo, Appl. Phys. Lett. 54, 896,1989.

Assessment of Internal Electric Fields in Polymer Films Using Electrochromic Dyes

G.T. Davis, A.S. DeReggi, and N. Tsutsumi[a]
National Institute of Standards and Technology
Gaithersburg, MD 20899

Polymer films with second harmonic generating properties can be produced by incorporating NLO molecules (e.g. electrochromic dyes) in the polymer which are then aligned preferentially in a high electric field[1]. When using amorphous polymers, the alignment is achieved above the glass transition temperature and the alignment is frozen in by cooling below Tg. With semicrystalline ferroelectric polymers such as polyvinylidenefluoride and its copolymers with trifluoroethylene, internal electric fields created by preferentially aligned polar crystallites can align the dye molecules in the non-crystalline regions of the polymer which are above Tg at ambient temperatures[2]. We have used measured changes in the UV-visible absorption spectra of electrochromic dyes in a variety of polymer films to deduce the internal fields to which they are subjected as well as to investigate the parameters which influence these fields. Dyes such as 4-dimethyl amino-4'-nitrostilbene and 4-amino-4'-nitroazobenzene are particularly useful because data on dipole moments, transition moments, and directions within the molecules have been reported.

[a] Present address: Kyoto Institute of Technology, Kyoto, Japan

[1] K.D. Singer, J.E. Sohn and S.J. Lalama, Appl. Phys. Lett. 49, 248 (198[illegible]).

[2] J.R. Hill, P. Pantelis and G.J. Davies, Ferroelectrics 76, 435 (198[illegible]).

SELF-ASSEMBLED NONLINEAR OPTICAL (NLO) STRUCTURE USING LANGMUIR-BLODGETT TECHNIQUE

SUDHA KUMAR, R. SAI KUMAR, LYNNE SAMUELSON, JAYANT KUMAR AND SUKANT TRIPATHY

DEPARTMENTS OF CHEMISTRY AND PHYSICS
UNIVERSITY OF LOWELL
LOWELL, MA 01854

ABSTRACT

Novel electroactive materials based on aromatic Schiff base compounds possessing large second- and third-order optical nonlinearities have been processed as Langmuir-Blodgett (L-B) thin films. The optimal process window for these classes of compounds has been extensively investigated. Film growth characteristics have been investigated as a function of (i) temperature and pH of the subphase; (ii) the nature of the polar end groups and composition of the material in the mixed monolayers. Solid state polymerization in appropriately assembled functionalized monolayers has been carried out.

The stable monolayer system including appropriately oriented electro-optic Schiff base compound is by definition a noncentrosymmetric structure. X- and Z-type growth or alternate layering with structurally different monolayer forming materials will lead to bulk noncentrosymmetric organizations. These superlattices are expected to possess unique combination of electronic and optical properties. Thus systems with large $\chi^{(2)}$ as well as large and fast $\chi^{(3)}$ are obtained by this technique. Results of these studies and spectral characterization of these mono- and multilayers on different substrates will be presented at the meeting.

OPTICAL NOTCH FILTERS FOR LASER PROTECTION

S.H. Chen and S.D. Jacobs
Department of Chemical Engineering and
Laboratory for Laser Energetics
University of Rochester
Rochester, NY 14627

An optical notch filter (ONF) is capable of rejecting incident optical radiation in a selected wavelength region while transmitting the rest of radiation. Existing technologies for the fabrication of ONF are based on holography, multilayer interference, and cholesteric liquid crystallinity. While holographic and liquid crystal filters suffer from the lack of long-term stability because of hygroscopic and fluid nature, respectively, multilayer interference filters require sophisticated processing techniques. To surmount the stability problem, there have been intensive research activities in recent years to design and synthesize polymer liquid crystals that exhibit the property of selective wavelength reflection.

Polymeric materials offer a unique advantage over low molar mass substances in that the needed cholesteric mesophase attained by annealing at a proper elevated temperature can be locked in the glassy matrix via subsequent quenching. Cholesteric mesophase is characterized by a helical structure at the supramolecular level. An ONF requires both right- and left-handed helices as induced in suitable materials. Although plenty of polymeric materials are known to possess the left-handed structure, there is a paucity of thermotropic polymers giving rise to the right-handed structure.

We will report on materials issues relevant to the optical applications of existing cholesteric liquid crystalline polymers and to design and synthesize novel, especially right-handed, polymeric systems with improved optical properties and processability into composite thin films with and without substrates. Fundamental issues related to structure-property relationships will also be discussed.

Corona Onset Poled Polymeric Films for Ultrashort Pulse Nonlinear Optics

By

A. Dienes, D. Yankelevich, M. A. Mortazavi,
A. Knoesen, and S. T. Kowel

Organized Research Program
on Polymeric Ultrathin Film Systems

and

the Department of Electrical Engineering
and Computer Science
University of California, Davis
Davis, CA 95616

Corona Onset Poled Polymeric Films for Ultrashort Pulse Nonlinear Optics

A. INTRODUCTION

The large hyperpolarizability of organic molecules can be utilized only if the molecules are organized into a noncentrosymmetric structure. One method of making such structures is to deposit polymeric films doped with the active molecules, and poling these films using an electric field. Recently, we reported a technique of poling [1,2] which resulted in more effective ordering than other methods: Corona Onset Poling at Elevated Temperatures (COPET). The resulting films exhibited effective $\chi^{(2)}$ significantly larger than commonly used inorganic crystals. There are two important areas in which these films may find applications. One is planar geometry guided wave optics, and the second is ultrashort pulse nonlinear optics in nonguided configurations. The latter is of special interest since for second harmonic or sum and difference frequency generation with femtosecond duration pulses, group velocity dispersion severely limits the useable length of the nonlinear medium. In some experiments, crystals as thin as 55 μm have been used [3]. Since the effective $\chi^{(2)}$ of the poled organic films is considerably larger than that of most inorganic crystals, films of the order of only a few micrometer thickness can give comparable signals. Since the film thickness is shorter than the coherence length, phasematching is not an issue and they may be used at different wavelengths. Additionally, they are very easy and inexpensive to make and have been shown to be rather durable. In this paper, we first give in Section B a brief summary of the COPET process and of the second order nonlinear properties of the resultant films. In Section C, we discuss some of the possible advantages of these films for ultrashort pulse nonlinear optics. In Section D, we give the results of an experiment which demonstrates for the first time that these films can be practically used in ultrashort pulse optics, followed by concluding discussions (Section E).

B. NONLINEAR CHARACTERISTICS OF COPET POLED FILMS

Figure 1 shows the experimental arrangement for the COPET method of poling. The details of this process have been recently reported. It involves subjecting the sample to a corona onset discharge, while raised to above the glass-rubber transition temperature. The large internal electric fields orientate the active dye molecules. Subsequently, the temperature is lowered and the discharge is removed. There is then a period of stabilization during which the orientational order drops because some of the lined up dipoles become disordered. However, after approximately 100 hours the orientational order and the resulting microscopic second order susceptibility completely stabilize and remain so for an extended period. Figure 2 shows the results obtained on a 1.2 μm thick film of PMMA doped with 2 x 10^{20} moles/cm^3 concentration of the dye Disperse Red 1. Measurement of the orientational order was obtained by an independent technique that involves comparison of the dichoic absorption after poling, with the unpoled absorption. The effective $\chi^{(2)}$

was measured relative to quartz using a direct comparison of second harmonic generation with that in a known quartz crystal. Both the stabilization of the ordering and the excellent properties of the stabilized film are clearly manifested. The stable orientational order is larger than obtained by other techniques and the value of $\chi^{(2)}$ is ≈ 10 times higher than the $\chi_{11}^{(2)}$ of quartz.

Figure 3 shows the basic geometry for the second harmonic generation. This will be relevant also for the ultrashort pulse experiment presented in Section C. The aligned dipoles are shown schematically. It has been shown that the ordered film has ∞ mm group symmetry and the effective $\chi^{(2)}$ for P-polarization and detection is given by [4]

$$\chi_{eff} = \left| (2\chi_{15} + \chi_{31}) \cos^2\theta \sin\theta + \chi_{33} \sin^3\theta \right| \qquad (1)$$

Without giving the exact analytical expression showing two symmetric peaks for the efficiency of the second harmonic generation (SHG), it is qualitatively obvious from Figure 3 and from equation (1) that the SHG will be zero at normal incidence and will peak around Brewster angle incidence. This is because the E field coupling to the nonlinear dipoles is zero at normal incidence and increases with increasing θ. However, the coupling of the P-polarized fields into and out of the film is most efficient at Brewster's angle. Figure 4 shows the variation of the SHG with the angle θ showing two symmetric peaks. Note also that, although there is no phase matching, there are no Maker fringes since the 1.2 μm thickness is much smaller than the coherence length.

C. POTENTIAL USES OF POLED POLYMERIC FILMS IN ULTRASHORT PULSE OPTICS

One area in which poled polymeric films may find applications is in nonlinear optics with femtosecond duration pulses. The reason for this is that group velocity dispersion in many cases severely limits the useable interaction length. Extremely thin crystals are rather difficult and expensive to produce. Poled polymeric films thus may replace thin inorganic crystals in some experiments if they can perform comparably. We will now examine briefly how GVD limits some second order nonlinearity dependent experiments, and thus attempt to ascertain the potential of poled organic films.

1. Second Harmonic Generation (SHG)

In SHG with femtosecond pulses, the useable length of the nonlinear medium is limited by the group delay difference between the fundamental and the second harmonic. This is given by [5]

$$\tau_D\left(\lambda_1 , \frac{\lambda_1}{2}\right) = \ell\left[\frac{1}{v_g(\lambda_1)} - \frac{1}{v_g(\lambda_1/2)}\right] = \frac{\ell\lambda_1}{c}\left\{\frac{dn}{d\lambda}\Big|_{\lambda_1} - \frac{1}{2}\frac{dn}{d\lambda}\Big|_{\frac{\lambda_1}{2}}\right\} . \qquad (2)$$

The SH pulses are not significantly broadened only if τ_D is shorter than the pulse duration. The physical explanation of this effect is straightforward. The "source" nonlinear polarization is generated by the fundamental and its envelope travels with group velocity $v_g(\lambda_1)$. The envelope of the SH itself, however, travels with group velocity $v_g(\lambda_1/2)$. Thus source and effect separate in time and if this separation is comparable or longer than the pulse duration of the SHG is broadened. In Figure 5, we show τ_D vs. fundamental wavelength λ for the nonlinear crystal βBaBo which has been used recently in intracavity femtosecond SHG[1]. The values were calculated using the Sellmeyer formula for this material. As can be seen from the figure, τ_D rapidly increases toward shorter wavelengths. For example, for SHG using a hypothetical 50 fs pulse at λ_1 = 520 nm (wavelength of mode-locked Coumarin dye laser [6]), to keep $\tau_D \leq 25$ fs and thus avoid broadening, the crystal would have to be less than 20 μm thick.

2. Correlation Measurements

To measure duration of ultrashort pulses, nonlinear correlations are commonly used. As shown schematically in Figure 6, two pulses are separated by a variable delay τ. The combination is introduced into a second order nonlinear material, where the sum frequency is generated, which is then detected by a slow detector which effectively integrates the output. The resultant signal, plotted vs. the delay τ, gives the correlation of the two pulse envelopes. If pulse 2 is the same as pulse 1 (delayed by τ) the second harmonic is generated and the output I vs. τ contains the autocorrelation of the pulse, thus measuring the pulse with itself. If the two pulses are at different frequencies then the sum frequency is generated and the output gives the crosscorrelation of the two pulses, i.e. measuring one pulse with the other.

The resolution of these type of measurements is also limited by GVD, but in a different way for the two cases [7]. For autocorrelation, although the SHG output is broadened by GVD in the manner described in the previous section (A1) this does not form a limitation since the output is time integrated by the slow detector. The only limitation is the GVD broadening of the fundamental pulses which influences the overlap. This effect is due to group velocity differences within the spectrum of the pulse and is much smaller than τ_D. Its value is given by

$$\tau_D^1 = \ell\Delta\left(\frac{1}{v_g}\right)_{\text{fundam.}} = \frac{\ell\lambda_1}{c}\,\Delta\lambda_1\,\frac{d^2n}{d\lambda^2} \qquad (3)$$

For example, for an 8 fs pulse at $\lambda_1 = 600$ nm and crystal thickness of 200 μm, we calculate for βBaBo $\tau_D^1 \approx$ 10fs and for KDP (commonly used for these measurements) $\tau_D^1 \approx 1$ fs. This is a much less severe limitation than that for second harmonic generation.

For crosscorrelations, however, the pulse overlap is affected by the delay due to GVD between the two different fundamental frequencies. The broadening parameter, which limits the resolution in a rather complicated way [7] is

$$\tau_D(\tau_1, \tau_2) = \ell\left[\frac{1}{v_g(\lambda_1)} - \frac{1}{v_g(\lambda_2)}\right] = \frac{\ell}{c}\left\{\lambda_1\frac{dn}{d_\lambda}\Big|_{\lambda_1} - \lambda_2\frac{dn}{d\lambda}\Big|_{\lambda_2}\right\} \qquad (4)$$

We note that for the special case when pulse 2 is the second harmonic of pulse 1, the broadening parameter $\tau_D(\lambda_1, \lambda_2)$ is the same as $\tau_D(\lambda_1, \lambda_1/2)$ given by equation (2). It's limiting effect, however, manifests in the crosscorrelation in a more complicated way [7]. This case is of special interest because ultraviolet femtosecond pulses which are generated by frequency doubling can be measured only by crosscorrelation with the fundamental. As the curve of Figure 5 shows, extremely short crystals must be used for crosscorrelation measurement of femtosecond duration pulses.

It is evident from the above discussion that the necessity for extremely thin nonlinear media for ultrashort pulse nonlinear experiments make poled polymeric films with their high nonlinear coefficients an attractive alternative. For example, using the known value of χ_{eff} for βBaBo and the value we measured at $\lambda_1 = 1.06$ μm for the Disperse Red 1 doped poled polymeric film, we estimate that a 4 μm thick film would give approximately the same amount of SH signal as a 21 μm thick crystal of βBaBo. In the above estimate, we assumed that βBaBo is phase matched, but that in the 4 μm thick film phase mismatch can be ignored. We also ignored absorption losses in the film. Given the low cost and ease of making poled films, it is clear that they may be suitable for some ultrashort pulse applications.

3. Factors Limiting Poled Film Performance

We must also examine some of the limitations of these films. Among these are (i) absorption of the active dye; (ii) lack of phase matching; (iii) power damage; and (iv) unknown effects of possible resonance enhancement. For simplicity, we discuss these effects for the case of SHG (either for its own sake or for the purpose of autocorrelations).

Absorption at the SH wavelength, together with lack of phase matching, introduces a factor $F(\alpha, \Delta k)$

$$F(\alpha, \Delta k) = \bar{e}^{\alpha \ell} \left| \text{sinhc} \frac{(\alpha + i\Delta k)\ell}{2} \right|^2 \tag{5}$$

into the SHG efficiency, where $\Delta k = k(2\omega) - 2k(\omega)$ and α is the power absorption coefficient. This factor multiplies the quadratic dependence on length and χ_{eff}. Thus,

$$I_{SH} \propto \chi^2_{eff}\, \ell^2\, F(\alpha, \Delta k) \tag{6}$$

Clearly, strong absorption can be a serious limitation and also the lack of phase matching limits the useful thickness to about one-half the coherence length ($\Delta k \ell_c = \pi$). In Figure 7(a), we show the absorption spectrum of the dye Disperse Red 1. At the fundamental wavelength of λ = 610 nm (RhGG CPM dye laser), there is essentially no absorption but at the SH wavelength there is finite absorbance giving $\alpha = 3 \times 10^{-5}$. In Figure 7(b), we show $\ell^2 F(\alpha, \Delta k)$ vs. film thickness for this value of α and $\Delta k = 6.6 \times 10^5\ m^{-1}$ which is a preliminary result found for the COPET Disperse Red 1 polymer film. Clearly, above $\ell \cong 4\ \mu m$, increasing film thickness is no longer useful for this particular system. With regard to power damage of the film, this can be due to two causes. If there is no absorption of the fundamental, the damage can be caused by the effect of the high optical frequency electric field on the active molecule. Furthermore, if there is a finite absorption at the wavelength of the high intensity fundamental beam, heating can cause damage. Fundamental absorption thus should be avoided. Fortunately, there exists a rich variety of dyes and proper choice for a given application should be able to minimize this problem.

Finally, with regard to possible resonance enhancement of the $\chi^{(2)}$ and how it may effect ultrashort pulse nonlinear optics in poled films, this question has not hitherto been investigated. Clearly, in the presence of nearby absorption bands some resonance enhancement may be present. Thus, a value of $\chi^{(2)}$ measured at a given wavelength may not be exactly the same at another. It is thus necessary to carry out wavelength dependent measurements of $\chi^{(2)}$ in these films. Additionally, there is the question of whether resonant enhancement may influence time response.

Second harmonic generation is, of course, an instantaneous effect. That is to say, the nonlinear polarization instantaneously disappears if the fundamental field is removed. However, resonance enhancement could cause population changes, as well as coherent state superposition whose finite decay could influence correlation measurements for which two fundamental pulses separated in time are involved. Although resonant enhancement of $\chi^{(2)}$ in dyes has been investigated [8] with slow pulses, possible effects in ultrashort pulse,nonlinear optics have not been studied.

D. EXPERIMENT

The experiment we report [8] is the autocorrelation measurement of a femtosecond pulse at 0.6 μm wavelength, using the COPET poled film described in Section B. The objective of the experiment is two-fold. One, to obtain a useful autocorrelation and thus to confirm the practical usefulness of these films. Second, to verify that no critical limitations exist, due to possible damage to the film, absorption losses, and other factors such as possible resonance enhancement, etc. We made no attempt here to measure the efficiency of the SHG. The source of the ultrashort pulses was a colliding pulse, modelocked CW dye laser operating at $\lambda_1 = 614$ μm. The experimental setup (Figure 8) consisted of a standard colinear autocorrelator and associated electronics. The pulses were first measured using a 200 μm thick KDP crystal and were found to be 220 fs long (assuming sech^2 shape). Then the crystal was removed and replaced by a sample of our poled film. The fundamental beam was focused onto the film by a 10x microscope objective. The fundamental and second harmonic output beams were spatially separated by Pellin-Broca prism. The film sample was a 1.1 μm thick film of PMMA doped with 2×10^{20} molecules/cm^3 DR1 deposited by spin casting onto a glass substrate and poled by COPET, and stabilized over a one month period. The sample was placed at the experimentally determined nonlinear Brewster angle (≈ 57°) which coincides with the maximum of the second harmonic intensity. The substrate used for the film deposition was a 1 mm thick BK7 substrate which has substantial absorption at the second harmonic wavelength (307 nm). In order to avoid attenuation of the second harmonic, the sample was placed such that the fundamental pulse train passed first through the glass. Because the pulses in this experiment were around 200 fs long, passage through the BK7 substrate does not significantly broaden them. However, for use with pulses of around 10 – 20 fs duration, the film system should be operated such that the fundamental pulse train is directly incident on the film. In this case, a substrate with negligible attenuation at the second harmonic wavelength is required. Note that in such a configuration, broadening of the second harmonic in the substrate does not effect the correlation measurement since this output signal is integrated by the slow detector.

Figure 7(a) shows that the effect of the absorption at the fundamental wavelength is negligible, but that at the second harmonic wavelength does cause a reduction of the signal [4]. The combined effects of this absorption and of Δk is approximately a factor of 0.8. This posed no problem in our experiment but would be a limitation for much thicker films. With regard to damage, it was found that by keeping peak power density of the fundamental below $\approx$ 200 MW/cm^2 damage to the film could be completely avoided. However, for fundamental intensity of $\approx$ 0.5 GW/cm^2 permanent damage was found to occur. This manifested itself in lower SH signal and a lower than expected contrast ratio. It is probably due to a small residual absorption of the strong 0.6 μm fundamental wave. Both the SH absorption and damage limitations can be improved by using a dye with spectrum slightly shifted toward longer wavelengths. The measured autocorrelation is shown in Figure 9b. It manifests the correct 3:1 contrast ratio, and gives a measured width of 220 fs, identical to that measured using the KDP crystal. We also show, for interest, the measurement for the case when damage was manifested (Figure 9a). The contrast ratio is seen to be 2:1, we have no detailed explanation at present for this effect.

It should be mentioned also at this point that in these measurements we saw no evidence of any time response limitations as speculated in Section C3. Whether this is due to the fact that any resonance enhancement in this experiment would be only at the weak SH or simply that resonant enhancement does not play a role here is impossible to tell from these results. Further theoretical and experimental work is necessary to answer these questions.

E. CONCLUDING DISCUSSION

In conclusion, we have examined in some detail how thin organic polymeric films poled by the COPET process can be used in ultrashort pulse, nonlinear optics. It is clear that due to their high nonlinear coefficient and the ease of making films of the order of 1 – 10μm thickness they have a strong potential for nonlinear optics application which utilizes femtosecond duration pulses. The main limitations are absorption (of either fundamental or of the SH) and lack of phasematching geometry. The limitation due to absorption can be overcome by choosing materials with narrow absorption spectra. Recently, our group reported COPET poling of a new type of organic film consisting of a PMMA backbone to which a coumarin chromophore is attached (CMMA-MMA) [9]. Compared to DR1/PMMA mixtures, CMMA-MMA sidechain polymers exhibit comparable second order nonlinearities but with significantly increased stability with respect to temperature changes. At 614 nm the absorption of the fundamental beam is negligible, the FWHM is approximately 60 nm (120 nm for DR1/PMMA), and the SH signal falls between absorption

peaks. As a result of these favorable characteristics, our research group is currently pursuing CMMA/PMMA for ultrashort pulse applications.

REFERENCES

[1] A. Knoesen, M. A. Mortazavi, S. T. Kowel, A. Dienes, and B. G. Higgins, Digest of Topical Meeting on Nonlinear Optical Properties of Materials (OSA, Washington D.C., 1988), pp. 244-247.

[2] M. A. Mortazavi, A. Knoesen, S. T. Kowel, B. G. Higgins, and A. Dienes, JOSA, v. 6B, pp. 733-741 (1989).

[3] D. C. Edelstein, E. S. Wachman, L. K. Cheng, W. R. Bosenberg, and C. L. Tang, Appl. Phys. Lett., v. 52, pp. 2211-2213 (1988).

[4] Y. R. Shen, The Principles of Nonlinear Optics (Wiley, N.Y., 1984).

[5] W. H. Glenn, IEEE J. Quantum Elec., v. QE-5, pp. 284-290 (1969).

[6] P. M. French, M. M. Opolinska and J. R. Taylor, Optics Letters, v. 14, pp. 217-218 (1989).

[7] A. W. Weiner, IEEE J. Quantum Elec., v. QE-19, pp. 1276-1283 (1983).

[8] M. A. Mortazavi, D. Yankelevich, A. Dienes, A. Knoesen, S. T. Kowel, and S. Dijaili, Appl. Optics, v. 28, pp. 3278-3279 (1989).

[9] A. Knoesen, M. A. Mortazavi, S. T. Kowel, J. M. Hoover, R. A. Henry, and G. A. Lindsay, OSA Annual Meeting, Orlando, Paper MC3 (1989).

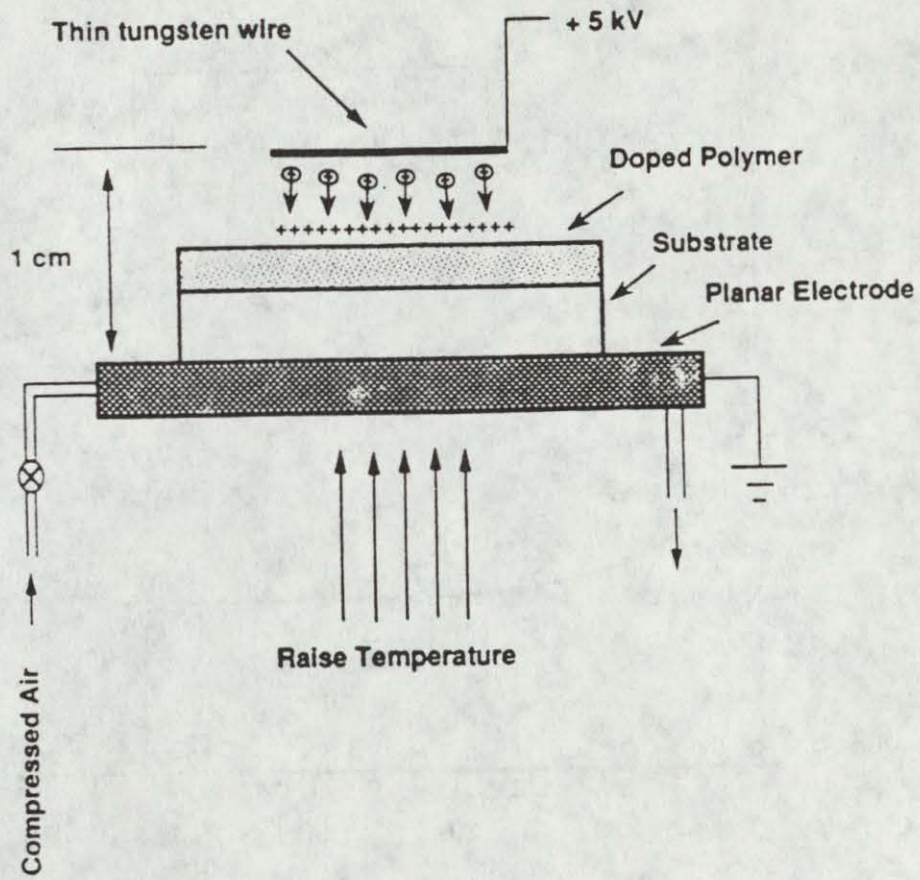

Figure 1 Experimental arrangement for COPET poling with wire electrode.

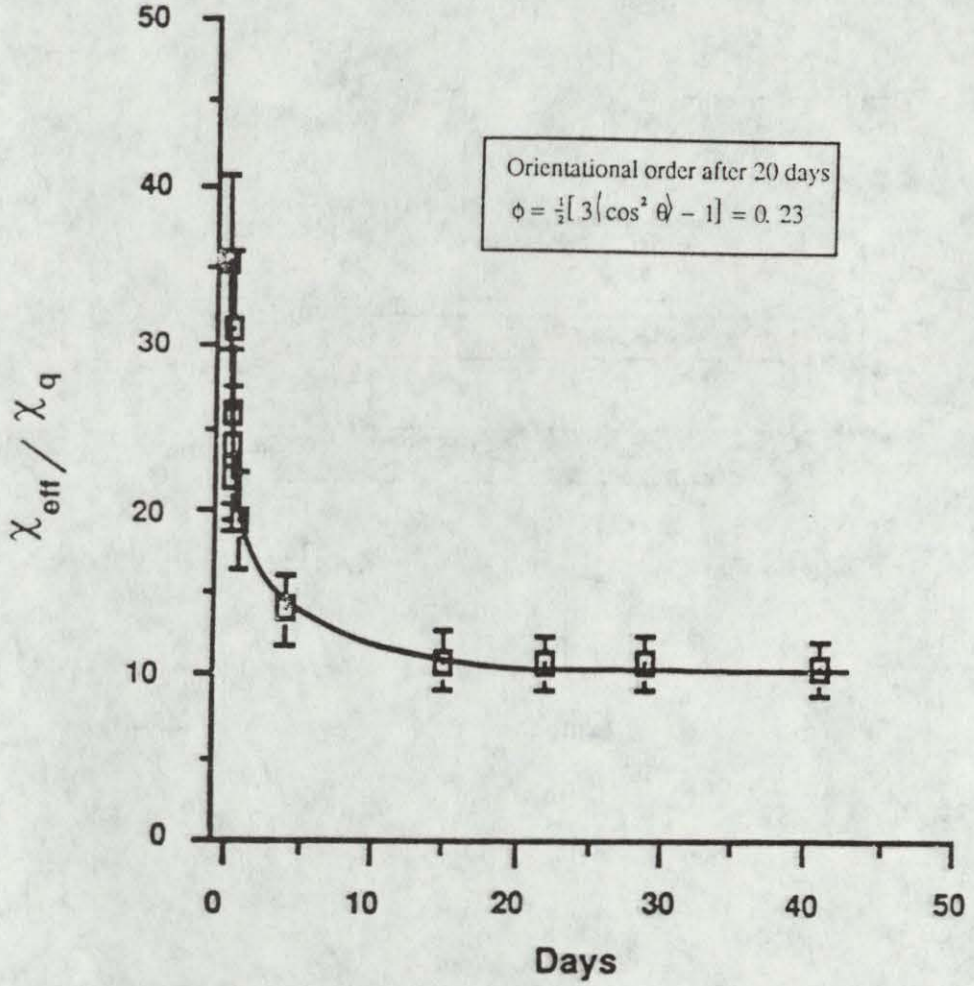

Figure 2 The second harmonic $\chi^2_{eff} / \chi^{(2)}$ quartz for COPET poled PMMA/DR1 films as a function of time.

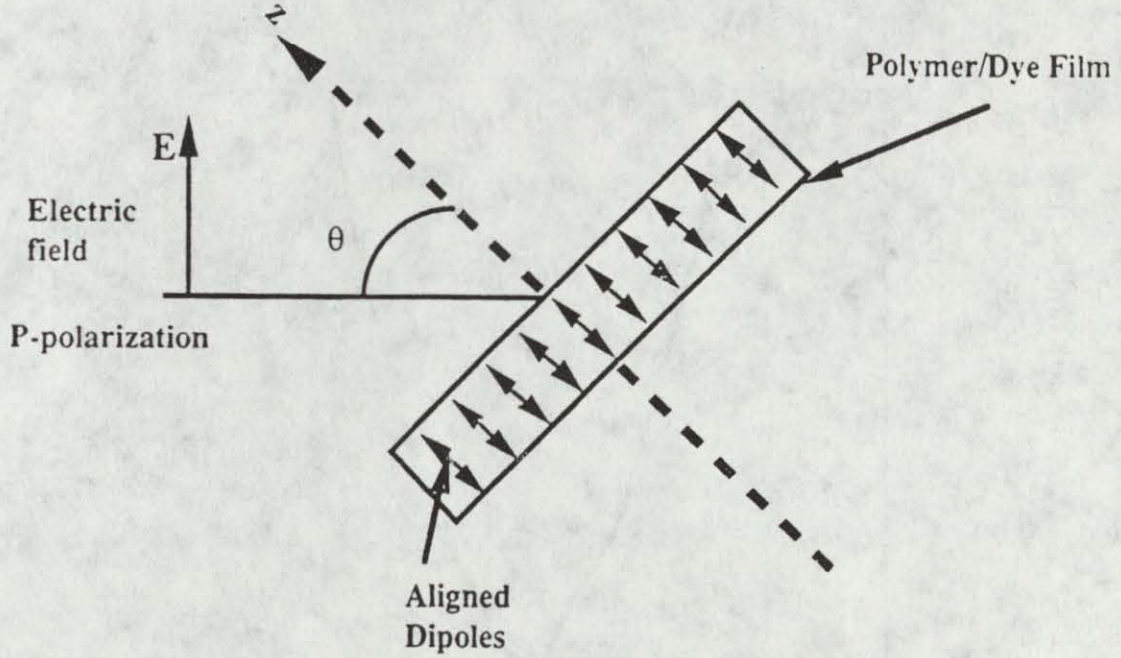

Figure 3 Geometry of SH generation in poled films. A P-polarized field is incident at the angle θ (Brewster angle). The arrows represent the dye molecule dipoles.

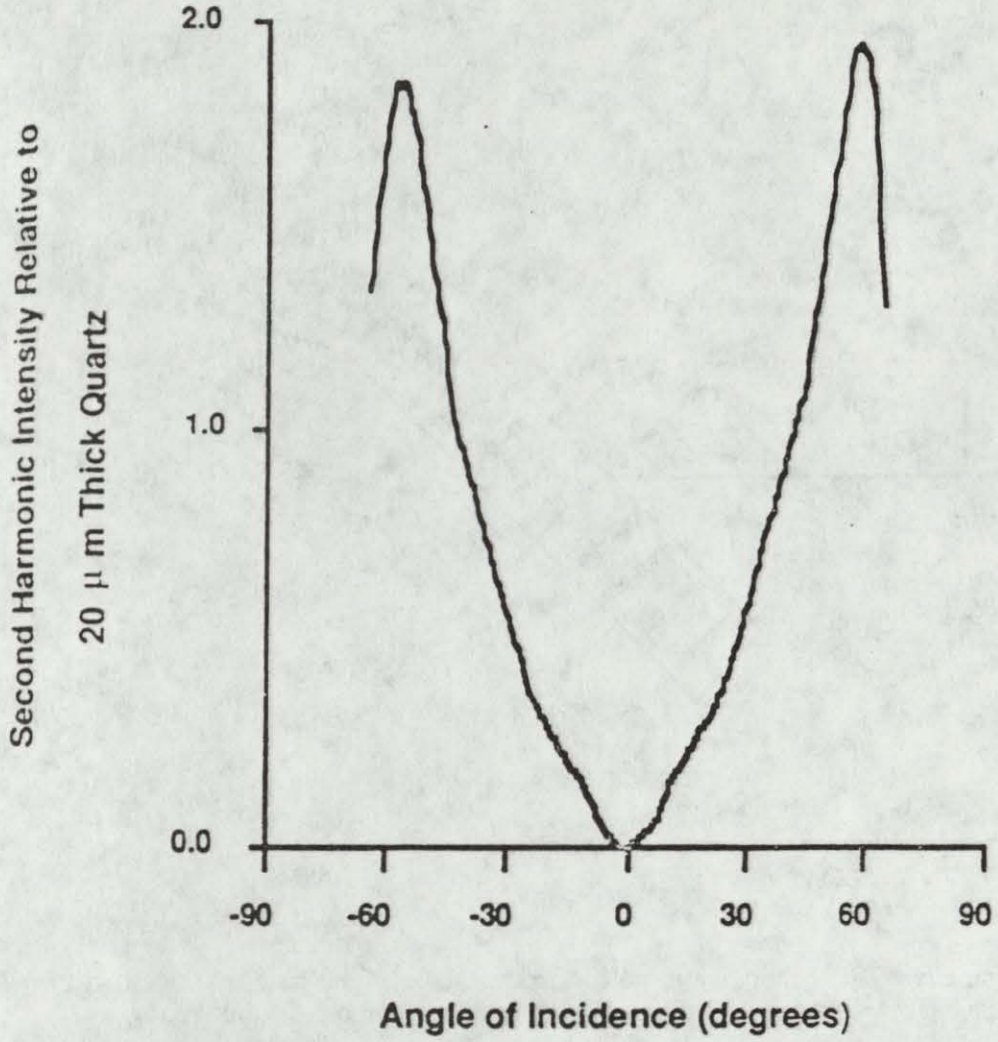

Figure 4 The second harmonic intensity from a PMMA/DR1 film relative to a 20 μm thick quartz plate.

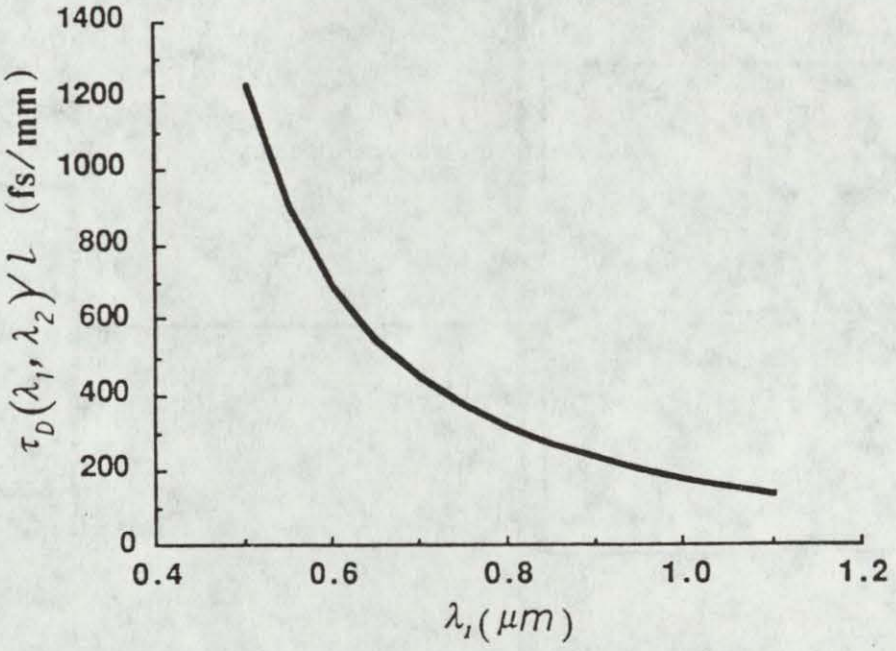

Figure 5 The broadening parameter $\tau_D(\lambda_1, \lambda_2)/\ell$ for βBaBo for the case when $\lambda_2 = \lambda_1/2$.

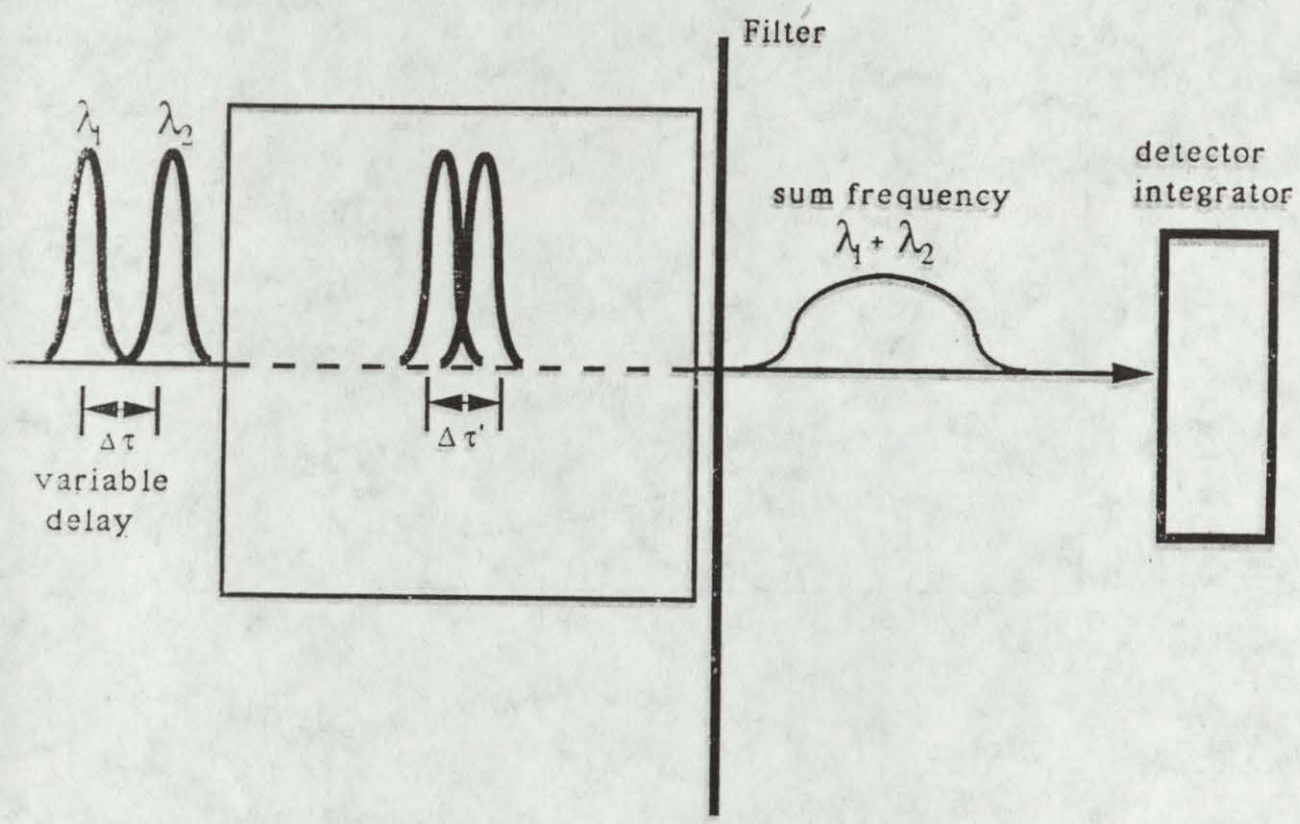

Figure 6 Schematic for nonlinear correlation measurements of ultrashort pulses.

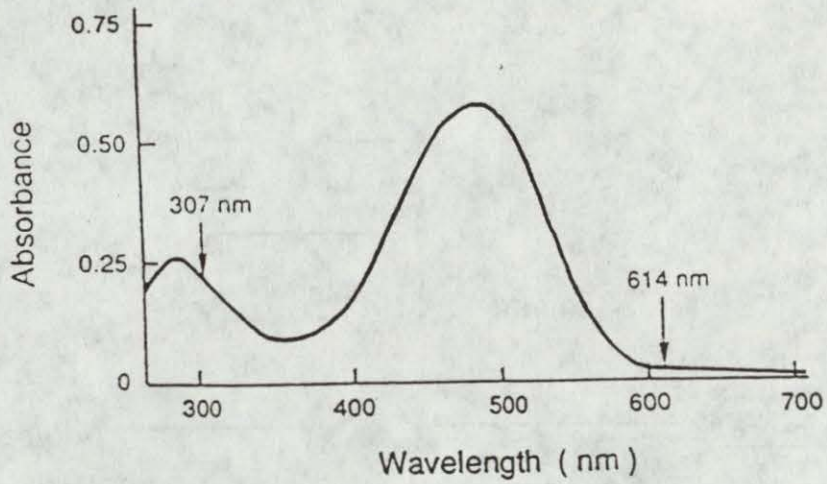

(a)

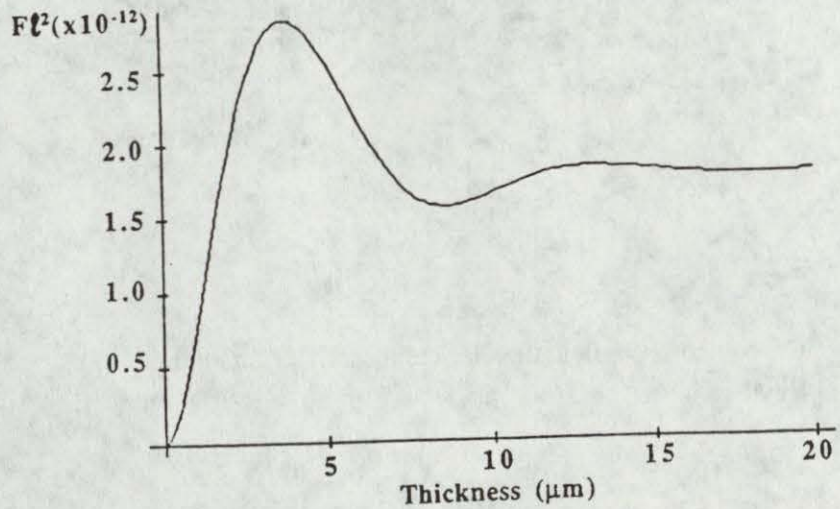

(b)

Figure 7 (a) Absorbance spectrum of the 1.1 μm thick film sample doped with 2×10^{20} molecules/cm^3 DR1 dye. (b) Theoretical wire for the effects of phase mismatch and absorption on the relative second harmonic intensity. ($\alpha = 3 \times 10^5$ m^{-1}, $\Delta k = 7 \times 10^5$ m^{-1}).

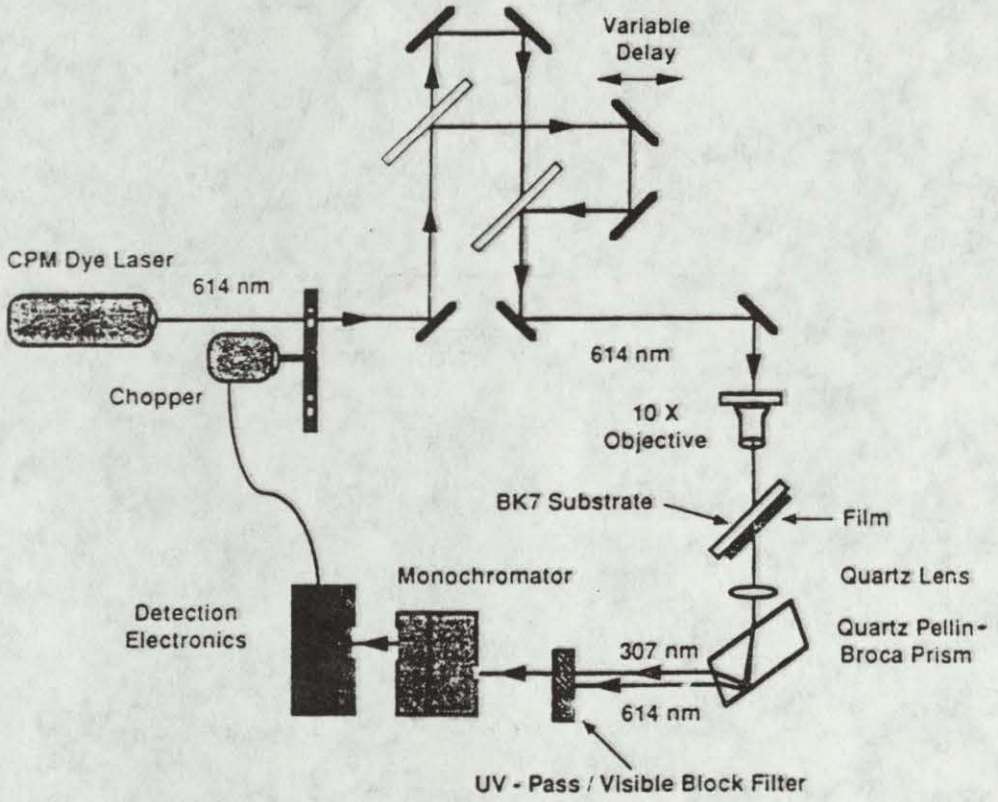

Figure 8 Experimental configuration for collinear SHG autocorrelation using a polymetric thin film.

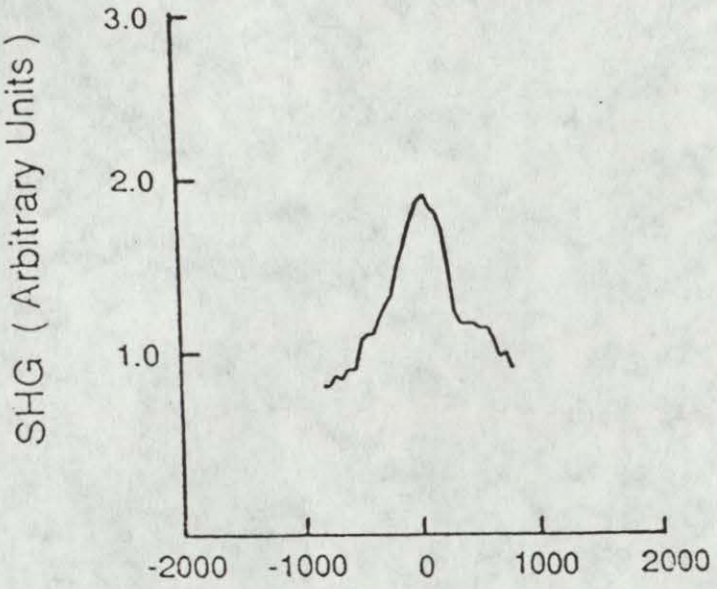

(a)

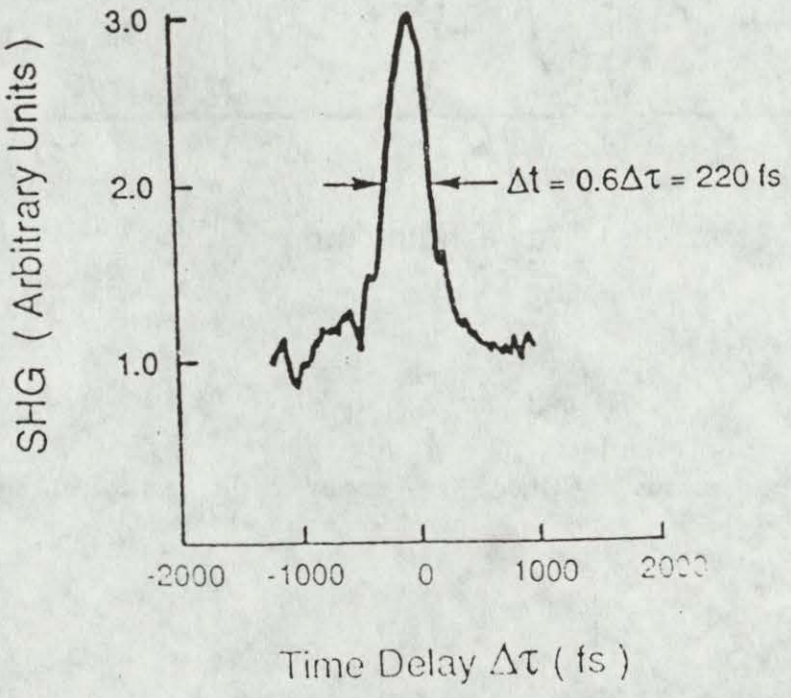

(b)

Figure 9 Autocorrelation traces using the film sample as SHG material. (a) Undamaged sample. (b) Damaged sample.

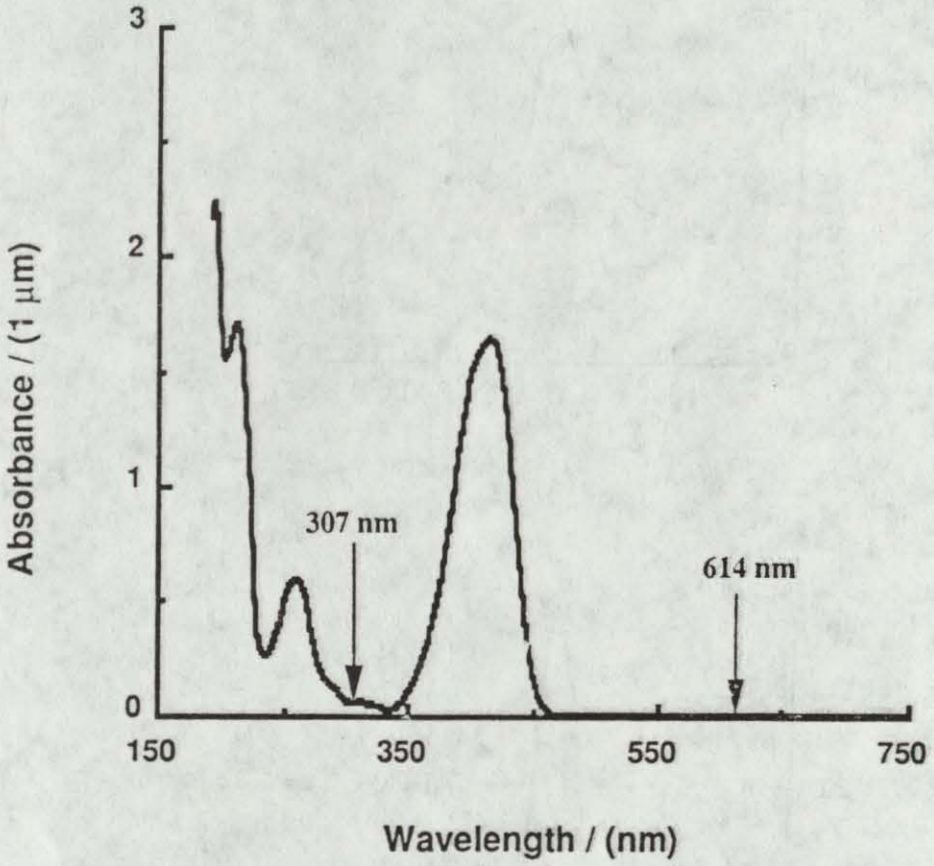

Figure 10 Absorption spectrum of COUM/PMMA copolymer film spin coated onto a quartz substrate.

Author Index

This document reports research undertaken at the US Army Natick Research, Development and Engineering Center and has been assigned No. NATICK/TR-80/028 in the series of reports approved for publication.